LBNL-38920
UC-2000

ERNEST ORLANDO LAWRENCE
BERKELEY NATIONAL LABORATORY

A Design Study for the Isolation of the 281-3H Retention Basin at the Savannah River Site Using the Viscous Liquid Barrier Technology

G.J. Moridis, P. Persoff, J. Apps, A. James,
C. Oldenburg, A. McGrath, L. Myer, L. Pellerin,
and K. Pruess
Earth Sciences Division

November 1996

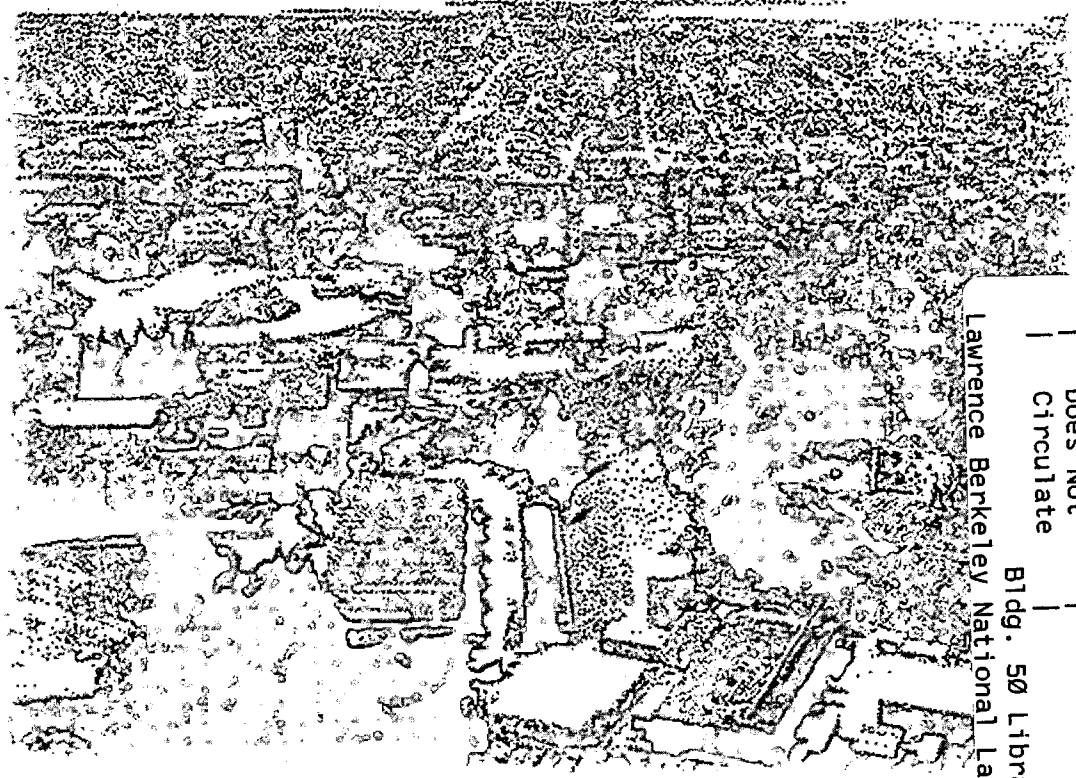

REFERENCE COPY
Does Not
Circulate
Bldg. 50 Library - Ref.
Lawrence Berkeley National Laboratory
Copy 1
LBNL-38920

DISCLAIMER

This document was prepared as an account of work sponsored by the United States Government. While this document is believed to contain correct information, neither the United States Government nor any agency thereof, nor the Regents of the University of California, nor any of their employees, makes any warranty, express or implied, or assumes any legal responsibility for the accuracy, completeness, or usefulness of any information, apparatus, product, or process disclosed, or represents that its use would not infringe privately owned rights. Reference herein to any specific commercial product, process, or service by its trade name, trademark, manufacturer, or otherwise, does not necessarily constitute or imply its endorsement, recommendation, or favoring by the United States Government or any agency thereof, or the Regents of the University of California. The views and opinions of authors expressed herein do not necessarily state or reflect those of the United States Government or any agency thereof or the Regents of the University of California.

LBNL-38920
UC-2000

A Design Study for the Isolation of the 281-3H Retention Basin at the Savannah River Site Using the Viscous Liquid Barrier Technology

G.J. Moridis, P. Persoff, J. Apps, A. James, C. Oldenburg, A. McGrath, L. Myer, L. Pellerin and K. Pruess

Earth Sciences Division
Lawrence Berkeley National Laboratory
Berkeley, CA 94720

November 1996

This work was supported by the U.S. Department of Energy, Office of Environmental Management, Office of Technology Development, Subsurface Contamination Focus Area, under Contract No. DE-AC03-76SF00098.

Recycled Paper

ABSTRACT

This report is a description of the design study for a pilot-scale field demonstration of the Viscous Liquid Barrier (VLB) technology, a new subsurface containment technology developed at the Lawrence Berkeley National Laboratory for waste isolation using a new generation of barrier liquids. The demonstration site was Retention Basin 281-3H, a shallow catchment basin at the Savannah River Site, which is contaminated mainly by radionuclides (^{137}Cs, ^{90}Sr, and ^{238}Pu). The goals of the field demonstration were (a) to demonstrate the ability to create a continuous subsurface barrier (with an average hydraulic conductivity of 10^{-9} m/sec and a minimum thickness of 0.9 m) in order to isolate the contaminants, and (b) to demonstrate the continuity, performance, and integrity of the barrier. The site was characterized, and preliminary hydraulic conductivity data were obtained from core samples. Based on the site characteristics and the functional requirements, a conceptual model was developed, the barrier specifications were defined, and lance injection was selected as the emplacement method. The injection strategy for the subsurface conditions at the site was determined using numerical simulations. An appropriate variant of Colloidal Silica (CS) was selected as the barrier liquid based on its relative insensitivity to interactions with the site soils, and the formulation for optimum site performance was determined. A barrier verification strategy, including hydraulic, pneumatic, tracer, and geophysical methods, was developed. A lance water injection test was conducted in order to obtain representative estimates of the hydraulic conductivity and its distribution for the design of the barrier emplacement. The water injection test demonstrated the lack of permeable zones for CS injection, and a decision not to proceed with the barrier emplacement was reached.

Abstract

TABLE OF CONTENTS

ABSTRACT iii
TABLE OF CONTENTS v
LIST OF FIGURES ix
LIST OF TABLES xi
1. INTRODUCTION 1
1.1. Conceptual Basis and Project Goals 1
1.2. Technology Needs 2
1.3. Technology Description 3
1.4. Application and Benefits 4
1.5. Brief Description of the Problem at the 281-3H Basin 5
1.6. Brief Discussion of the Isolation Approach 5
1.7. Brief Discussion of Important Issues and Assumptions 7

2. OBJECTIVES AND ACTIVITIES 9
2.1. Design Parameters, Issues, Implications and Requirements 9
2.2. Objectives and Criteria 9
2.3. Site-Preparation Activities 10
2.4. Pre-Injection Activities 10
2.5. Activities During Emplacement 11
2.6. Post-Injection Activities 11

3. SITE DESCRIPTION 13
3.1. Design Parameters, Issues, Implications and Requirements 13

3.2. Geological Site Characterization 14
3.2.1. Background Information 14
3.2.2. Basin Subsurface Geology 15
3.3. Pedological Analysis 16
3.3.1. Soil Cores from the HAA-3AA Area 16
3.3.2. Soil Cores from the HR3-13 Area 19
3.3.3. Hydrologic Implications 20
3.4. Chemical Site Characterization 21
3.4.1. Groundwater Chemical Characterization 22
3.4.2. Soil Chemical Characterization 25
3.4.3. Total Organic Carbon (TOC) Analyses 28
3.5. Hydrologic Characterization 29
3.5.1. Data Requirements 29
3.5.2. Data Availability and Evaluation 30
3.5.3. Permeability Analyses 31
3.5.4. Soil Particle Size and Mineralogic Analysis 36
3.6. Contaminant Characterization 36
3.7. Foreign Bodies in the Basin 38

4. BARRIER SPECIFICATIONS 39
4.1. Design Parameters, Issues, Implications and Requirements 39
4.2. Barrier Geometry 41
4.2.1. Basin Dimensions 41
4.2.2. Barrier Conceptual Model 41
4.2.3. Barrier Geometry and CS Grout Volumes 46
4.3. Selection of Barrier Emplacement Technique 47
4.3.1. Advantages of the Lance Injection Technology 47
4.4. Machinery and Instrumentation Requirements 50
4.4.1. The Lance-Pushing System 50
4.4.2. Lances and Lance Instrumentation and Monitoring 50
4.4.3. The Grout Injection System 50

4.5. Emplacement Design Calculations 51
4.5.1. Injection Strategy and Grids 51
4.5.2. Injection Under Variably Saturated Conditions 57
4.5.3. Implications 61
4.5.4. Grouting Around Buried Foreign Objects (Rip-Rap) 61

5. THE BARRIER LIQUIDS 63
5.1. Design Parameters, Issues, and Implications 63
5.2. Background Information 63
5.3. Colloidal Silica Samples 66
5.4. Soils 67
5.5. Laboratory Testing 67
5.5.1. Standard Tests 68
5.5.2. Gel Time Jar Tests Without Soil 68
5.5.2. Gel Time Jar Tests With Soil 69
5.6. Special Tests 69
5.6.1. Drain-In Test 69
5.6.2. Column Injection Test 69
5.6.3. Column Gel-Time In Soil Test 70
5.7. CS Evalution Results and Discussion 71
5.7.1. CS in Native and Simulated Soils 71
5.7.2. CS Variant Selection 75
5.7.3. CS Permeation and Gelling in Sludge 84
5.7.4. CS Permeation and Gelling in Remolded S1 Soil 84
5.7.5. Effect of γ-Radiation 88

6. MONITORING AND VERIFICATION 89
6.1. Design Parameters, Issues, Implications and Requirements 89
6.2. Sensors and Equipment for Barrier Verification 90
6.2.1. Overview 90
6.2.2. Drive Point Piezometers 90
6.2.3. Multifunction Hydrologic Probes (MHP) 92

6.2.4. Dual-Function Probes (DFP) 92
6.2.5. Gas Tracer Analysis and GPR Instrumentation 92
6.3. Pre-Injection Monitoring- and Verification-Related Activities 95
6.4. Monitoring and Verification During Emplacement 96
6.5. Post-Emplacement Verification 96

7. THE LANCE WATER INJECTION TEST (LWIT) 101
7.1. Objectives of the LWIT 101
7.2. Synopsis of the LWIT Results 101
7.3. Conclusions and Implications 103

8. SUMMARY AND CONCLUSIONS 105

9. ACKNOWLEDGEMENTS 109

10. REFERENCES 111

11. APPENDIX 115

LIST OF FIGURES

Figure 1.1. A schematic of the subsurface barrier using lance injection. The barrier is created by overlapping CS grout bulbs. 6

Figure 1.2. Plan view of the subsurface barrier using lance injection (not to-scale). 7

Figure 4.1. Map of H-Area retention basin (281-3H). 42

Figure 4.2. A schematic of the basin immediately before the barrier emplacement. 43

Figure 4.3. Conceptual model of the barrier to be emplaced at the retention basin 281-3H. 44

Figure 4.4. Specifications of the barrier walls. 47

Figure 4.5. The principles of the lance injection technology 48

Figure 4.6. Truck-mounted lance injection system. 49

Figure 4.7. Single source grout injection adjacent to a closed wall boundary. 53

Figure 4.8. Double port grout injection in an infinite acting system. 53

Figure 4.9. Close up of double port grout injection. 54

Figure 4.10. Simultaneous 2 port grout injection. 54

Figure 4.11. Staggered middle port injection. 55

Figure 4.12. Two-dimensional radial mesh for the injection simulations. 57

Figure 4.13. Initial hydrostatic conditions for the unsaturated injection scenario. 58

Figure 4.14. Injection curves for unsaturated conditions (water injection).....60
Figure 4.15. Injection curves for saturated conditions (water injection).....61
Figure 4.16. Bulb radius of injected CS grout, as affected by injection pressure and permeability (saturated conditions, water injection).....64

Figure 5.1. Isomorphic substitution of Si by Al on the CS surface in surface-modified CS formulations.....66
Figure 5.2. S2 soil effect on the gel time of CS-1A.....72
Figure 5.3. S2 soil effect on the gel time of CS-2A.....73
Figure 5.4. S2 soil effect on the gel time of CS-3A.....74
Figure 5.5. Effect of temperature on the complex viscosity of CS-3A.....83
Figure 5.6. Effect of sludge on the gel time of CS-3A.....85
Figure 5.7. Pressure and flow rate during CS-3A injection into remolded S1 soil.....86
Figure 5.8. Gel time of CS-3A effluent from a column of remolded S1 soil.....87

Figure 6.1. Schematic of (a) the Dual-Function Probe (DFP) and (b) the Multifunction Hydrologic Probe (MHP).....91
Figure 6.2. Locations of piezometers (squares) and MHPs (circles), as well as layout of the tube and cable conduits for data aquisition.....93
Figure 6.3. Layout of the DFP array.....94
Figure 6.4. Layout of the GPR vertical access tubes.....98

LIST OF TABLES

Table 3.1. Partial Chemical Analysis of Groundwater from Well HAA-3D (pH=6.2, T = 18 °C) 22

Table 3.2. Calculated Speciation at T = 18 °C 24

Table 3.3. Calculated Mineral Saturation Indices (SI) 25

Table 3.4. Soil Analysis of the S1 Soil 26

Table 3.5. Soil Analysis of the S2 Soil 26

Table 3.6. TOC of Soils at the H-Area Basin 29

Table 3.7. Laboratory Hydraulic Conductivity Measurements from Shelby Tube Samples at the HAA-3AA Location 33

Table 3.8. Laboratory Hydraulic Conductivity Measurements from Shelby Tube Samples at the HR3-13 Location 34

Table 3.9. Laboratory Hydraulic Conductivity Measurements from Split-Spoon Samples 35

Table 3.10. Particle Size Analysis of Soils at the H-Area Basin 37

Table 4.1. Parameters for the Injection Curve Simulations 58

Table 5.1. Jar-Test Gel State Codes 65

Table 5.2. Compliance of CS Variants to Specifications 76

Table 5.3. Performance of the CS Variants in Test 1 With a 1 hr Design Gel Time 77

Table 5.4. Performance of the CS Variants in Test 1 With a 2 hr Design Gel Time 78

Table 5.5. Performance of the CS Variants in Test 1 With a 4 hr Design Gel Time 79
Table 5.6. Performance of the CS Variants in Test 1 With a 8 hr Design Gel Time 80
Table 5.7. Performance of the CS Variants in Tests 2 and 3 81
Table 5.8. CS Testing Results in Tests Not Included in the RFP (Savannah River Soil S2)....82

1. INTRODUCTION

This report is the design study for a pilot-scale field demonstration of a new subsurface containment technology for waste isolation developed at the Lawrence Berkeley National Laboratory, which uses a new generation of barrier liquids for permeation grouting. The demonstration site is Retention Basin 281-3H, a shallow catchment basin at the Savannah River Site (SRS) originally built to control contaminated runoff for the H Reactor, and which has been contaminated mainly by radionuclides.

Several parties are involved in this effort. Where needed in the subsequent sections, the responsible parties for the various activities are clearly identified. These parties include:

- The Department of Energy (DOE), the site owner
- The Landfill Stabilization Focus Area (LSFA), the funding agency of the project
- The Westinghouse Savannah River Company (WSRC), the Management and Operations contractor for the facility
- The Lawrence Berkeley National Laboratory (LBNL), the design agency with technical responsibility over the project,
- MSE, a contractor to the Western Environmental Technology Office (WETO) of the Department of Energy and the Contract Administrator for field operations;
- The Sandia National Laboratories (SNL), responsible for an independent evaluation of the barrier verification effort.
- The DOE field offices (Savannah River, OAKland, ALbuquerque) associated with the various project activities.

1.1. Conceptual Basis and Project Goals

LBNL staff have developed a subsurface containment technology [*Moridis et al.*, 1993a,b; 1995a,b; 1996a,b; Finsterle et al., 1994a,b; Persoff et al., 1994, 1995] using a new generation of viscosity-sensitive barrier liquids which, when set in porous media, cause the media to exhibit near-zero permeabilities and permit containment of contamination in the

subsurface by entrapping and isolating both the waste source and the plume by a chemically and biologically benign physical barrier.

The current phase of the project involves a pilot-scale field demonstration of the LBNL viscous barrier technology, and represents a scale-up from the first small-scale (feasibility) field test conducted in January 1995 [*Moridis et al.*, 1995a,b]. The goals of the current phase of this project are:

(a) To demonstrate the ability to create a continuous subsurface barrier isolating the contaminated Retention Basin 281-3H at SRS. This effort constitutes a pilot-scale field demonstration/application of the technology to an actual contaminated site of realistic size (220 ft long by 150 ft wide by up to 25 ft deep) rather than a demonstration at a clean site.

(b) To demonstrate the continuity, performance, and integrity of the barrier, and its compliance with the functional requirements of the related Treatability Study [*WSRC*, 1996].

1.2. Technology Needs

The development of an effective *in situ* containment technology is needed both to prevent further release of contaminants from buried sources and to contain existing contaminant plumes. Without such technology, contaminants from buried wastes or from contaminated soil in the vadose zone can be mobilized and migrate toward previously uncontaminated regions of an aquifer. The alternative contaminant removal from the subsurface by pumping or excavation is expensive, very slow, and usually ineffective. Contaminants sorb tenaciously to subsurface materials (especially clays), and traditional physical extraction methods are slow and ineffective. Excavation of contaminated soils and disposal in protected facilities may pose environmental health and safety problems, is expensive and often impractical.

Despite the obvious need, containment technologies have been limited largely to expensive *brute-force* approaches involving trenching, and cut-off and slurry walls. The applicability of these methods is restricted to cases of lateral movement of contaminants, and their effectiveness is limited by practical considerations. Currently there is no effective technology available to prevent the downward migration of wastes toward deeper and uncontaminated parts of the subsurface.

Subsurface barriers, formed by injection of barrier fluids that gel or solidify *in situ*, can contain contaminants on-site and control the groundwater flow pattern, thus reducing or eliminating an off-site threat. Furthermore, containment is also needed to prevent the spread of mobilized contaminants caused by application of treatment technologies (e.g., soil flushing, alcohol flooding, surfactant mobilization) that increase contaminant mobility.

1.3. Technology Description

The LBNL viscous barrier technology employs barrier liquids which, when injected into the subsurface, produce chemically benign nearly impermeable barriers through a very large increase in viscosity. The low-viscosity liquids are emplaced through multiple injection points in the subsurface and the intersecting plumes merge and completely surround the contaminant source and/or plume. Once in place, they gel or cure to form a nearly impermeable barrier. The technology can be applied to encapsulate wastes in the subsurface. In applying this technology, however, it is important to match the fluid to the waste and to the soil conditions, and to control the gel time and emplacement of the fluid to form the barrier [*Moridis et al.*, 1993a; *Persoff et al.*, 1994, *Moridis et al.*, 1995a, 1996a]

Two general types of barrier liquids have been used. The first is **C**olloidal **S**ilica (CS), an aqueous suspension of silica microspheres in a stabilizing electrolyte. It has excellent durability characteristics, poses no health hazard, is practically unaffected by filtration, and is chemically and biologically benign. The increase in viscosity of the CS following injection is due to a controlled gelation process induced by the presence of a neutralizing agent or a concentrated salt solution, either of which are added immediately prior to injection at ambient temperatures. The CS has a tendency to chemically interact with the geologic matrix, and therefore, special formulations or techniques are required to minimize or eliminate the impact of such interactions which can result in loss of *gel-time* control. Due to the expected conditions of the subsurface at the retention basin, CS was selected as the barrier liquid for the SRS demonstration.

The second type of barrier belongs to the **P**oly**S**ilo**X**ane (PSX) family, and involves vinyl-terminated silanes with dimethyl side groups. The increase in viscosity in PSX is caused by the cross-linkage of the injected liquid and the formation of a matrix of essentially infinite viscosity after the addition of a catalyst through a process akin to vulcanization. The cross-linking process is controlled by the quantities of the catalyst, crosslinker, and (occasionally) retardant added to the PSX prior to injection.

Both materials pose no health hazard (have been approved by FDA for food contact), are unaffected by filtration, have low initial viscosity (under 10 cP), are chemically and biologically benign, and have been shown to be effective barrier liquids. Control of the setting time is an essential component of the process because premature or late setting can result in incomplete filling of the pore space and thus reduces the effectiveness of the technology.

There are three ways to apply the containment technology. The first, conditions permitting, results in permanent immobilization of the contaminants in the affected aquifer region by sealing and entombing them in a *monolith* of impermeable material. This represents a radical deviation from the currently practiced approach, which either allows the contaminants to remain in a free state by seeking to lower their rate of migration by decreasing the permeability of the porous medium, or is used in attempting to neutralize them by a chemical reaction.

In the second option, an impermeable container *(box)* is created to surround and isolate the contaminated area, which can then be treated at a later time. Alternatively, such a *box* could enhance or even make possible remediation techniques (such as soil flushing) which currently face regulatory approval problems due to concerns about contaminants escaping into previously unaffected areas of the subsurface. The design of the pilot-scale field demonstration discussed in this report is based on the impermeable container approach.

Finally, the third option allows sealing of permeable aquifer zones, thus concentrating the effects of traditional cleanup techniques (such as pump and treat) in inaccessible and difficult-to-treat less permeable zones.

1.4. Application and Benefits

The LBNL viscous barrier technology can be applied at any site where hazardous wastes (radionuclides, heavy metals, organics, mixed wastes) have contaminated the subsurface environment, and includes isolation of ponds and buried tanks, cap and liner repairs at landfills, etc.

The LBNL containment technology offers a number of significant advantages:

- On-site containment and control of the groundwater flow pattern which limits the off-site threat and could supply a long-term solution.
- Site disturbance, if any, is minimal, as no excavation of possibly contaminated soils is required.
- Risk of human exposure is minimized.
- It is applicable to the whole spectrum of wastes and a wide variety of sites.
- It enables the complete isolation of the affected area from the regional groundwater flow by providing barriers to both horizontal and vertical flow (the only technology currently capable of providing horizontal barriers (bottoms) in containment systems).
- It is usually cheaper and more effective than conventional (baseline) methods.
- The effectiveness of traditional clean-up techniques can be enhanced by allowing natural degradation and bioremediation to occur without risk of contaminant migration.
- Additionally, more intensive remediation technologies (such as soil washing, alcohol flooding, etc.) are possible without the risk of mobilizing and spreading the contaminants.

1.5. Brief Description of the Problem at the 281-3H Basin

Basin 281-3H is a shallow retention/seepage basin at the Savannah River complex, and is contaminated mainly by radionuclides. Of particular concern are ^{137}Cs, ^{90}Sr, and ^{238}Pu. The basin dimensions were originally designed to be 200 ft by 120 ft by 6 ft, but are expected to be somewhat larger due to bank erosion. The groundwater table is thought to be shallow (possibly a perched water table) and to vary seasonally between 4 and 12 ft from the surface. Rainfall in the area averages 45 inches/year.

Most of the contamination is believed to be in the first 1-2 ft from the surface and from the basin bottom. In addition to the contamination in and around the pond, a pile of contaminated excavated soil is located on the west side of the basin. A detailed description of the pond, contamination, and the prevailing conditions at the site can be found in the report WSRC-RP-94-499, Rev. 1 (Phase II, Revision 1, Remedial Investigation Work Plan for the H-Area Retention Basin (281-3H)(U), October 1994). A summary of this report by *Kuelske* [1995] includes the most important information on the specifics of the basin.

Current plans for Retention Basin 281-3H call for removal of the contaminated water from the basin, moving the contaminated soils into the basin, and isolating the basin from the surrounding environment. Waste isolation includes (a) prevention and elimination of future contamination of groundwater, and (b) placement of a low permeability cap on top of the contaminated material.

1.6. Brief Discussion of the Isolation Approach

The LBNL subsurface barrier technology is being employed to provide a hydraulic barrier for waste containment and isolation to prevent further groundwater contamination from current sources. The current source of contamination is believed to be a 1-2-ft thick zone at the bottom of the basin and at the soil surface. Radionuclide-laden water migrates towards the water table through infiltration of rainwater or when a rising watertable intercepts the contaminated zone, and creates a plume carried by the regional groundwater flow. Waste containment and isolation are a prerequisite for placement of the soil pile in the basin.

The humid conditions at the basin site dictate the use of Colloidal Silica (CS): CS is water based, and as such it can easily seal the water-filled pores. The particular PSX formulation that LBNL has been using is not hydrophilic, and it would be practically impossible to achieve a complete displacement of the water in the pores or bond with the soil particles. A large portion of the pore space (the irreducible saturation, up to 25% of the pore space) would remain unsealed, which would leave a continuous

aqueous film through which contaminants could migrate. No such problem exists with CS.

Compared to the other baseline technologies (such as slurry walls and removal and disposal) the LBNL subsurface barrier technology offers several advantages. It entirely isolates the affected area from the regional groundwater flow by providing barriers to both horizontal and vertical flow. It makes possible the isolation of waste through the least intrusive approach. Because it relies on permeation, no soil (possibly contaminated) is excavated during injection and the risk of human exposure is substantially reduced.

Application of the LBNL subsurface barrier technology to the contamination problem of Basin 281-3H entails the creation of a containment system (isolation chamber) using Colloidal Silica (CS). After evaluation of a number of alternative emplacement methods of the subsurface barriers, a technique using lances to inject the CS was selected. This approach leads to creation of an impermeable barrier by permeation grouting beneath the bottom of the basin (**Figures 1.1** and **1.2**) by lancing through the cover and contaminated material.

Figures 1.1 and **1.2** are used **only** to illustrate the approach, and represent a simplified statement of the problem reflecting idealized conditions. A more realistic and accurate depiction of the emplacement approach (as it pertains to the subsurface conditions at the site) can be found in Section 4.

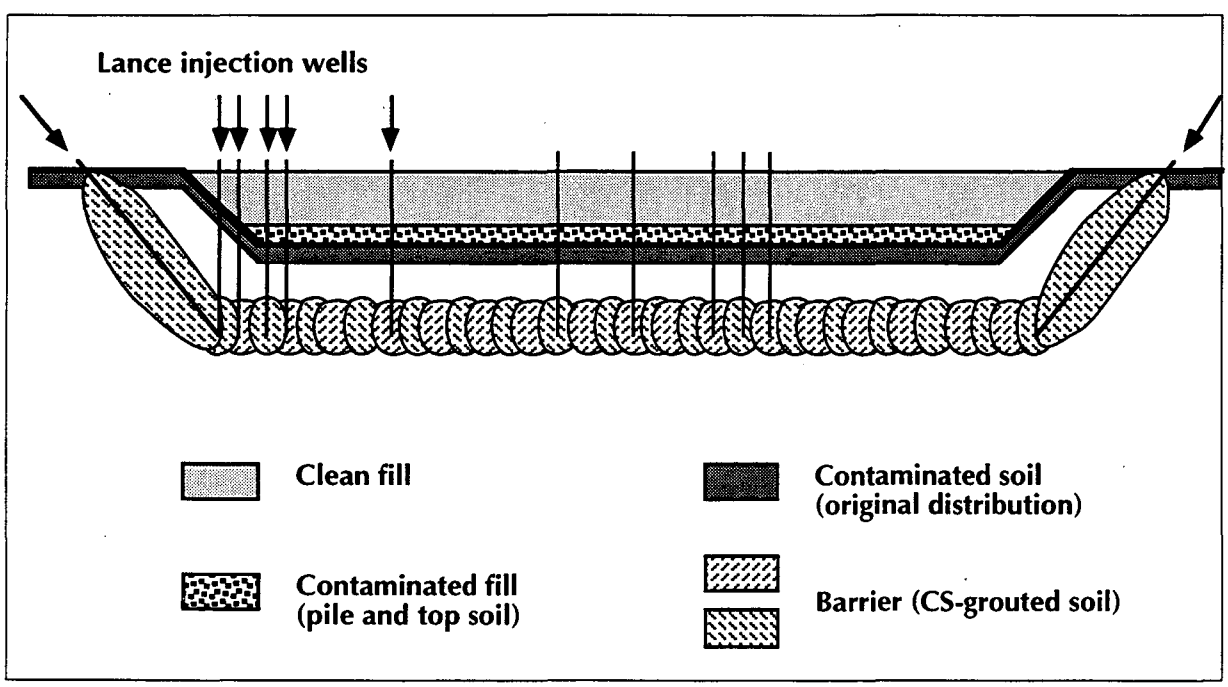

Figure 1.1. A schematic of the subsurface barrier using lance injection. The barrier is created by overlapping CS grout bulbs.

Although lance injection for barrier emplacement is slightly intrusive, as it requires piercing the contaminated zones, it minimally disturbs the contaminated soils and offers significant health, safety, cost and time advantages because it obviates drilling and completion of wells. The selection of the emplacement method is discussed in Section 4.

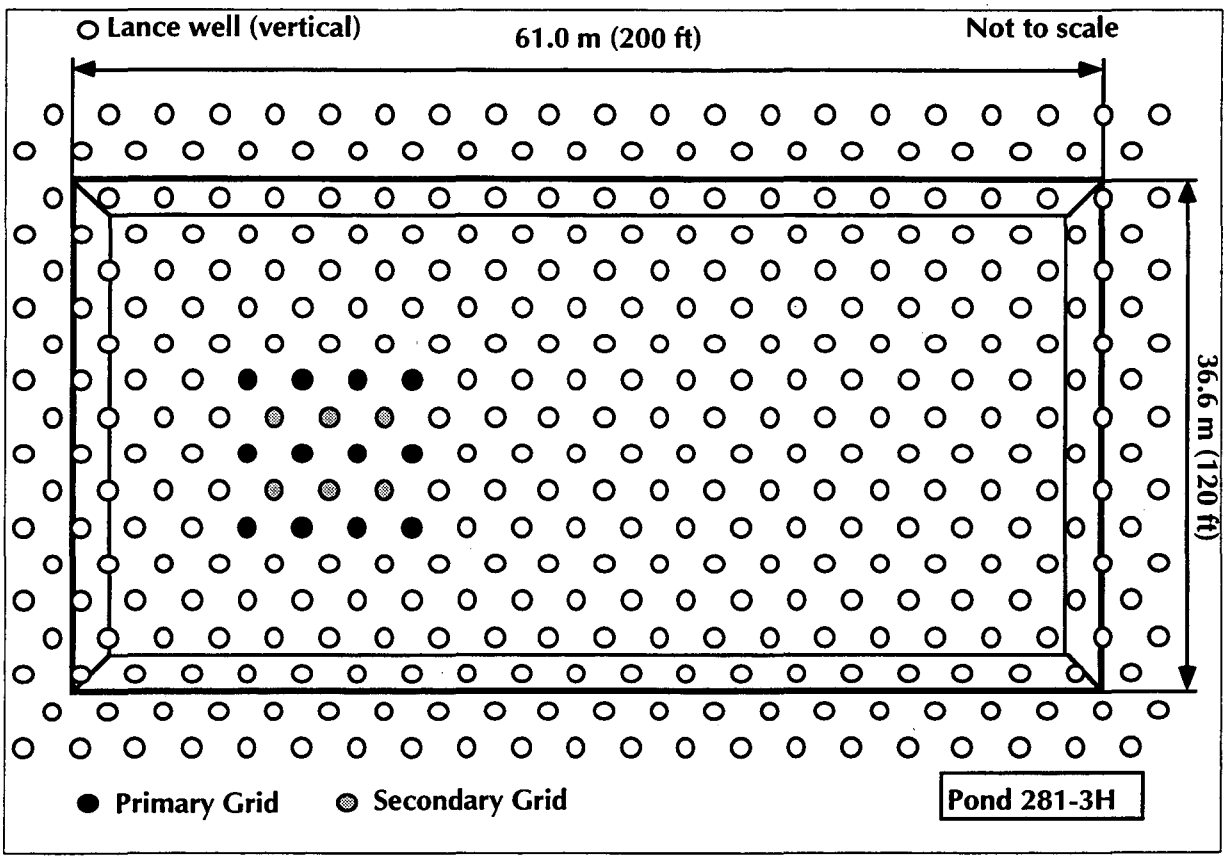

Figure 1.2. Plan view of the subsurface barrier using lance injection (not to-scale).

1.7. Brief Discussion of Important Issues and Assumptions

In the present report we discuss the activities deemed necessary to isolate Basin 281-3H using the LBNL subsurface containment technology, and present a design study for use in the development of the engineering design package and work plan. At the inception of this project, site characterization information was very limited. In light of the considerable uncertainties, the underlying assumptions of this proposal and the corresponding implications must be clearly articulated. More specifically:

(a) Detailed characterization of the contamination and its distribution at the Basin 281-3H area is needed. The proposed sampling activities listed in the *WSRC* [1994] report are expected to provide sufficient information about the extent and distribution of contamination. Soil sampling and analysis are expected to occur before the inception of field operations. This information is vital for delineating the extent of contamination and designing the containment system.

(b) This design package is based on the assumption that contamination is limited to the shallow zone at the surface and the bottom of the basin, which can be contained and isolated by the proposed design [*Kuelske*, 1995; *WSRC*, 1996]. The preliminary plans and designs are conservative and seek to isolate the bulk of the sources, as well as adjacent material that may be contaminated by migrating waste. If upon soil analysis, it should become evident that the extent of contamination is much greater than originally expected (and/or that the existing plume is large in size and high in radioactivity, thus acting as a secondary source), then it may be necessary to redesign the containment system to isolate a much larger soil volume.

(c) Because of existing contamination, the objectives and success criteria, as well as the methodology and means of success verification, are different than those at a pristine site. These are clearly identified in Sections 2 and 4.

These issues are discussed in detail in the ensuing sections of this document.

2. OBJECTIVES AND ACTIVITIES

In this section we discuss the project objectives and the criteria for success. The sequence of all the events and activities necessary for the project completion are listed in strict chronological order.

2.1. Design Parameters, Issues, Implications and Requirements

(a) The success criteria for this project are defined by the Treatability Study, TS [*WSRC* , 1996].

(b) To meet the TS functional requirements, the barrier
- must have an average hydraulic conductivity of 10^{-9} m/sec or less, and
- the minimum cumulative thickness of the grouted soil horizons in the direction of potential flow must be 0.9 m (3 ft).

(c) Barrier emplacement operations were expected to begin on 9/23/96 and to be completed by 11/31/96.

2.2. Objectives and Criteria

The specific objectives of this effort are:

(a) To demonstrate the ability to create a continuous subsurface barrier isolating the contaminants in Retention Basin 281-3H at SRS.

(b) To demonstrate the continuity, performance, and integrity of the barrier, and its compliance with the functional requirements of the related TS [*WSRC* , 1996].

The performance/success criteria are defined by the TS, and include:

(1) Spatially averaged hydraulic conductivity between the isolated soil volume and the surroundings of 10^{-9} m/sec or less.

(2) Demonstrated lack of hydraulic communication between the isolated volume and the surrounding soils.

(3) Minimum cumulative thickness of the grouted soil horizons in the direction of potential flow of 0.9 m (3 ft) or more.

It must be clearly stated that this project

- does not involve removal of the contamination from the subsurface,
- targets for isolation a specific contaminated zone (see Section 4) and not all the potentially contaminated soils.

2.3. Site-Preparation Activities

2.3.a. Vegetation is removed from the basin.

2.3.b. The standing water in the basin is removed.

2.3.c. The initial and current basin boundaries are delineated, and a topographic map of the empty basin is prepared.

2.3.d. The contaminated soils are relocated inside the basin, which is then covered by 0.61 m (2 ft) of clean soil to provide protection from radiation.

2.4. Pre-Injection Activities

2.4.a. 9.1-m (30-ft) continuous cores are obtained from 5 locations (within the basin boundaries) for contaminant characterization, and the resulting wells are completed and equipped for Ground Penetrating Radar (GPR) studies. If contamination is detected below the 9.1 m-level, the approach and design will have to be reconsidered.

2.4.b. Horizontal wells are drilled underneath the target area for GPR measurements from below the barrier.

2.4.c. GPR surveys (surface, using the 5 vertical wells from 2.4.a, and subsurface) of the site are conducted.

2.4.d. 10 drive-point piezometers are installed outside the perimeter of the basin using the lance system.

2.4.e. 35 **M**ultifunction **H**ydrologic **P**robes (MHP, see Section 6) are installed on a regular grid within the perimeter of the basin using the lance system.

2.4.f. Hydrologic data collection from the piezometers begins.

2.5. Activities During Emplacement

2.5.a. Just prior to the beginning of field injection operations, the lance system is tested using the design CS grout at a clean location near the basin. Adjustments are made to the CS component ratio, design lance spacing, injection rates and pressures, as well as to any other pertinent parameters of interest. The grouted soils at the test location may be used to test final permeability and compliance with the TS requirements.

2.5.b. The field CS injection for barrier emplacement begins using the lance injection system.

2.5.c. The MHPs in the covered (grouted) areas are connected to the data collection system and data recording begins.

2.6. Post-Injection Activities

2.6.a. All MHPs are connected to the data collection system.

2.6.b. 24 vertical access tubes (12 inside and 12 outside the basin) for GPR measurements are installed using the lance system.

2.6.c. GPR surveys (surface, using the 5 vertical wells and the 24 access tubes, and subsurface) of the site are conducted.

2.6.d. 63 **D**ual-**F**unction **P**robes (DFP, see Section 6) are installed on a regular grid within the perimeter of the basin above the barrier using the lance system.

2.6.e. Air and gaseous tracers are injected underneath the barrier, the responses of the various sensors are recorded, and the areal distribution of the barrier permeability is determined.

2.6.f. Based on the results of 2.6.e (as supported and enhanced by the GPR analysis in 2.6.c), weak areas of the barrier with incomplete CS coverage are identified.

2.6.g. Following the data analysis in 2.6.f, if areas of the barrier are found to be not in compliance with the design criteria of permeability and thickness, finishing and *touch-up* CS injection operations begin, targeting incompletely grouted horizons.

2.6.i. Activities 2.6.e through 2.6.g are repeated until the compliance criteria are met or a maximum of three times.

2.6.j. The pressure transducers from the DFP are removed, and the DFPs are grouted in place. Similarly, the 12 access tubes within the enclosed volume are grouted in place.

3. SITE DESCRIPTION

The site geology, pedology, geochemistry, and hydrology are presented in this section. Hydraulic conductivity data from the laboratory analysis of Shelby tube cores from the site of the basin are tabulated, and the implications discussed. The current state of knowledge on the contaminant characterization is reviewed, and the necessary activities to fill important knowledge gaps are discussed.

3.1. Design Parameters, Issues, Implications and Requirements

(a) Preliminary assessment based on laboratory analysis (see subsection 3.5) indicates that the subsurface soils at the basin site

- are predominantly clay-rich with low to very low natural hydraulic conductivities (10^{-7} to 10^{-9} m/sec),
- contain layers of locally higher permeability (10^{-5} to 10^{-6} m/sec).

The more permeable layers (see **Tables 3.1** through **3.3**) will be targeted for injection. These findings are subject to revision based on the results of a field water injection test (see Section 7).

(b) The extent and continuity of the more permeable layers are unknown. Based on information from other sites within the same geologic formation, these layers are assumed to be discontinuous, and the subsurface is expected to be very heterogeneous.

(c) The water bearing horizon closest to the surface seems to be confined or semi-confined; the piezometric surface varies between 1.5 to 4.0 m (5 to 13 ft) from the surface. The top of the water-saturated formation seems to be 7.9-8.5 m (26-28 ft) below the original soil surface.

(d) The water saturation conditions of the soils underneath the pond are unknown, but they are assumed to be saturated, possibly forming a perched watertable.

(e) Foreign bodies (rip-rap, broken concrete, asphalt) are present in the basin, and must be accounted for during the barrier emplacement operations. A drill rig will be situated on site to replace the lance system when needed to ensure penetration (see subsection 3.7).

(f) A useful set of illustrations has been developed, which relate laboratory hydraulic conductivity measurements to soil textures (based on Shelby tube and split-spoon cores from the site) together with a narrative of the geological, pedological, and geochemical analysis of the cores. These figures can be found in the Appendix.

3.2. Geological Site Characterization

3.2.1. Background Information

The Savannah River Site is underlain by consolidated and unconsolidated Tertiary sands clays and gravels. The Tertiary rocks are in turn underlain by Upper Cretaceous argillites and sandstones. These sedimentary rocks rest upon rifted Paleozoic basement rocks consisting of acid intrusives and mafic metavolcanics. A buried Triassic graben filled with impermeable mudstones has also been delineated beneath the site.

The overlying Upper Cretaceous-Tertiary sediments are wedge shaped and vary in thickness between approximately 244 m (800 ft) on the northwestern side to 274 m (1730 ft) on the southeastern side of the site, [*Kegley*, 1993]. The Tertiary sediments are primarily fluvio-deltaic in origin, with characteristic abrupt vertical and lateral changes in lithology.

The so-called 10 m thick Miocene *Altamaha Formation*, or *Upland Unit*, [*Huddleston*, 1988; *Nystrom and Willoughby*, 1992] is believed to be present at the surface in the vicinity of the H Area retention basin. In an area 2 km NE of the H Area, *Kegley* [1993] found that this formation consisted of multi-colored clays, sandy clays and clayey sands. Beneath the *Altamaha Formation* lies the ≈21 m thick Tobacco Road Sand and underlying ≈17 m thick Dry Branch Formation of the Late Eocene Barnwell Group. The former is generally characterized as consisting of red, purple and pink, coarse-to-medium grained, poorly-to-moderately sorted sands and clayey sands, whereas the latter is a tan-yellowish-orange, coarse-to-medium grained clayey sand [*Kegley*, *loc. cit.*].

3.2.2. Basin Subsurface Geology

Numerous shallow wells have been sunken throughout the H-Area since construction, particularly around the present rubber-lined retention basin immediately to the west of the old H Area retention basin, 281-3H. Of particular importance is monitoring well No. HAA-3AA, which is located immediately outside the retention basin boundary at the northeast corner. A geologic field log was prepared for Well No. HAA-3AA to a depth of 91.4 m (300 ft) [*Kuelske*, 1995]. Subsequently, 3 cone penetration tests, HCPT-02, HCPT-03 and HCPT-04, were conducted immediately outside the H-Area retention basin enclosure on the north and east sides to a depth of 18.3 m (60 ft) [*Serrato,* 1996a]. These tests allowed for preliminary extrapolations of the stratigraphy within the boundaries of the enclosure.

The penetrometer information, while useful in targeting general intervals of the stratigraphic column for injection, was, never-the-less interpretive but lacking sufficient resolution, and therefore direct sampling and recovery of intact core samples was required for mineralogical and hydrologic characterization.

Accordingly, six Shelby tube penetrations were made to depths of approximately 9.1 m (30 ft). Four of these penetrations were made in the vicinity of monitoring well No. HAA-3AA and two were made in the vicinity of well No. HR3-13, which is located adjacent to Road E immediately north of the northern boundary fence of the H area retention basin [*Williams*, 1996]. Subsequently, a further three holes, designated HAA-3AA-1, HAA-3AA-2 and HR3-13-3, using a split spoon sampler were drilled to depths up to 7.6 m (25 ft) in order to recover core suitable for permeability tests.

Bulk samples of sediment/soil were also collected from the east side of the retention basin boundary fence, just south of the HAA-3AA well cluster, using a back hoe. The samples were segregated by intervals. Soil from the 1.5-3.0 m (5-10 ft) zone below the surface will be hereafter referred to as *Soil S1*. Soil from the 3.0-6.1 m (10-20 ft) zone below the surface will be hereafter referred to as *Soil S2*. The purpose in collecting the samples was to perform various soil compatibility tests with CS.

Within the primary target interval for injection of CS between 3.0 and 9.1 m (10 and 30 ft) below ground surface, all sources of information indicate the presence of heterogeneous poorly consolidated clay, silt and silty-sand horizons, with occasional narrow intervals containing coarse angular 0.0064-0.019 m (0.25-0.75 in) quartz pebbles embedded in a silty matrix. These quartz pebble horizons, particularly at approximately 3 m (10 ft) and 5.8-6.4 m (19-21 ft) in depth prevented penetration of the Shelby tube and necessitated auguring [*Serrato,* 1996b,*Williams*, 1996].

Clay horizons predominate, however, and show greater apparent continuity than the thin and apparently discontinuous silt and sand horizons. There is no evidence of any pronounced marker horizons with a distinctive lithology, which would permit a stratigraphic correlation between the various sampled intervals. Those sandy intervals that were preserved

during split spoon coring, varied between 0.05 to 0.23 m (2 to 9 inches), with most being towards the shorter end of the range. Both Shelby tube and split spoon recoveries were incomplete suggesting that the missing intervals might have been unconsolidated permeable sands.

Iron oxides provide distinctive staining. In the homogenized back-hoe samples, the S1 soil is a rusty brown, suggesting the presence of ferric oxyhydroxides, whereas the S2 soil is stained a *hematite* red. It is possible that localized redox reactions induced by the biogenic oxidation of translocated organic matter from the uppermost soil horizon is responsible for the differing nature of the iron oxides in the S1 soil sample.

3.3. Pedological Analysis

3.3.1. Soil Cores from the HAA-3AA Area

In this section we discuss the pedological analysis of the cores obtained from the cluster of holes HAA-3AA-1 through 4. The soil profile is incomplete, because some subsurface horizons could not be sampled (and subsequently analyzed) due either to excessively friable or to cemented soil conditions.

0-0.038 m (0-1.5 in) A moderately to weakly developed surficial soil (A horizon), with low concentrations of Organic Matter (OM). The surface may have been eroded and soil began developing again.

0.025-0.3m (1-12 in) A red-brown clay-rich B or AB horizon. The red color is indicative of greater oxidation than lower horizons, and the structure appears to be that of a more loosely aggregated layer with 15-25% clay. The brown color is indicative of residual OM that has leached through the surface layers of soil. The brownish hue in this layer is indicative of a more mature soil than the thin A, surficial horizon, indicates.

0.3-0.49m (1-1.6 ft) A yellow, possible iron-rich (goethite) sediment below 1 ft, a BC1 horizon with obvious weathering, but with a lower degree of oxidation and transformation. The presence of goethite without red, hematite mottling (as seen in lower horizon) is indicative of some residual OM present which inhibits transformation into hematite and therefore stabilizes the goethite (this is based on conjecture without chemical data to support this assumption).

0.49-1.22m (1.6-4 ft) A Yellow, possibly iron-rich (goethite) layer with mottles of hematite, a BC2 horizon with weathering and pebbles (<2.5 cm in diameter). The clay content is approximately 10-15% with significant sand and clay films of iron oxides within the matrix. The lithic fragments,

pebbles, are quartz rich, implying that the sediment has undergone weathering.

1.22-1.82m (4-6 ft) A mottled layer, with predominantly goethite coloring, rich in kaolinite (potentially a BC3 horizon formed prior to the surface erosion and formation of the current surface soil). The mottling is composed of yellow (goethite), brown (mixtures of goethite, hematite, and kaolinite), and red (hematite) mottles and with quartz pebbles (predominantly ≤2.5 cm with larger fragments of 3-5 cm) and sand present. The permeability sample #10 was taken from the 1.52 to 1.66 m (5 to 5.5 ft) section of this core, and it has a preliminary texture determination of sandy clay (clay content of ~25%). This layer is quite massive and compact (although this may partly be a result of the coring procedure). The kaolinite concentration in this horizon appears to increase with depth, giving the lower portion a grey to white color between mottles of red and yellow. The kaolinite appears to be responsible for the dense, lithified nature of portions of this layer.

1.82-2.44+ m (6-8+ ft) This is a dense clay layer with highly weathered minerals such as hematite and kaolinite. Little-to-no goethite is present, and there appears to be a sharp transition (discontinuity) into this oxidized, weathered layer at approximately 1.82 m (6 ft).

2.44-3.81 m (8-12.5 ft) There is a gap in the shelby tube samples between 2.1 to 2.4 m (7 or 8 ft) and ~3.8 m (~12.5 ft), where recovery of the sediment using shelby tubes was impossible. Split spoon samples through this section revealed that the sediment is of similar composition to the overlying sections with more quartz pebbles surrounded by a hematitic clay matrix. It is difficult to determine the actual composition of this layer after split spoon aquisition.

3.81-5.18 m (12.5-17 ft) The composition and degree of weathering indicate that this layer was not weathered as part of the current soil development processes. It has many of the same minerals found in the layers between 1.82-2.44 m (6-8 ft), but the concentration of highly crystallized hematite and kaolinite appear to be greater. Undulating layers of kaolinite form streaks through the red to purple, well crystallized hematite. Some mica (vermiculite?) and sand are present, but the clay concentration is high (25+%). The clay is derived from either highly altered material (Eocene coastal sedimentary rock that has been highly weathered and buried) or from buried, highly weathered Pleistocene soil. Without further information regarding the history of the site, it is impossible to resolve this question. The permeablility sample #9 was taken from the 4.57-4.72 m (15-15.5 ft) increment of this series of cores. It is predominantly kaolinite with stains of goethite on the edges of the hematite-kaolinite margins. The permeability in this layer is expected

to be very low. Sample #8 was taken from the 5.03-5.18 m (16.5-17 ft) depth in a kaolinite/hematite mixed sample where the ratio was approximately 50/50.

5.49-7.32 m (18-24 ft) A quartz rich layer missing in cores (split spoon sampling has shown that it is a quartz conglomerate layer with a kaolinite and hematite matrix). Despite the high concentration of pebbles in this layer, the matrix contains a high concentration of clays, suggesting that the permeability is very low.

7.32-8.23+ m (24-27+ ft) A red oxide conglomerate layer with purple stains on pebbles due to well crystallized hematite. Banding of goethite and hematite in the matrix enclosing sands and pebbles form layers of alternating yellow and red. Although the texture of this layer is skeletal (i.e. matrix enclosing a conglomerate layer) the matrix is composed of well lithified clays with low concentrations of sands. Both permeability samples #6 and 7 were taken from this layer at a depth of 7.62-7.77 m (25-25.5 ft). The proximity to the water table changes the appearance of this layer dramatically from well hole to well hole. As a result, adjacent holes have cores with very different appearances. Sample #5 was taken at a depth of 7.85 to 8 m (25.75 to 26.25 ft) in a layer with an approximate texture of clayey loam (~15% clay)

The water table appears to be somewhere between 7.92 and 8.53 m (26 to 28 ft) feet in depth. This can be determined both by the degree of saturation in the sediments removed by the cores, but also from the increasing concentration of goethite and lighter yellower colors.

8.53-9.14+ m (28-30+ ft) This is a layer that is high in clay and quartz sand (25-30% clay). It is difficult to determine its original morphology because of the proximity of the water table and the degree of saturation of the sediments (cores appear to be slurries of the original samples). These layers appear very mixed and yellower in color due to the presence of hydrated iron oxides. Samples #4 and 3 were removed from this series of layers, with 4 taken out of a layer of unconsolidated sandy material at 8.23 to 8.38 m (27 to 27.5 ft). This material appears to be quite permeable. Sample #3 came from a depth of 8.61 to 8.76 m (28.25 to 28.75 ft) in a sandy clay layer with mottling of goethite within a matrix mixture of hematite and goethite.

A sandy clay loam layer occurs below the water table at 8.99 to 9.14 m (29.5 to 30 ft), where sample #2 was obtained (~15% clay). A clayey sand texture was found at approximately 9.14 to 9.29 m (30-30.5 ft) where sample #1 was taken. The mineralogy of both samples is similar; a matrix of goethite and small amounts of hematite dominate the profile. The presence of goethite is indicative of recycled

iron and possibly the presence of stabilizing organic material.

In summary, the sediments at the aforementioned locations appear to be a series of buried soils with specific features that outline the morphology. A highly weathered soil layer with kaolinitic-hematitic mineralogy must have been exposed at the surface for a significantly longer period of time than the overlying and subsequent layers. Horizons below the ultisol layer are not as weathered, implying that they were not exposed to the surface for a long period of time, supporting the idea that the overlying horizon was a soil, and not deposited material that was then buried and altered in place. The textures and mineralogy of the sediments support the conclusion that all of the examined layers are expected to have low permeabilities.

3.3.2. Soil Cores from the HR3-13 Area

In this section we discuss the pedological analysis of the cores obtained from holes HR3-13-1 and 4 which are located roughly 80 m away from the HAA-3AA cluster of holes. As with the previous cluster of holes, the soil profile is not complete because some subsurface horizons could not be sampled (and subsequently analyzed) due either to an excessively tight or to loose state of aggregation.

0-6.1 m (0-20 ft) A single core from 4.88 to 5.18 m (16 to 17 ft) was recovered from this section, and it appears to have similar mineralogy to the 5.5-m (18-ft) section of well HAA-3AA-1 to 4. There are fewer quartzite pebbles in this core, and no kaolinite present. Sample #15 was removed from this layer between 4.95 and 5.10 m (16.25 and 16.75 ft). The sample layer was described as a pebble rich sandy clay.

6.1-6.71 m (20-22 ft) At 6.1 m (20 ft) recovery of cores using shelby tubes was possible showing that the mineralogy and composition of the sediment was very similar to the overlying layers at 4.88-5.18 m (16-17 ft), but with more goethite present altering the color to a lighter brown-yellow hue. Sample #14 was taken at a depth of 6.17 to 6.32 m (20.25 to 20.75 ft) in a mixed hematite-goethite mineralogy with loamy sand texture tending to goethite conglomerate at the bottom of the sample.

6.71-7.32 m (22-24 ft) This layer appears to be in the capillary fringe above the water table where the transition from red sediments to yellow sediments occurs (~23 ft). Sample #13 was taken from a layer at a depth of 7.09 to 7.24 m (23.25 to 23.75 ft), where the texture was sandy clay, and although the layer was more lithified than the overlying one, it was wet and high in both hematite and goethite.

7.32-8.23 m (24-27 ft) This is a continuation of the transition layer in the capillary fringe, in which the goethite increases dramatically over 0.9 m (3 ft). Sample #12 was taken at a depth of 7.62

to 7.77 m (25 to 25.5 ft), in the center of this clay rich mixed mineralogy zone.

8.23-8.84 m (27-29 ft) At the bottom of the transition layer, 8.15 to 8.23 m (26.75 to 27 ft), there is a sharp transition to goethite-rich, yellow sediments with hematite and kaolinite mottling. It is a loamy clay with dense layers of kaolinite throughout the horizon, and smaller pockets of hematite. Sample #11 comes from a depth of 8.53 to 8.68 m (28 to 28.5 ft).

This core appears to correlate well with Wells HAA-3AA, but there is a discrepancy in the depth to the water table and the continuity of the sedimentary layers found in each of the two different sets of cores (HAA-3AA and HR3-13). What is apparent is that the sediments are of similar origin and composition. The discrepancy in the depth of the samples and the apparent height of the water table needs to be examined. The HR3-13 samples have a much sharper mineralogical transition ,which is indicative of a higher water table, but the depths measured by the corers may also be inaccurate.

3.3.3. Hydrologic Implications

The mottled colors exhibited by the sediments beneath the H Area retention basin are indicative of the presence of different forms of iron oxide. The reddish form is probably due to hematite (Fe_2O_3), which is the most stable of the Fe(III) oxides, and can form quite rapidly in the absence of organic matter at neutral pH. Its formation from other less stable oxides is also favored with increase in temperature. Yellowish colored forms are commonly indicative of microcrystalline goethite (FeOOH), color variation being due to variable crystallinity (when coarsely crystalline, goethite is a deep honey-yellow color.)

Goethite, although less stable than hematite, commonly persists in the natural environment, because it is believed that the adsorption of organic matter on its surface inhibits dissolution, which would otherwise allow it to precipitate as the more stable form. A brown rusty colored coloration is due to the presence of the least stable form of iron oxide, ferrihydrate, or hydrated ferric oxide. The formula is sometimes represented as $Fe(OH)_3$, but more recent work indicates that this is not strictly correct. This material is substantially amorphous, and persists only because of its limited solubility, the inhibitive effects of adsorption of organic species on its surface and through its participation in biogenic processes.

Aerobic bacteria require the presence of an electron acceptor to permit them to oxidize organic matter as a source of energy. To accomplish this, they release siderophores into the surrounding environment, powerful complexing agents for Fe(III) (and Pu(IV)). The siderophores solubilize ferric ions, which are then transported to the cell. The cell, in turn absorbs and uses them in coupled redox reactions in which organic matter is oxidized. Upon the death of the cell, the iron in either ferric or ferrous state is released to the environment, where it immediately oxidizes and precipitates as the amorphous hydrated ferric hydroxide. This form is

readily soluble in hydroxylamine hydrochloride solution and provides a measure of the adsorptive capacity of iron oxides in the soil or sediment, as it is presumed that its specific surface area greatly exceeds other forms of iron oxide.

If we assume that presently exposed Miocene sediments had undergone diagenesis, then most of the iron would have been stabilized as hematite. Subsequent exposure at the surface, and weathering under humid temperate ultisol conditions presently at SRS, is likely to result in the remobilization of the ferric iron by bacteria, through dissolution of hematite and the precipitation of less stable forms of ferric oxide. The rust staining, in contrast to the reddish hematite color, is therefore indicative of the penetration of groundwaters containing bacteria, organic matter and oxidants (probably dissolved oxygen).

The heterogeneous and irregular zones of rust colored clay and sand reveal the presence of past and present channel ways for groundwater migration. The variable coloration illustrates the underlying heterogeneity of hydraulic pathways through the soil and shallow sediments. It should be emphasized, however, that the coloration could be due to relic pathways, which may persist for thousands of years after the pathways become inactive.

3.4. Chemical Site Characterization

Colloidal silica and its stabilizing electrolyte have a tendency to react with soil constituents such as certain clays, organic compounds (e.g. humic acids) and carbonates. Necessary precautions must therefore be taken to characterize the chemical environment before injection, and interpret the chemical properties of the site in order to ensure that injection proceeds in a controlled and predictable manner. Characterization of the soil chemical environment is also of value in predicting the mobility of radionuclides in that environment.

As noted previously, the surficial sediments at the Savannah River Site, and particularly at the H Area Retention Basin, consist of poorly consolidated to unconsolidated discontinuous argillaceous sands and clay horizons. Analysis of soil samples from the site (see subsection 3.5.4) indicates that the dominant clay is kaolinite with minor quantities of vermiculite and traces of illite. Smectite does not appear to be present. The surficial soils and sediments therefore appear to be representative of temperate ultisol development. Ultisols are characterized by subsurface horizons of kaolinitic clay accumulation and a low basic cation supply. The soils are usually moist for most of the year, particularly during the growing season. They form through the progressive leaching of exchangeable cations in clays by acid groundwater containing organic acids formed from the abundance of vegetation and the accumulation of forest litter.

3.4.1. Groundwater Chemical Characterization

A comprehensive sampling program of waters from monitoring wells at the Savannah River Site confirms that the ground waters are generally acid in composition with pH values ranging from 4.2 to 6.5 [*Kuelske*, 1996]. A typical water sample from Well HAA-3D, collected on March 7, 1995, indicates that the total dissolved solids content is very low (TDS = 105 ppm). The depth of the water below the well collar was 5.8 ft., suggesting that the water should be representative of shallow groundwaters in the region. Data from this chemical analysis was adapted to an input file for the distribution-of-species code, EQ3, version 7.0 [*Wolery*, 1992] as shown in **Table 3.1.** Major species are listed, together with species that participate in reactions involving precipitation or dissolution of soil minerals, e.g. Al, Fe(III) and SiO_2(aq).

A preliminary evaluation of the data indicated that the charge imbalance was significant, about 30 %, which is not unusual for extremely dilute solutions, as is the case for the present analysis, the most likely cause being a discrepancy in pH caused by the degassing of carbon dioxide from the sample between sampling and analysis. Although this interpretation is reasonable and consistent with an ultisol environment, it would require further evaluation to prove its validity. However, the charge imbalance was corrected through addition of HCO_3^-.

Table 3.1. Partial Chemical Analysis of Groundwater from Well HAA-3D (pH=6.2, T = 18 °C)

Constituent	Concentration (mg/L)	Constituent	Concentration (mg/L)
Na	16.1	Fe(II)	Assumed trace
K	1.07	Mn	0.0098
Ca	4.97	SO_4	6.98
Mg	0.674	Cl	5.03
Al	Assumed saturation with kaolinite	NO_3	2.436
F	Assumed trace	HCO_3	34.0
Fe(III)	0.164	SiO_2 (aq)	7.47
TDS	105		

The measured aluminum concentration in the water was also excessively high for waters in equilibrium with kaolinite, the dominant aluminosilicate in the soil at the site. This may be due to the presence of aluminum bearing colloids, or to aluminum complexing with organic compounds in the water, or to both, as is discussed further below. However, it should be noted that the analyzed concentration of total organic carbon in the well water was only 0.523 mg/L. The distribution of species in the groundwater, calculated using EQ3 is given in **Table 3.2.**

The partial pressure of $CO_2 = 10^{-1.6}$ atm in the water is almost two orders of magnitude higher than is found in the atmosphere, and is due to the presence of a considerable concentration of carbonic acid. Although a portion might be attributed as an artifice of the charge balancing procedure, the groundwater has probably evolved as the result of the bacterial oxidation of decaying organic matter, and is probably responsible for the recycling of ferric iron from a hematitic form to the less stable ferrihydrate as suggested by the color differences in the various soil horizons. This suggests, but does not prove, that the mottling of the clay horizons observed in drill cores from the H Area may be a reflection of the differential movement of surficial acid oxidizing waters percolating through a variably permeable vadose zone and accumulating in permeable horizons below the water table.

The EQ3 code also calculates the saturation indices (SI = log(Q/K)) of all minerals containing the aqueous components incorporated in the initial analysis used in the input file. **Table 3.3** lists the saturation indices of those minerals that have been identified in mineral analyses of SRS soils, or are suspected or could be present in such soils.

The groundwater is intermediate in saturation with respect to α–cristobalite and quartz, which is reasonable for a soil mineral composition consisting dominantly of quartz and kaolinite. However, the high levels of supersaturation of iron and manganese oxides suggest that the chemical analyses for Fe and Mn might have been affected either by the presence of colloids of the oxides and/or complexing of these metals with organic compounds in the groundwater.

As noted above, the aluminum analysis of 0.256 mg/L may similarly reflect the presence of colloids and/or organic complexing agents. Given the ubiquitous occurrence of detrital organic leaf-fall material overlying ultisol profiles, and the acidic conditions generated by organic acids and carbonic acid, which could be favorable for the formation and stabilization of colloids, it is perhaps reasonable to conclude that the anomalously high Al, Fe(III) and Mn analyses can be attributed to colloid formation or organic complexation, but this remains to be proven. Evidence for the existence of organic contamination from the overlying vegetation in soil horizons between 5 and 10 ft. and 10 and 20 ft. respectively, is given in a subsequent section. However, as noted above, the actual total concentration of organic carbon in the well water was quite low (only about 0.5 mg/L), suggesting that colloids predominate.

Table 3.2. Calculated Speciation at T = 18 °C

Species	Concentration (*M*)	Species	Concentration (*M*)
CO_2 (aq)	1.058×10^{-3}	$Fe(OH)_2^+$	2.725×10^{-5}
HCO_3^-	7.054×10^{-4}	$Fe(OH)_3$ (aq)	1.431×10^{-6}
Na^+	6.994×10^{-4}	$CaHCO_3^-$	8.250×10^{-7}
Cl^-	1.419×10^{-4}	$CaSO_4$ (aq)	7.913×10^{-7}
SiO_2 (aq)	1.243×10^{-4}	$NaHCO_3$ (aq)	7.426×10^{-7}
Ca^{++}	1.224×10^{-4}	H^+	6.552×10^{-7}
SO_4^{--}-	7.128×10^{-5}	$MgSO_4$ (aq)	3.065×10^{-7}
NO_4^--	3.926×10^{-5}	$NaSO_4^-$	2.706×10^{-7}
K^+	2.736×10^{-5}	$MgHCO_3^+$	1.788×10^{-7}
Mg^{++}	2.725×10^{-5}	Mn^{++}	1.754×10^{-7}

Measured Al (mg/L)	0.254
Calculated Al (mg/L)	0.000008
Measured HCO_3^-(mg/L)	34.0
Calculated HCO_3^-(mg/L)	43.03
Redox State (Eh)	0.791 Volts
Soil PCO_2	2,562.9 Pa (0.0253 atm)
Atmospheric PCO_2	33.4 Pa (0.00033 atm)

Table 3.3. Calculated Mineral Saturation Indices (SI)			
Mineral	**SI**	**Mineral**	**SI**
α-cristobalite	-0.322	Goethite	5.533
Gibbsite	-0.466	Illite	-2.941
Hematite	12.006	Kaolinite	0.000 (specified)
Manganite	-0.469	Pyrolusite	2.813
MnO_2 (aq)	1.237	Quartz	0.244
Todorokite	6.669		

3.4.2. Soil Chemical Characterization

In order to characterize the interaction of soils and groundwaters, representative samples from the soil horizons targeted for CS injection should be characterized in terms of their physical and chemical properties. The resulting data can then be reconciled through modeling and testing using independent checks.

The two soil samples S1 and S2 taken from a back-hoe cut trench in the vicinity of the H-Retention Basin (see subsection 3.2.2) were homogenized from intervals at 1.5-3.0 m (5-10 ft) and 3.0-6.1 m (10-20 ft) respectively, and analyzed for the following:

- Chemical analysis of major cations and anions in the soil saturation extract (i.e. Na, K, Mg, Ca, Sr, NH_4, Al, SO_4, Cl, NO_3, PO_4), SiO_2(aq), alkalinity, pH and electrical conductivity
- Total cation exchange capacity (meq/100g)
- Exchangeable cations (H^+, Na, K, Mg, Ca, Sr, NH_4, Al)
- Soil pH

The information is summarized in **Tables 3.4** and **3.5**

Groundwater samples should also be collected from the same horizons as those of the soil samples, and analyzed for the same chemical constituents as the soil saturation extract noted above. The temperature of the soil horizon at the time of sampling should also be noted. In the absence of such data, reliance must be placed on extant data collected nearby, as is the case with chemical analyses reported from Well HAA-3D, noted above. A comparison of the groundwater composition (**Table 3.1**) with the soil saturation extracts in **Tables 3.4** and **3.5** shows that the chemical compositions are essentially similar where comparisons with individual constituents can be made.

Table 3.4. Soil Analysis of the S1 Soil			
Exchangeable Cations (ppm)			
Sodium	70	Strontium	0.9
Potassium	54	Ammoniacal Nitrogen	<39
Magnesium	30	Aluminum	0.4
Calcium	510		
Cation Exchange Capacity		**43 meq/100 g**	
Soluble (Soil Saturation) Extract (ppm)			
Bicarbinate alkalinity	17	Strontium	0.11
Carbonate alkalinity	<1	Ammoniacal nitrogen	<39
Hydroxide alkalinity	<1	Sulfate	110
Calcium	43	Chloride	8.8
Magnesium	3.3	Nitrate	<2
Sodium	4.9	Phosphate	<2
Potassium	4.8	Silica	3.3
pH		6.8	
Electrical conductivity		0.32 mmho/cm	

Table 3.5. Soil Analysis of the S2 Soil			
Exchangeable Cations (ppm)			
Sodium	77	Strontium	0.6
Potassium	45	Ammoniacal Nitrogen	<39
Magnesium	32	Aluminum	0.4
Calcium	85		
Cation Exchange Capacity		**72 meq/100 g**	
Soluble (Soil Saturation) Extract (ppm)			
Bicarbinate alkalinity	11	Strontium	<0.08
Carbonate alkalinity	<1	Ammoniacal nitrogen	<39
Hydroxide alkalinity	<1	Sulfate	4.7
Calcium	2	Chloride	9.2
Magnesium	0.74	Nitrate	<2
Sodium	5.4	Phosphate	<2
Potassium	5.5	Silica	7
pH		5.4	
Electrical conductivity		0.071 mmho/cm	

A comparison of the S1 and S2 soils in **Tables 3.4** and **3.5** shows that they are essentially similar. The most obvious difference is in exchangeable Ca (510 ppm in soil S1 vs. 85 ppm in soil S2) and soluble Ca (43 ppm vs 2 ppm). The reason for the the higher Ca concentration and higher pH of the S1 soil is not obvious.

The chemical analyses can be reconciled using ECHEM [*Morrey*, 1988], a computer code developed at Pacific Northwest Laboratories from an earlier distribution of species code, MINTEQ. The EQ3 code cannot be used, as the present version does not contain algorithms for calculating ion exchange on clays or sorption on iron oxy-hydroxides. The procedure for evaluating the data is as follows:

(a) The soil saturation extract is checked for charge balance, and the pH, alkalinity and electrical neutrality reconciled using ECHEM. Saturation indices of those mineral phases observed to be present from the mineralogical characterization will be calculated. In general they should be in the region of zero

(b) A similar exercise is conducted on groundwater analyses from the same soil horizon as the soil saturation extract. The results of the soil saturation extract and groundwater should be comparable, although some deviations are permissible. Thus, for example, the soil saturation extract may not have fully reached equilibrium with respect to the soil minerals. In contrast, the groundwater should normally be close to saturation with respect to most clay minerals.

(c) The total exchange capacity of the soil should be reconcilable with the total of exchangeable cations and the calculated exchange capacity of the clays as determined from the mineralogical analysis. Some discrepancies might be expected if the soil contains significant concentrations of carbonates or gypsum, but this is not expected to be the case for soils beneath the H Area Retention Basin. These calculations are performed using ECHEM.

(d) The measured distribution of exchangeable cations should be the same as that predicted by the ECHEM code.

(e) The analysis of hydroxylamine HCL extractable iron is used to calculate the **H**ydrated **F**erric **O**xide (HFO) adsorption sites on the soil, and hence the concentration of adsorbed cations and anions and their distribution between the soils and the aqueous phase. These calculations are again performed using ECHEM.

3.4.3. Total Organic Carbon (TOC) Analyses

The TOC measurements in **Table 3.5** indicate that the TOC of the S1 soil is 2,160 mg/kg, significantly higher than the TOC of the S2 soil (372 mg/kg). This was expected because of the shallower origin of the S1 soil. **Table 3.6** also shows the TOC in the solids and the water of sludge similar to the one at the bottom of the 281-3H basin.

Table 3.6. TOC of Soils at the H-Area Basin		
Sample	**Analysis**	**TOC (mg/kg)**
S1 Soil	EPA 9060	2160
S2 Soil	EPA 9060	372
Sludge	EPA 9060	12,600
Sludge water	EPA 415.1	49

The TOC in the sludge is 12,600 mg/kg, while the sludge water TOC is an exceptionally high 49 mg/kg. The relative TOC values substantiates our hypothesis that organics could retard the CS gelation (see Section 5). Increasing amounts of TOC correspond to longer gel-times.

3.5. Hydrologic Characterization

3.5.1. Data Requirements

The importance of relevant and accurate data on the hydraulic properties of the soils at the site of the basin cannot be overemphasized. Such data are necessary for the development of the design package, and must include

- a conceptual hydrogeologic model of the 281-3H retention basin area, as well as hard data on
- *in situ* permeability,
- porosity,
- capillarity, and
- heterogeneity.

This information represents the **absolute minimum** requirement, and deficiencies would in essence preclude any reasonable or responsible design. This information is positively indispensable for

(a) clarifying the hydrogeologic conditions that are responsible for the ponding of water at the basin and the strong observed sensitivity of the water level to rainfall events,

(b) identifying a target horizon for barrier emplacement and determining its continuity,

(c) understanding the distribution of heterogeneity of hydraulic properties over the target isolation area,

(d) developing a flexible strategy (and a work plan) for barrier emplacement, which can cope with variable water saturation regimes and different-scale heterogeneity conditions.

3.5.2. Data Availability and Evaluation

The information available on the basin hydrology at the beginning of this study was rather limited and did not satisfy the minimum requirements of the design for the barrier installation. That information included the following:

(a) An indirect textural analysis of the soil in the immediate vicinity of the basin, based on empirical correlations between Cone Penetrometer (CPT) tip resistance and soil texture.

(b) Some geological information on the site developed within the context of a geostatistical assessment of the seismic performance of soils in the same general area of the basin.

(c) Water level data from wells located near the boundaries of the retention basin, as well as inferred water level distributions based on these measurements. Based on these data, the groundwater table is shallow, i.e.78.6 to 81.1 m (258 to 266 ft) above MSL, where the soil surface elevation is 83.2 m (273 ft). It also varies seasonally between 1.5 m and 3.7 m (5 and 12 ft) from the surface. Rainfall in that area averages 1140 mm/year (45 in/year).

This information, while useful, was insufficient for the design of the barrier emplacement for the following reasons:

(a) Very limited quantitative data on the important parameters (discussed in item 1) were available. Based on in the H-Area Treatability Study [*WSRC*, 1996], hydraulic conductivity data for the existing soil around and below the basin are not known, but are expected to be in the range of 10^{-6} m/sec and $5x10^{-6}$ m/sec. There was no supporting documentation. This range was considered in the LBNL design calculations, and was shown to be at or above the feasibility limit for field injection (see Section 4). Permeabilities below this level are technically feasible but impractical because of the excessive injection times required.

(b) Examination of the Shelby tube and split-spoon cores did not confirm the CPT-deduced soil texture. This was probably due to insufficient resolution of the CPT measurements and/or an imperfect theoretical or empirical relationship between tip resistance and soil texture.

(c) The geostatistical assessment of seismic performance was of limited usefulness, because it was not based on data from the immediate vicinity of the basin.

(d) The inferred water table elevation could not be supported by the water levels observed in the soil cores (Shelby tubes and split-spoon samples) available to LBNL, which placed the water level significantly lower than what previous data would suggest. More specifically, evidence from (i) the well behavior at a well completed in the zone of interest, (ii) the saturation distribution of the soil cores and (iii) chemical evidence (oxidation states of Fe) tended to support the thesis that

- the water bearing horizon closest to the surface was confined or semi-confined, with the piezometric head varying between 1.5 to 4 m (5 to 13 ft) from the surface,
- the top of the water-saturated formation (in a sense, the watertable) was 7.9-8.5 m (26-28 ft) from the original soil surface,
- it was rather stable at this level,
- the subsurface had a relatively thick unsaturated zone of 7.6-9.1 m (25-30 ft).

This impression was supported by a recent report [*Hasbrouck et al.*, 1996] which placed the water level at a depth of ~10.7 m (~35 ft) from the surface in the same formation at the adjacent F-area of the SRS.

(5) There is an indication that the water level fluctuations in the basin are much more pronounced after rainfall events than what the amount of rainfall would suggest. A possible explanation is that the fluctuation was caused by the gravel bed on which the abandoned inlet pipe to the basin rests, which may act as a collector and a conduit channeling water into the basin.

Another possibility involves the presence of a conductive pathway between the basin bottom and the underlying shallow confined aquifer, in which case the water level fluctuations in the basin could be significantly influenced by changes in the piezometric head. Such a scenario is supported by geochemical evidence (see Section 4), which indicates that young water (rich in organic acids) could reach the groundwater relatively quickly through highly permeable pathways. There is, however, no hard evidence to support these theses.

3.5.3. Permeability Analyses

The permeability distributions of the soils at the 281-3H basin site are determined from

- analysis of 44 soil samples from the Shelby tube and split-spoon cores, and more importantly

- hydraulic data from a water injection test in the immediate vicinity of the 281-3H basin (see Section 7).

Hydraulic conductivity measurements were conducted on 44 representative sections selected from the site soil cores available to LBNL and appropriately prepared. The laboratory measurements of horizontal and vertical hydraulic conductivity are presented in **Tables 3.7** through **3.9**. Note that the reported depths are approximate due to depth-calibration uncertainties during coring. The split-spoon samples seem to be considerably less permeable than the Shelby tube samples, a difference which may be due to differences in the degree of soil disturbance caused by the two sampling techniques (split-spoon sampling disturbs the soil considerably more).

Based on the permeability data in **Tables 3.7** through **3.9**, the preliminary conclusion was that while the majority of the soil matrix appeared to have low permeability, there was an indication of thin zones (less than 0.15 in thickness) with locally higher permeability which could support CS permeation grouting.

Although these data are extremely valuable, they cannot accurately describe the subsurface conditions because (a) they may include significant distortions due to the soil disturbance during the coring process, (b) they represent point data and (b) they are based on an incomplete data set, as no sample recovery was possible in some sections because of the presence of very friable or indurated soils. The laboratory analysis only provides an estimate, as the cores are disturbed, permeability is known to be scale-dependent, and permeability measured in the laboratory is known to deviate from the *in situ* values. Therefore, because of the significant uncertainties discussed above, the permeability information from the tables is insufficient for the design of the barrier system.

The most accurate and relevant information can be obtained only from the *in situ* injection test. The pilot injection test provides the most representative information on the *in-situ* hydraulic properties, as well as some indication on the spatial heterogeneity of the site. The results of the water injection test, their importance and the corresponding implications are discussed in detail in Section 7.

A useful set of figures has been developed, which relates laboratory hydraulic conductivity measurements to soil textures (based on Shelby tube cores from the site), and which includes a narrative of the geological, pedological, and geochemical analysis of the cores. This set can be found in the Appendix.

Table 3.7. Laboratory Hydraulic Conductivity Measurements from Shelby Tube Samples at the HAA-3AA Location

Sample Depth From Furface (ft)	Sample No.	Horizontal Hydraulic Conductivity (m/sec)	Vertical Hydraulic Conductivity (m/sec)
5-5.5	10	4.3×10^{-7}	1.2×10^{-5}
15.0-15.5	9	2.4×10^{-6}	2.8×10^{-6}
16.5-17.0	8	4.9×10^{-7}	4.8×10^{-7}
24.5-25.0	7	Not testable	Not testable
25.0-25.5	6	Not testable	Not testable
25.8-26.3	5	1.2×10^{-8}	1.5×10^{-8}
27-27.5	4	9.5×10^{-9}	1.2×10^{-5}
28.2-28.5	3	2.6×10^{-8}	1.1×10^{-8}
29.5-30.0	2	1.7×10^{-6}	7.2×10^{-7}
30.0-30.5	1	6.0×10^{-8}	4.7×10^{-8}

Table 3.8. Laboratory Hydraulic Conductivity Measurements from Shelby Tube Samples at the HR3-13 Location

Sample Depth From Furface (ft)	Sample No.	Horizontal Hydraulic Conductivity (m/sec)	Vertical Hydraulic Conductivity (m/sec)
16.2-16.6	15	2.5×10^{-7}	1.2×10^{-7}
20.2-20.6	14	2.2×10^{-7}	1.7×10^{-8}
23.2-23.7	13	8.9×10^{-7}	1.5×10^{-7}
25.0-25.5	12	1.6×10^{-7}	7.2×10^{-9}
27.7-28.2	11	1.3×10^{-8}	5.0×10^{-8}

Table 3.9. Laboratory Hydraulic Conductivity Measurements from Split-Spoon Samples

Sample Borehole	Sample Depth From Surface (ft)	Sample No.	Hydraulic Conductivity (m/sec)
HAA-3AA-1	15-15.7	A1	2.2×10^{-8}
HAA-3AA-1	17.0-17.3	A2	2.9×10^{-7}
HAA-3AA-1	21.0-21.3	A3	4.7×10^{-9}
HAA-3AA-1	23.5-24.0	A4	3.5×10^{-9}
HAA-3AA-2	10.7-10.8	B1	1.5×10^{-8}
HAA-3AA-2	14.7-15.1	B2	1.6×10^{-9}
HAA-3AA-2	16.0-16.8	B3	1.6×10^{-8}
HAA-3AA-2	20.0-20.5	B4	3.3×10^{-9}
HAA-3AA-2	20.8-21.3	B5	3.3×10^{-9}
HAA-3AA-2	22.8-23.4	B6	4.5×10^{-9}
HR3-13	16.9-17.5	C1	1.5×10^{-8}
HR3-13	19.2-19.7	C2	8.1×10^{-9}
HR3-13	20.7-21.0	C3	6.7×10^{-8}
HR3-13	25.0-25.4	C4	1.1×10^{-8}

3.5.4. Soil Particle Size and Mineralogic Analysis

The particle size analysis given in **Table 3.10** covers the S1 and S2 soils, as well the Shelby-tube and split spoon soil samples used in the permeability analysis. The sample numbers in the first column of **Table 3.10** refer to the corresponding sample numbers identified in **Tables 3.7** through **3.9**.

The particle size analysis confirmed previous qualitative observations (based on feel, appearance, and permeability measurements) regarding the high content of fines (silt and clays) in the soils, which exceeded (with one exception) 20wt% and could be as high as 45wt%. The very poor sorting of the soils were indicative of low permeability, and the permeability analyses confirmed this observation.

A related mineralogic analysis of S2 soil [*Altaner*, 1996] showed the following composition: 28wt% kaolinitic clay, 60wt% quartz, 6wt% goethite and 6wt% hematite. The clay mineralogy analysis (<2 mm size fraction) showed 99% kaolinite and 1% vermiculite.

3.6. Contaminant Characterization

Detailed characterization of the contamination and its distribution at the Basin 281-3H area is currently unavailable. This information is important in establishing the baseline conditions, which will provide the basic criterion for the evaluation of the barrier performance.

Existing information is limited to discussion of chemical analyses of samples from a number of locations within the pond and the soil pile, and is listed in *Kuelske* [1995]. The 281-3H basin is contaminated mainly with radionuclides. Of particular concern are ^{137}Cs, ^{90}Sr, and ^{238}Pu, with maximum concentrations of 33000, 7000 and 238 pCi/g respectively, as well as a total of 139215 pCi/g of non-volatile beta-emitters. These figures provide some indication of the conditions to be expected, but are insufficiently informative since they do not discuss distribution with depth.

The proposed sampling activities listed in the *WSRC* [1994] report report are expected to alleviate this significant knowledge gap and to provide sufficient information about the extent and distribution of contamination.

According to the Treatability Study (TS), samples from the soil pile and surrounding contaminated areas indicate a total radionuclide inventory possibly as high as 200 Ci. This figure is 20 times higher than the previously quoted level (handout circulated during the 2/1/1996 project meeting) on which the original design had been based. This higher radioactivity level has a significant impact on the barrier design (see Section 4), and necessitates an accurate inventory of radioactivity to resolve this uncertainty.

Table 3.10. Particle Size Analysis of Soils at the H-Area Basin

Sample No.	Particle Size (wt%)				Soil Texture	ϕ %
	>1mm	Sand	Silt	Clay	Classification	
S1	38.65	59.72	8.29	31.99	sandy clay loam	
S2	40.14	59.72	8.92	31.36	sandy clay loam	
1	13.17	79.97	11.28	8.75	loamy sand	45
2	15.30	85.00	6.25	8.75	loamy sand	39
3	20.63	67.50	15.23	17.27	sandy loam	38
4	54.91	79.99	11.26	8.75	loamy sand	40
5	20.93	73.63	11.91	14.46	sandy loam	45
8	10.33	59.58	21.91	18.51	sandy loam	44
9	18.60	54.50	20.50	25.00	sandy clay loam	47
10	31.37	58.75	13.75	27.50	sandy loam	38
12	16.44	73.52	13.98	12.50	sandy loam	44
13	17.30	83.64	6.36	10.00	loamy sand	39
14	50.09	62.25	12.75	25.00	sandy clay loam	41
15	42.67	67.50	12.50	20.00	sandy clay loam	42
A1	30.98	25.83	25.64	48.53	clay	48
A2	26.98	68.32	12.72	18.97	sandy loam	35
C4	6.77	72.56	11.59	15.85	sandy loam	42
C3	45.27	65.00	12.64	22.36	sandy clay loam	38
B4	18.95	64.79	13.32	21.89	sandy clay loam	42
B2	7.61	56.16	20.95	22.89	sandy clay loam	41
B1	19.31	70.06	11.19	18.75	sandy loam	38
A4	62.25	59.90	12.91	27.20	sandy clay loam	40

3.7. Foreign Bodies in the Basin

Foreign bodies in the pond area include units of rip-rap in the inlet and outfall, concrete outfall structures and asphalt pieces from the adjacent waste pile. Also present are a ditch and graveled areas. The asphalt pieces could be dispersed throughout the basin area. The rip-rap will be broken up and left in place. A number of subsurface pipes in the area of the basin will also be removed.

Reinforced concrete structures at the outlet of the pond will remain in place. The most significant implication for lance grout injection is the chance of hitting a foreign body with the lances. The lance injection system will undoubtedly be unable to force the lance past a direct hit with such foreign bodies.

In order to address this potential problem, a drill rig will be situated on site to replace the lance system when required. Should a foreign body be encountered, the lance will be removed and a drill of a slightly smaller diameter lowered into the hole to drill through the obstruction. Once the obstruction is cleared, the drill will be removed and the lance reinserted to continue lance penetration. Necessary precautions will be required to deal with drilling debris.

4. BARRIER SPECIFICATIONS

In this section we discuss the barrier concept, geometry, specifications, and related requirements. The lance injection technology is presented in detail, and functional requirements are determined. The injection patterns, as influenced by the saturation conditions of the subsurface, are analyzed. Some baseline calculations and numerical simulations are conducted to determine the effect of soil conditions and properties on the injection pressure and flow rates.

4.1. Design Parameters, Issues, Implications and Requirements

(a) At the beginning of the barrier operations, the basin will be filled to grade (or slightly above grade) with contaminated soils and overlaid with 2 ft of clean soil.

(b) The footprint of the basin is about 67 m by 46 m (220 ft by 150 ft). The barrier footprint will be 76 m by 46 m (250 ft by 150 ft), because the area between the edge of the pond and the western boundary with basin 281-8H will be covered. CS injections will start at a depth ranging from 0.6 m (2 ft) from the surface at the barrier walls to 1.5 m (5 ft) within the basin.

(c) This barrier isolates all potential sources of contamination down to a depth of 6.1 m (20 ft) from the original soil surface.

(d) The composite barrier to be installed will seal all the permeable zones to a depth of 6.1 m (20 ft) and will incorporate

- a minimum of 0.9 m (3 ft) and a maximum of 1.2 m (4 ft) of cumulative thickness of grouted horizons, coupled with (and complementing)
- the naturally very low permeability soil horizons at the basin site.

(e) The top of the barrier will seal the bottom of the basin where the most contaminated materials will be located (*in situ* sludge and contaminated soils moved from outside the basin) and where the hydraulic conductivity will be the highest (expected to exceed 10^{-5} m/sec) due to incomplete soil consolidation. The top 0.3 to 0.6 m (1 to 2 ft) of the barrier will be inside the basin; the barrier will continue downward below the current bottom of the basin.

(f) The area between the west boundary of the basin and the fence to the adjacent basin 281-8H (i.e. the area where the soil pile is currently situated) will be completely grouted to a depth of 6.1 m (20 ft) from grade.

(g) The inlet and outlet pipes and the underlying sand and gravel beds will be grouted over a distance of at least 15.2 m (50 ft).

(h) The walls of the barrier inside the basin will range in thickness from 0.6 to 3 m (2 to 10 ft).

(i) The amount of CS to be injected depends on the soil porosity and permeability, and is expected to range between 0.91M and 2.15M kg (2M and 4.7 M lbs).

(j) Injections will proceed on a regular grid, and will involve

- a primary (first pass) injection for the emplacement of the bulk of the CS and
- a secondary (second pass) injection to seal the unfilled pore space remaining after the primary injection. Upon testing the barrier integrity, more localized *touch-up* injections may be needed.

Grid spacing of both the primary and secondary injections will vary between 0.6 and 1.5 m (2 and 5 ft). The secondary injection grid will be offset from the primary and located at the centers of the primary injection grid. The water injection test (see Section 7) was expected to provide information leading to a more accurate estimate of the grid spacing.

(k) Lance injection technology will be used for the barrier emplacement. Commercially available lance injection technology will be used. The truck-mounted lancing system must be able to deliver a minimum force of 6,740 N (15,000 lbs). More than one lance system operating simultaneously might be needed.

(l) Mixing equipment capable of mixing the grout components in line and at variable volumetric ratios will be needed. The injection system must be clean and free of any lime contamination. The CS residence time in the injection system should not exceed 30 minutes. Equipment for mixing CS and a fine sand to a slurry for backfilling the lance holes during lance withdrawal will also be needed.

(m) The lance injection system will be instrumented with tip resistance sensors, pressure transducers and flow meters, as well as with data acquisition systems.

(n) Baseline calculations and numerical simulations are conducted to determine the effect of soil conditions and properties on the injection pressure and flow rates (see subsection 4.5). Maximum injection pressures will be determined based on the results of the water injection test.

4.2. Barrier Geometry

4.2.1. Basin Dimensions

Figure 4.1 is a map of retention basin 281-3H. **Figure 4.2** is a cross-section of the basin at the beginning of the barrier emplacement. The soil pile (i.e. the most contaminated soil) is first placed at the bottom of the basin and is distributed as uniformly as possible. The top 2 ft of the soil of the area within the basin fence are then stripped and placed in the basin. It is expected that the volume of the contaminated soil will equal or slightly exceed the basin capacity. The contaminated soil will then be covered with 2 ft of clean soil (fill) to provide the necessary protection for the barrier emplacement operations.

The original basin dimensions were 61 m by 36.6 m by 1.8-2.4 m (200 ft by 120 ft by 6-8 ft). Because of bank erosion, the current basin dimensions have increased to 67 m by 46 m (220 ft by 150 ft). The current basin depth, however, is unknown. After draining the pond, the original and current basin boundaries will be delineated (and marked) and a topographic study of its depth will be conducted.

4.2.2. Barrier Conceptual Model

The basic barrier geometry is shown in **Figures 1.1** and **1.2**. For the needs of the basin 281-3H, however, a safer alternative barrier design is proposed. This concept is shown in **Figure 4.3**, and involves the creation of a compound barrier system that seals all the permeable zones to a depth of 20 ft and incorporates

- a minimum of 0.9 m (3 ft) and a maximum of 1.2 m (4 ft) cumulative thickness of grouted horizons, coupled with (and complementing)
- the naturally very low permeability of soil horizons at the basin site.

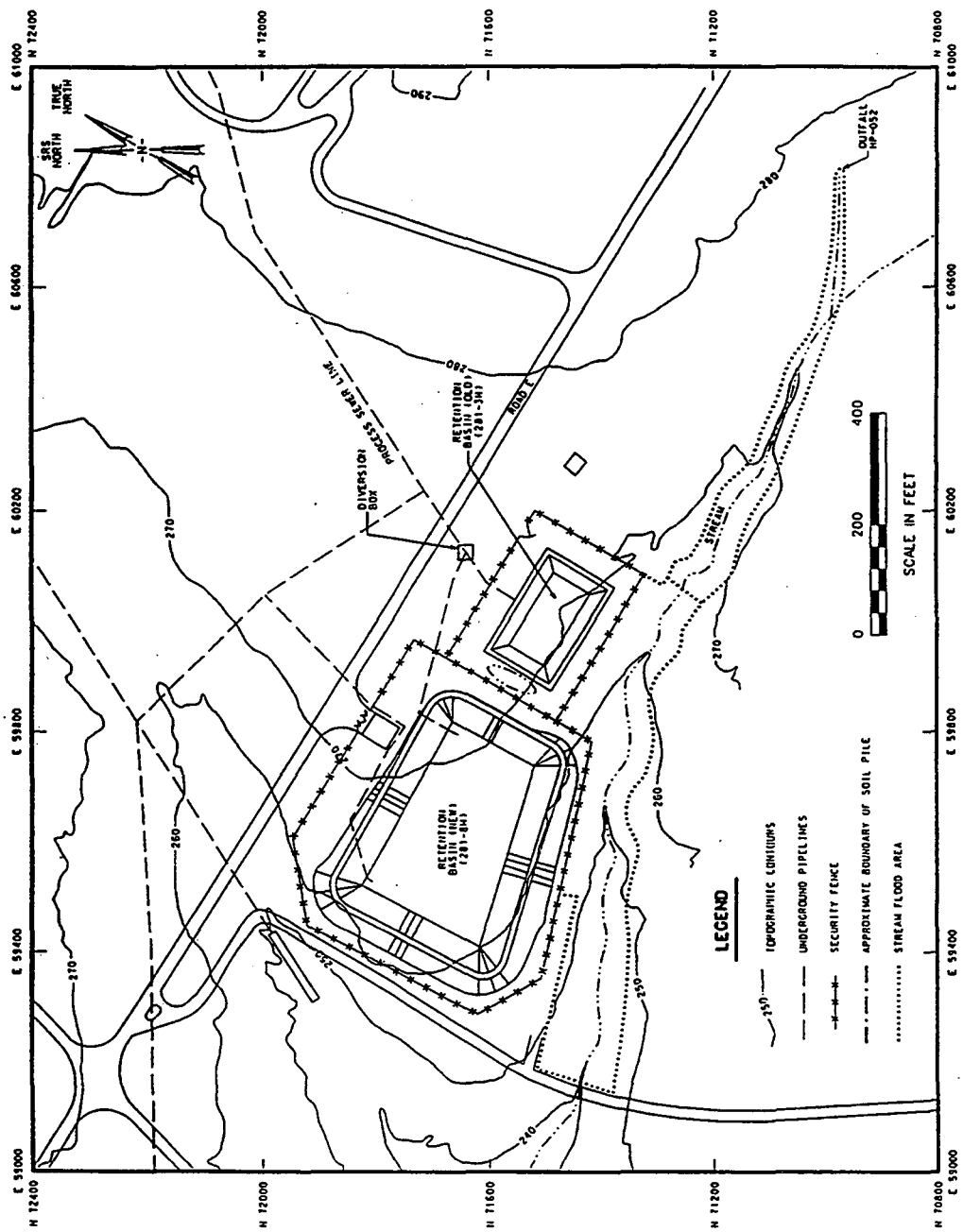

Figure 4.1. Map of H-Area Retention Basin (281-3H).

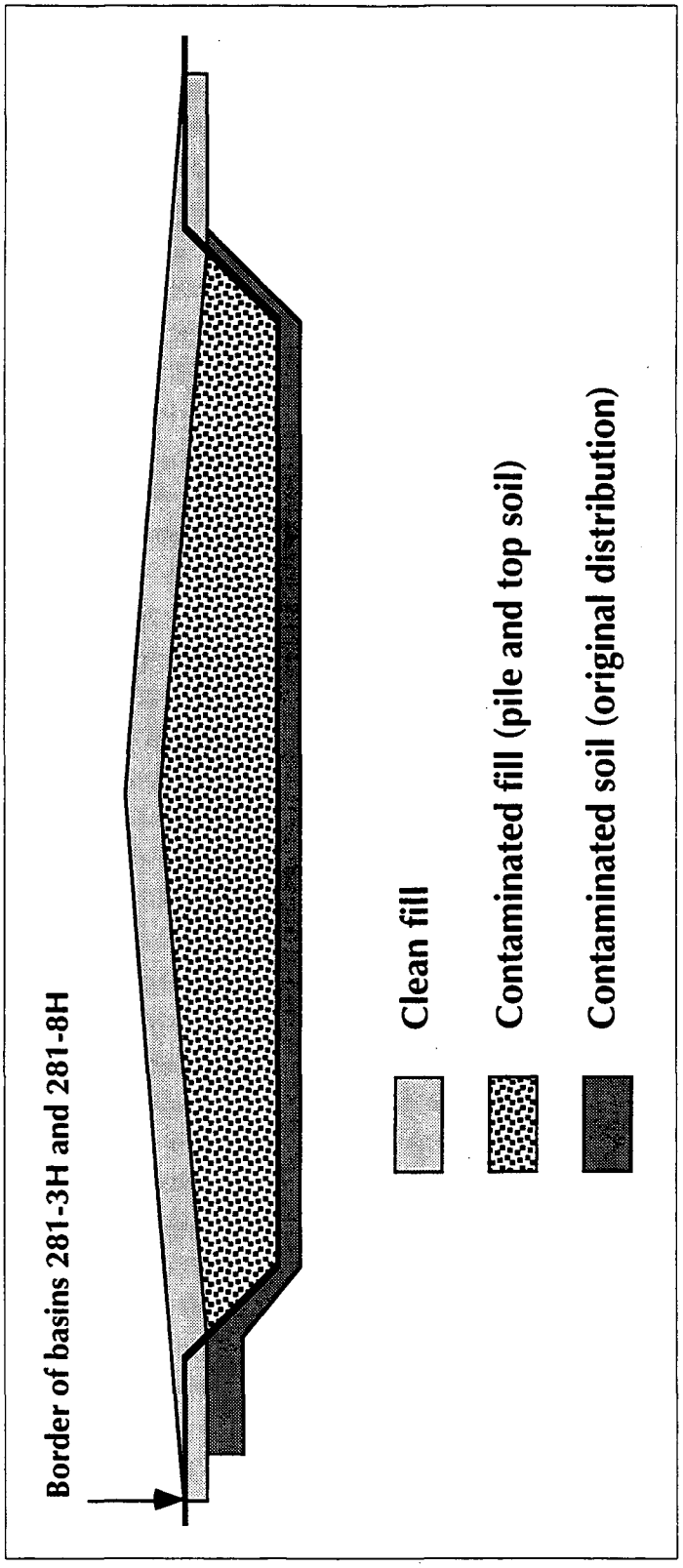

Figure 4.2. A schematic of the basin immediately before the barrier emplacement.

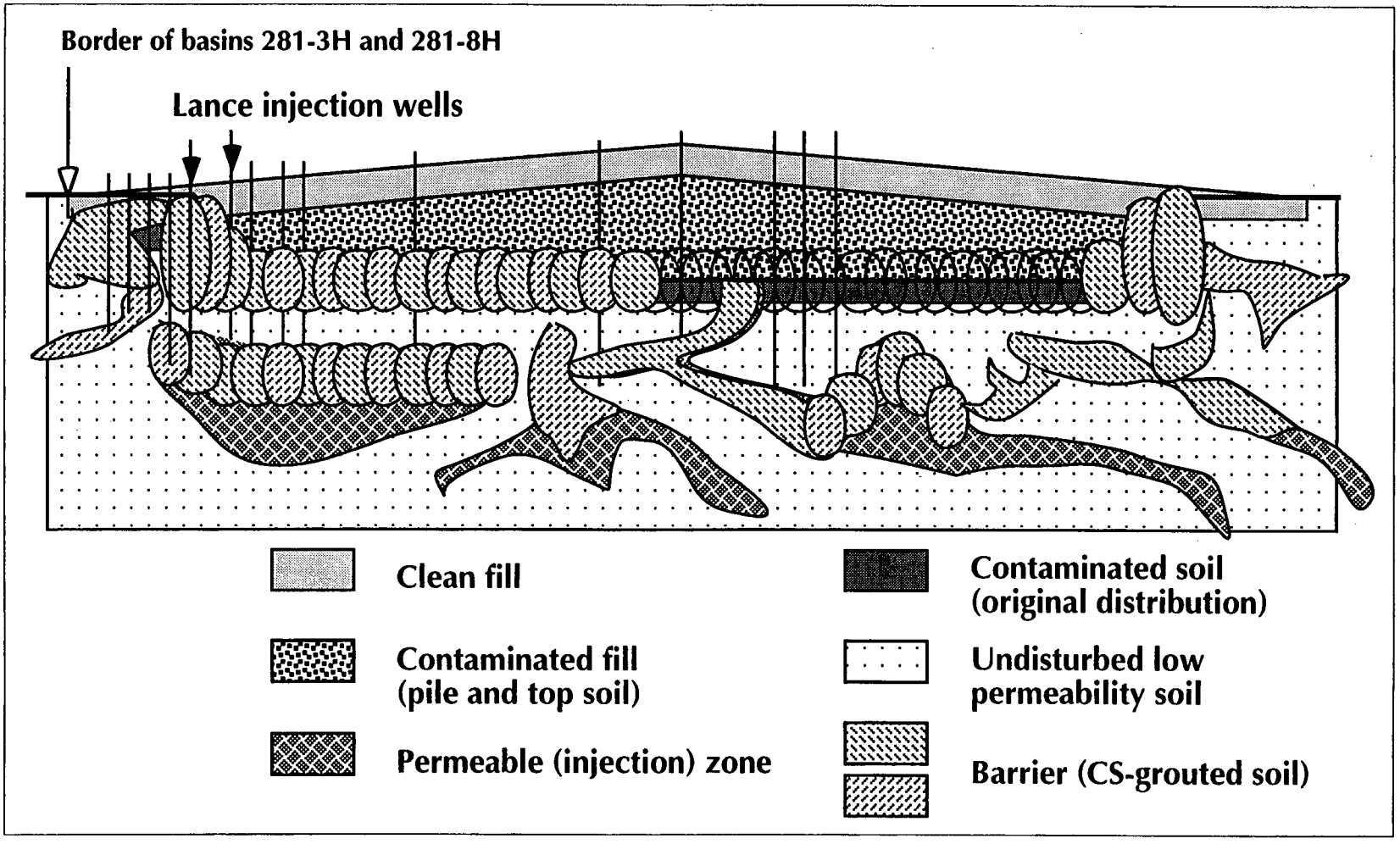

Figure 4.3. Conceptual model of the barrier to be emplaced at the retention basin 281-3H.

This design provides a needed additional level of safety and protection and isolation of all potential primary and secondary sources of contamination to a depth of 6.1 m (20 ft) from current grade. The primary sources are the contaminated soils inside the sealed basin, and the secondary sources are created by contaminants outside the basin. An examination of the Shelby tube soil data (see Section 3) indicates that acceptable permeable zones in the soil profile to a depth of 6.1 m (20 ft) are rather few and quite thin. Emplacement of this barrier in essence involves injections in multiple target zones, but the total aggregate thickness of CS-grouted horizons will not exceed 0.9-1.2 m (3-4 ft).

There are several important reasons for adopting this approach. The most important is because the level of radioactivity is now estimated at 200 Ci (and may be significantly exceeded), and is expected to be concentrated mainly in the soil pile, which will be placed at the bottom of the basin.

Although most of the water will have been drained from the basin, a significant amount of water, the primary migratory vehicle of the contamination, will remain in contact with highly contaminated materials. The additional level of safety dictated by the increased amount of radioactivity necessitates the sealing of any conductive pathways between the bottom of the basin and the groundwater (such conductive pathways are suggested by the fact that the water level fluctuations in the basin cannot be fully accounted for by rainfall and evapotranspiration).

In the same spirit of increased safety, the proposed approach is deemed more effective in isolating the basin from water (a) inflow (through the gravel bed underlying the inlet pipe) and (b) outflow (from the rip-rap area). These two areas constitute "supply or drain pipe" zones and are assumed to have high permeabilities. If the barrier depicted in **Figure 1.1** is defective at these points, it may lead to water accumulation in the basin (raising the level of radioactive water in the original basin up to the surface) and then drain through the basin outlet. In the proposed approach all the permeable strata from the basin bottom to 6.1 m (20 ft) below current grade will be completely sealed in the vicinity of the inlet and outlet, and moreover the pipe and the surrounding gravel area will be grouted over a distance of at least 15.2 m (50 ft). Isolating only a short distance from the inlet will be insufficient to divert the suspected major water supply path to the basin.

The proposed approach seems to be significantly more effective in sealing potentially high permeability pathways between the bottom of the basin and the groundwater, thus providing a higher level of protection from radionuclide migration. Such a hydraulic communication is suggested by two observations. Water level fluctuations in the basin are much more pronounced after rainfall events than what the amount of rainfall would suggest. As noted previously, this may be caused by the gravel bed on which the inlet pipe to the basin rests (which may act as a collector and a conduit channeling water into the basin). It may also be due to the presence of a conductive pathway between the basin bottom and the underlying shallow confined aquifer, in which case the water level fluctuations in the basin could be significantly influenced by changes in the piezometric head. Such a scenario is supported by geochemical evidence (see Section 3),

which suggests that young water (rich in organic acids) reaches the groundwater relatively fast through highly permeable pathways.

The barrier conceptual model in **Figure 4.3** is based on the assumption that low permeability sediments are present underneath the basin, with discontinuous zones of locally high permeability. Such a soil profile is suggested by the Shelby tube soil cores and has been observed by *Hasbrouck et al.* [1996]. Should the natural sediments underneath the pond involve zones with hydraulic conductivities of 10^{-6} m/sec or higher in a matrix with a predominant hydraulic conductivities of 10^{-8} m/sec, the creation of the barrier would be in essence an effort to complement the naturally low permeability. In this sense the barrier emplacement in the lower (underneath the basin) horizons involves identification and sealing of the permeable layers, while the CS at the bottom of the basin will prevent contaminant migration from the basin toward the groundwater.

4.2.3. Barrier Geometry and CS Grout Volumes

The barrier footprint will be larger than the 220 ft by 150 ft footprint of the basin because the area between the western side of the basin and the fence at the border with the 281-8H basin (the site of the pile) will also be grouted to a depth of 6.1 m (20 ft) to alleviate potential migration problems of contaminants from the soil pile. The cumulative grouted thickness of the barrier will be between a minimum of 0.9 m (3 ft) and a maximum of 1.2 m (4 ft). It is expected that, depending on conditions, a grouted layer between 0.3 and 0.6 m (1 and 2 ft) thick will be emplaced at the bottom of the basin. The walls of the barrier will be somewhat thicker. Barrier specifications at the boundaries (i.e. the walls) appear in **Figure 4.4**. Note that case (b) applies only to the western wall (i.e. the area under the soil pile); case (a) applies to all other walls.

In addition, the area around the outlet will be completely grouted. The inlet pipe will be grouted (probably using a cementitious grout), as well as the high permeability gravel bed underneath it using CS. To prevent the possibility of a *supply conduit* to the basin, this bed will be grouted to a total of 15.2 m (50 ft) back from the inlet.

As noted earlier, the total volume of CS needed for the barrier operations is estimated between a minimum of 916,000 kg (2,000,000 lbs) and a maximum of 2,153,000 kg (4,700,000 lbs). The CS grout volume will be 20% larger than the CS alone because of the addition of the gelling electrolyte.

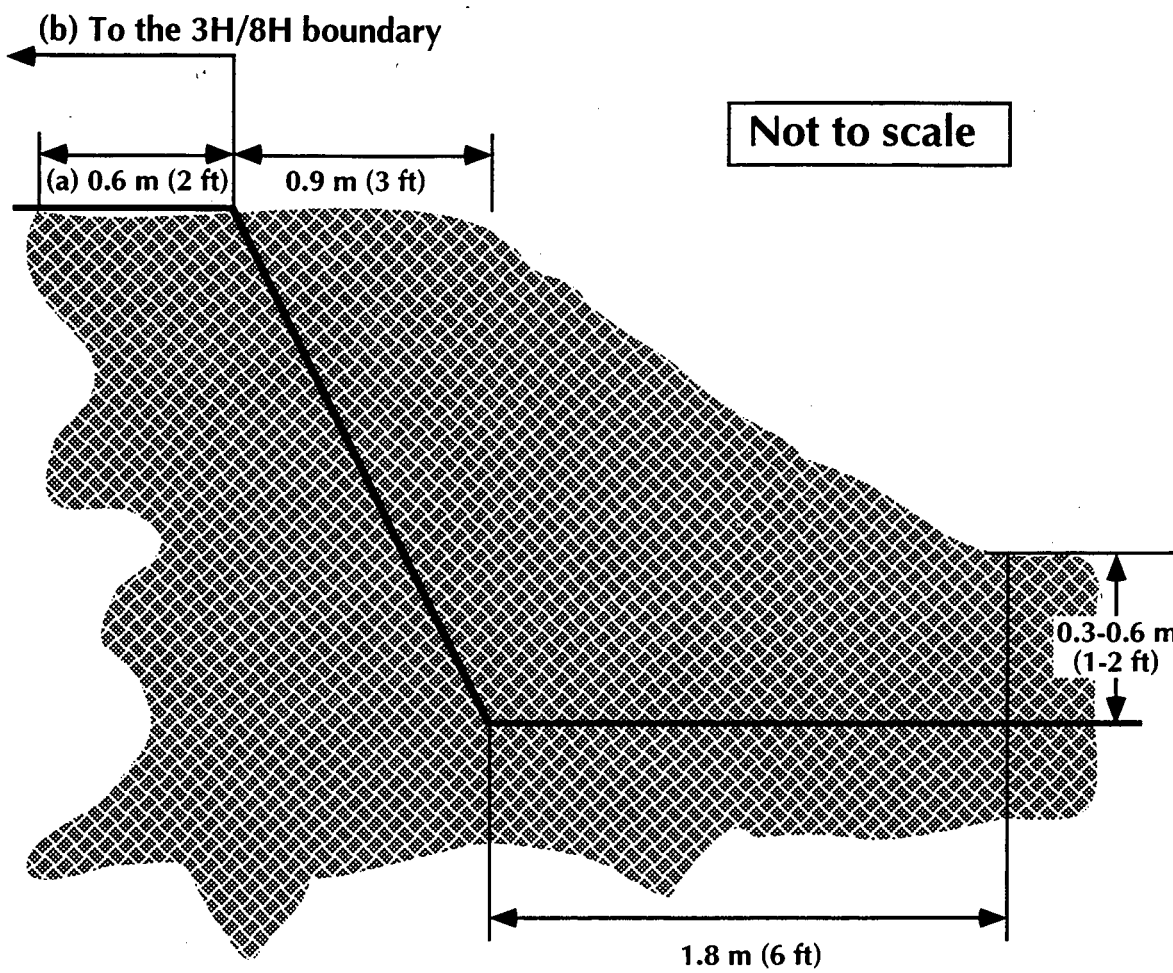

Figure 4.4. Specifications of the barrier walls.

4.3. Selection of Barrier Emplacement Technique

After evaluating several barrier emplacement alternatives, lance injection was selected as the barrier emplacement method. Lance injection (shown in **Figures 4.5** and **4.6**) offers a number of attractive features.

4.3.1. Advantages of the Lance Injection Technology

The injections using lance injection technology are closely spaced, and accurate emplacement is easy to achieve. It requires no drilling fluids, and no cuttings or slurry are expelled during penetration. The lances are forced into the soil using a hydraulic mechanism, thus eliminating the risk of contaminant dispersion in the air, which could pose a problem when using pneumatic techniques such as ODEX for well drilling.

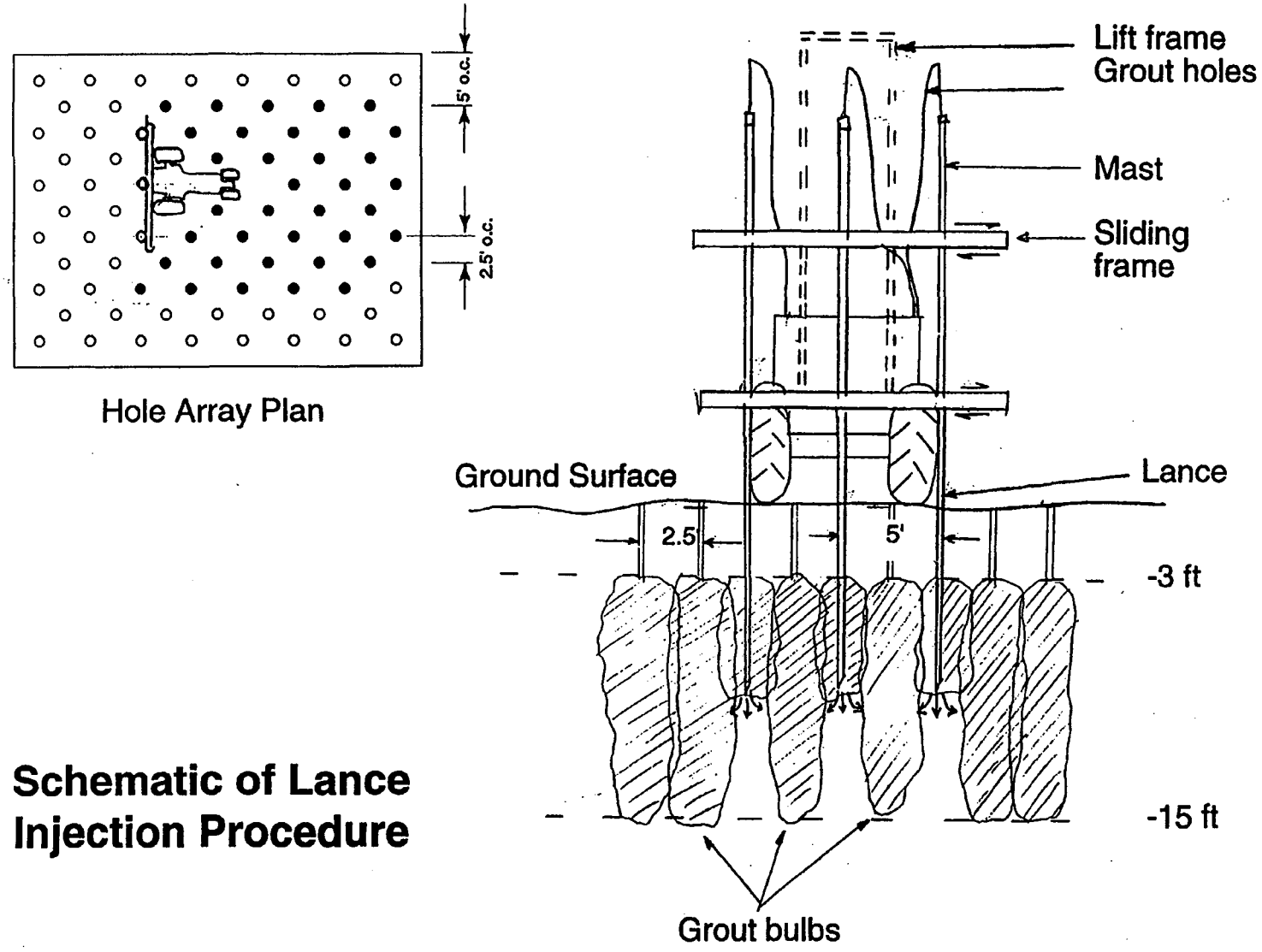

Figure 4.5. The principles of the lance injection technology. The dimensions and spacings on these illustrations are only indicative. Lance spacing is an important design parameter to be determined from numerical simulation and preliminary field tests.

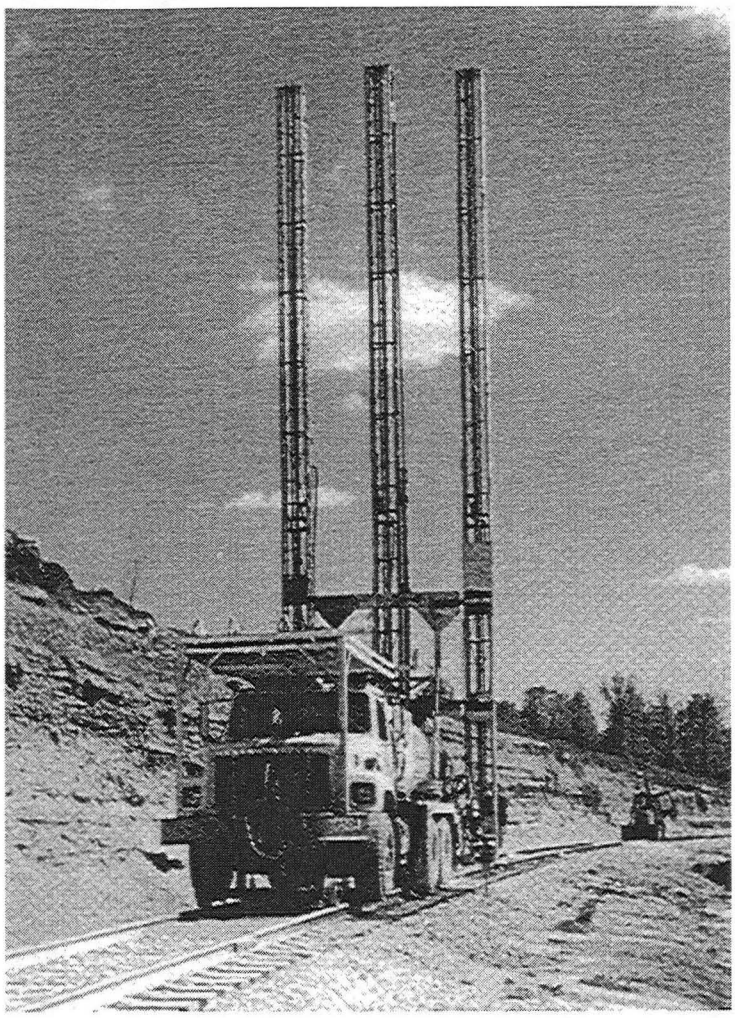

Figure 4.6. Truck-mounted lance injection system.

It has a significant cost advantage compared to traditional well drilling techniques because it does not require well completion. The chemical grout injection begins from the top of the intended injection zone, and proceeds downward (downstage method). It eliminates the downward spread of contaminants, a common problem of drilling methods.

Lance injection results in a barrier consisting of overlapping grout bulbs (see **Figure 4.5**), and allows repeated injections and/or re-treatment of the grouted zones. It allows visual monitoring of work at all times, and is compatible with many methods of emplacement and post-injection barrier verification. Using lance injection, application of the technology can be designed using a flexible modular approach which may provide isolation in a multi-stage process for greater flexibility in terms of scheduling and budgeting.

4.4. Machinery and Instrumentation Requirements

4.4.1. The Lance-Pushing System

As already noted, the truck-mounted lancing system must be able to deliver a minimum force of 6,740 N (15,000 lbs) and/or be able to penetrate the site strata. Based on CPT and Shelby tube coring data, this force is needed to penetrate the compact/cemented quartz pebble horizons of the soil profile (see Section 3).

4.4.2. Lances and Lance Instrumentation and Monitoring

Commercially available lance tips will be used. The lance system will be instrumented with pressure transducers, and with flow meters.

4.4.3. The Grout Injection System

The grout injection system will include the mixing equipment (capable of mixing the grout components (CS and electrolyte) in line and at variable volumetric ratios), the injection pumps, and the hose system. The injection system must be clean and free of any Ca contamination. The CS residence time in the injection system should not exceed 30 min.

The holes left by the lances will be backfilled using a CS-sand slurry. The sand alone will have a hydraulic conductivity of about 10^{-4} cm/sec, and will be mixed with the CS grout system in line immediately prior to injection. The amount of slurry required for each hole is estimated at about 4 liters (1 gallon).

4.5. Emplacement Design Calculations

4.5.1. Injection Strategy and Grids

The injection pattern involves two grids (see **Figure 1.2**) : the primary grid (i.e. the first pass) and the secondary grid (second pass), which is offset from the primary grid and injects at the midpoints between the primary grid. The grid spacing is expected to range between 0.6 and 1.5 m (2 and 5 ft). A more accurate estimate could be obtained by using the permeability value determined from the pilot water injection test (see section 7).

The injection strategy is dictated by the state of saturation of the subsurface, and differs for saturated and unsaturated conditions. The unsaturated condition allows somewhat higher pressures (see subsection 4.5.2), simultaneous injection from all three lances (in 3-pronged systems), and shorter gel times. The saturated condition precludes simultaneous use of more than two lances (to avoid less than satisfactory coverage), and requires lower injection pressures and longer gel times (several hours long).

Simulations of constant pressure CS injection into a fully saturated two-dimensional Cartesian mesh have been performed in order to continue the exploration of gel content between multiple side by side injection ports. For all simulations, CS with an initial viscosity of 4.5 cP is injected into a horizontal, **2-D**imensional (2-D) water saturated domain with a uniform permeability of $k = 5\times10^{-12}$ m^2. (Note: to obtain hydraulic conductivity K in m/s, multiply the intrinsic permeability k by 9.81×10^6, e.g. when $k = 5\times10^{-12}$ m^2, $K = 4.91\times10^{-5}$ m/s.)

The first series of simulations was performed with the purpose of illustrating the interaction of two identical injection ports, which can be simulated using a closed boundary at the line of symmetry between the two ports (method of images). The finely discretized, simplified 2-D system is illustrated in **Figure 4.7**. The domain is surrounded on 3 sides by constant pressure boundaries to create an infinite-acting system in these directions. The fourth side, the left hand side in **Figure 4.7**, is a closed boundary. Close to the wall, grid blocks are 1 mm in length in the x-direction. Further away from the wall, grid blocks are sized to 1 cm. CS barrier liquid is injected into the domain at a constant pressure of 2.026×10^5 Pa (2 atm). The initial pressure conditions throughout the domain are atmospheric pressure, i.e. 1.013×10^5 Pa (1 atm). Injection occurs for 60 s (1 min.), after which the system is allowed to evolve naturally. Observations are taken at 300 s (5 min.). **Figure 4.7** illustrates the spread of CS in the domain with gel mass fraction contour lines at intervals of 0.1. High gel concentrations extend all the way to the closed boundary wall.

Figure 4.8 shows the results of the second simulation, in which the closed boundary is replaced with a mirrored grid system to the left hand side in order to allow two identical injection ports. Injection occurs exactly as described above. Observations of CS spreading for this simulation are exactly the same as for the closed boundary system. **Figure 4.9** offers a close up of the gel contours between the two ports. This exercise has

illustrated the obvious, that the line of symmetry between injection ports can be used in simulation efforts. It also shows that a zone of low gel content will not occur given enough time for injection.

The second series of simulations reproduces previous work but with updated port spacing and pressures expected in field application, and simulates two different injection scenarios in order to maximize gel content between ports. **Figure 4.10** illustrates CS placement after 1800s (0.5 hrs.) of simultaneous 2 port injection and 1.5 hrs. natural evolution. Observations are made at t = 2 hrs. Port locations are labeled and the 2-D grid is halved along the line of symmetry at port 2. Grid blocks between injection ports 1 and 2 are 1 mm in length (x axis). Initial pressure conditions throughout the domain were set at roughly 2.22091×10^5 Pa (2 atm or 32 psi) based on a subsurface depth of 4.57 m (15 ft). The constant pressure injection was set at 6.89×10^5 Pa (100 psi).

Contour lines of gel mass fraction in **Figure 4.10** indicate that there is a zone between the two injection ports with a gel mass fraction of less than 0.1 due to this injection scheme. If injection were continued for a very long time, this area would eventually be filled with gel and a low gel zone would not exist. The relevancy of this series of simulations is to show that for a given finite injection period, there may exist a zone between injection ports of low gel content. If this is the case, a manner in which to maximize gel coverage in the area between the injection ports is the selection of optimal injection schemes.

Figure 4.11 shows grout placement at t = 2 hrs. for the second injection scheme, a staggered gel injection. Gel injection occurs via port 1 for 0.5 hrs at 6.89×10^5 Pa (100 psi), followed by injection from port 2 at the same constant pressure for the next 0.5 hrs. The system is then allowed to evolve naturally. Comparison of these two simulations shows that the staggered scheme increases gel content in the zone between ports for the same time allowed for injection from all ports and essentially the same amount of injected gel. There is roughly 1 kg (2.2 lbs.) difference in the amount of gel recorded in the domain for the two injection schemes, 21.52 kg for the staggered and 20.23 kg for the simultaneous but this could be attributed to more gel moving into the inactive boundary grid blocks to the right hand side of the domain. Overlaying **Figure 4.10** and **Figure 4.11** shows that gel contours support this explanation.

The conclusion favoring the staggered injection scheme is consistent with the results of the first series of simulations. An important difference between the present simulations and the earlier work is the use of the grout viscosity of 4.5 cP. Previous work was performed using a water-like gel.

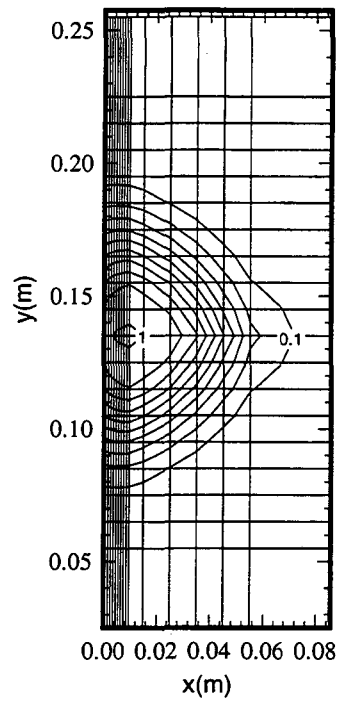

Figure 4.7. Single source grout injection adjacent to a closed wall boundary. Shown are contours of the mass fraction of injected grout at 0.1 intervals.

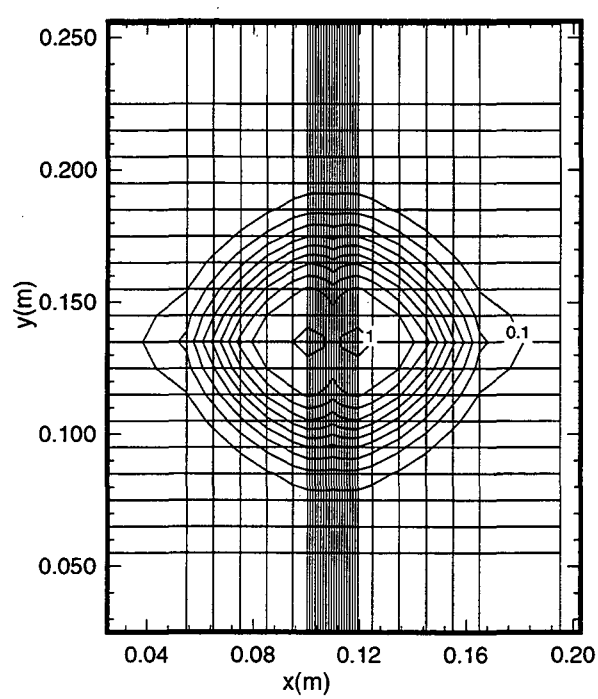

Figure 4.8. Double port grout injection in an infinite acting system. Contours of the fraction of injected grout are shown at 0.1 intervals.

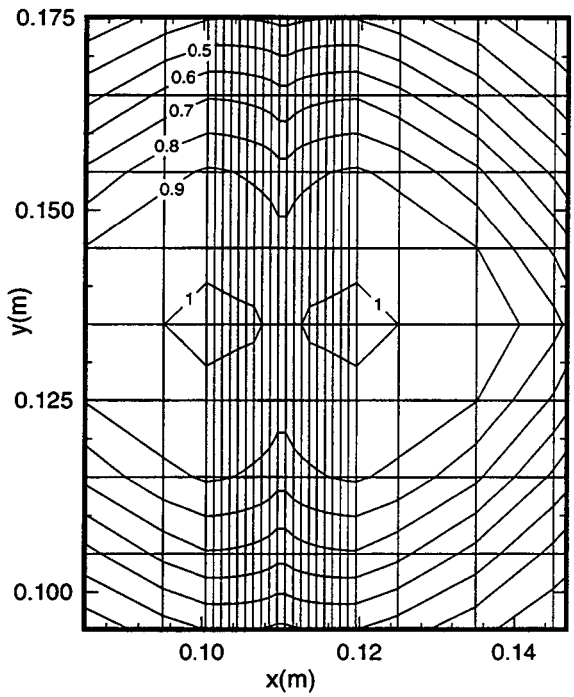

Figure 4.9. Close up of double port grout injection.

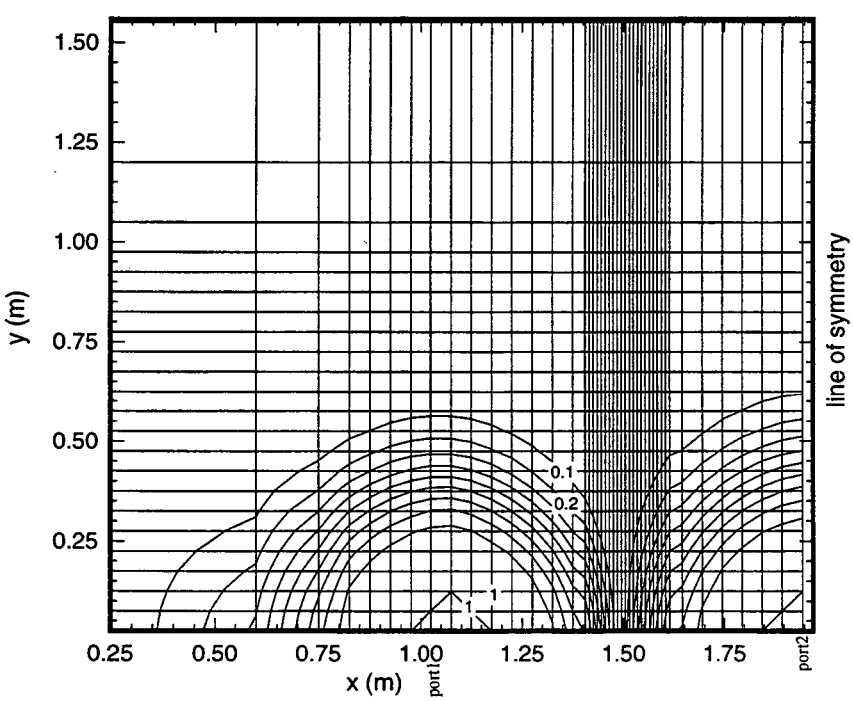

Figure 4.10. Simultaneous 2 port grout injection.

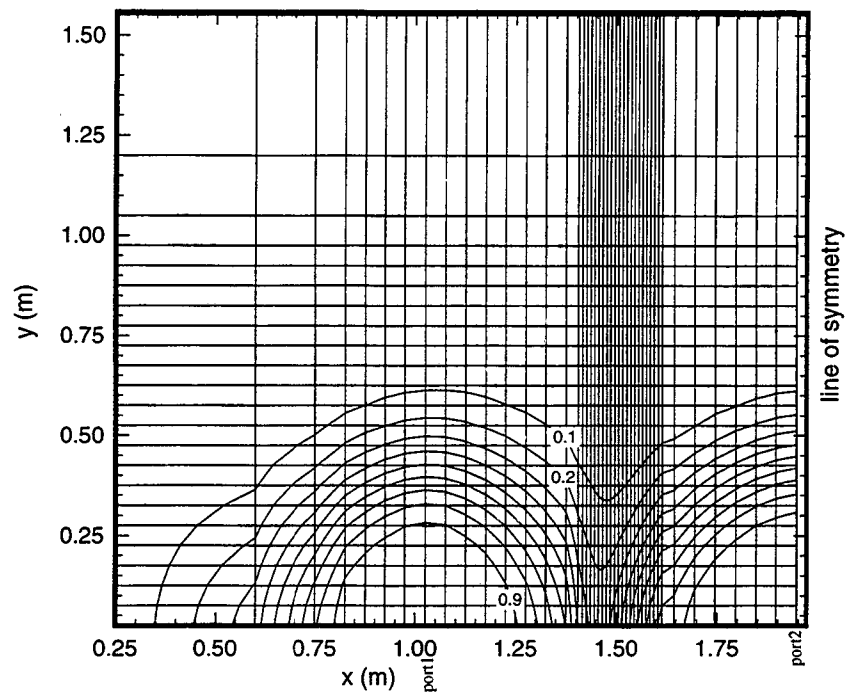

Figure 4.11. Staggered middle port injection.

4.5.2. Injection Under Variably Saturated Conditions

To aid in the design of both a field hydrologic test (see Section 7) as well as actual grout injection, we have used EOS11 [*Finsterle et al.*, 1994b] (the TOUGH2 gelation module) to perform preliminary simulations of water injection under both saturated and unsaturated conditions. For these preliminary calculations, we inject water only with no CS present. Then, from a series of simulations, we are able to construct injection curves, which are plots of water injection rate *vs.* lance tip pressure for injection at constant pressure for various permeabilities. The approximately linear relations between pressure (P), permeability (k), injection rate (q), and viscosity (μ) in the system allow relatively easy interpolation between the curves, and a direct approximation of injection rates and pressures for injections of viscous gelling fluids.

The conceptual model of the system considers a single lance injection in a two-dimensional radial (r-z) system with homogeneous isotropic permeability. Parameters for the problem are presented in **Table 4.1.** Because we expect the injection pressure to be of overwhelming importance in the system, we have used linear capillary pressure and relative permeability functions for these preliminary calculations.

The discretization is shown in **Figure 4.12**. The injection interval for the lance is assumed to be 6 in. (0.1524 m). We have modeled this approximately by using a finely discretized region around the injection location. Grid blocks are 0.16 m x 0.16 m (~6 in x ~6 in) in the finely discretized region. Water is injected at a constant pressure into a particular gridblock (maintained at the same constant pressure). Thus water moves upward, downward, and to the right from this grid block over three interfaces of 0.16 m length, and varying interfacial areas in this *r-z* system. The injection location is fixed in the problem at a depth of 6.5 m.

The boundary conditions are closed on the bottom and right-hand side. The top boundary conditions are held constant at conditions corresponding to the gravity capillary equilibrium for the given capillary pressure function and water table location. For the unsaturated injection scenario, initial conditions are gravity-capillary equilibrium with the water table at a depth of 8 m (**Figure 4.13**). For the saturated injection scenario, initial conditions are gravity capillary equilibrium with the water table at a depth of about 4.5 m.

In Figures **Figure 4.14** and **Figure 4.15** we show the injection curves for unsaturated and saturated injection scenarios, respectively. The injection rate plotted is the time averaged mass injection rate over the first 10 minutes of injection. Each curve is defined by 3 points corresponding to injection simulations at 689.5, 344.8, and 206.8 kPa (100, 50 and 30 psi) respectively. A fourth point is used for the zero injection rate corresponding to 0 psi injection pressure.

Table 4.1. Parameters for the Injection Curve Simulations

Parameter	Symbol	Value
porosity	ϕ	0.3
compressibility	COM	4.4×10^{-8}
permeability	k	$10^{-11} - 5\times10^{-14}$ m^2
temperature	T	15 °C
viscosity of injected water	μ	1.136×10^{-3} Pa·s
lance injection interval	L_i	0.16 m
lance injection depth	d_i	6.49 m
max. capillary pressure	$P_{cap\ max}$	10^5 Pa
residual liquid saturation	S_{lr}	0.20

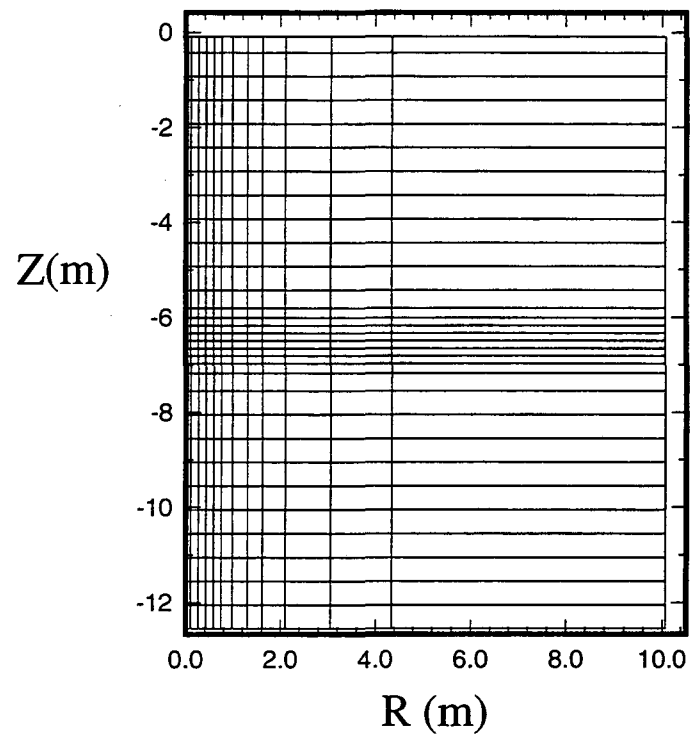

Figure 4.12. Two-dimensional radial mesh for the injection simulations.

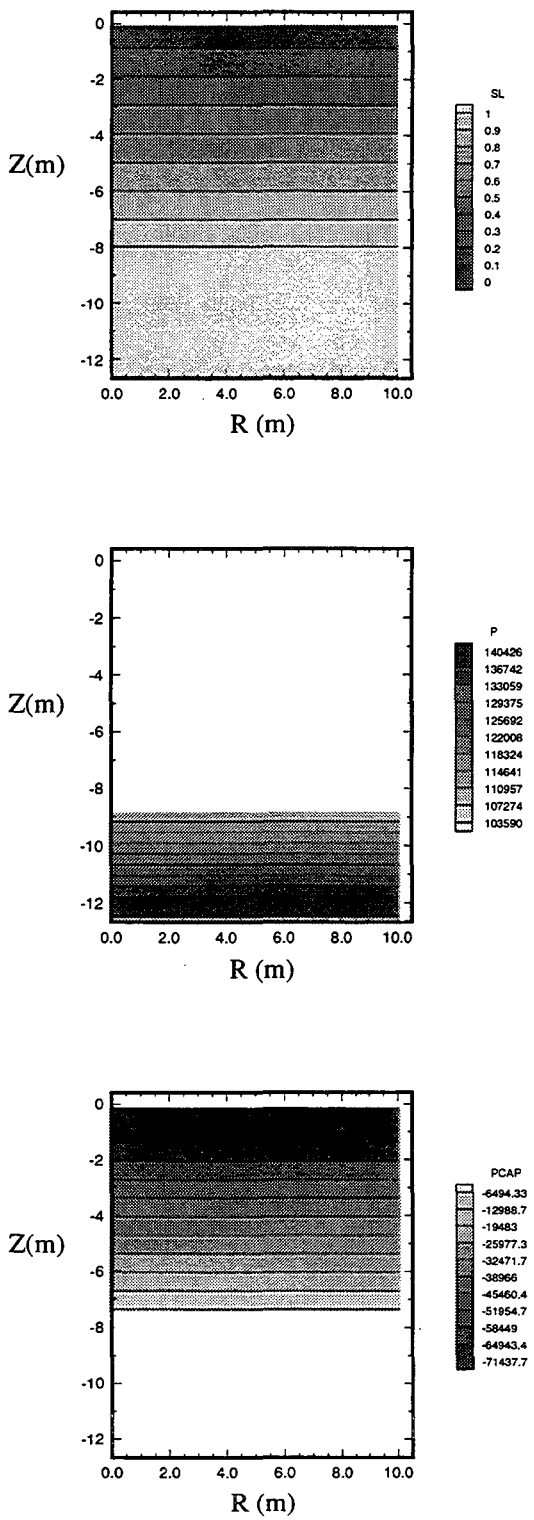

Figure 4.13. Initial hydrostatic conditions for the unsaturated injection scenario.

The injection curves for unsaturated conditions (**Figure 4.14**) show that injection rates are relatively small for the low permeability formations expected at the site. We see further that there is a permeability below which we effectively cannot inject water over any reasonable time period due to the low injection rate. Note that injection curves for all lower values of permeability will plot between the x-axis and the $k = 5\times10^{-14}$ m^2 curve. Thus the surface defined by the constant permeability curves has a very sharp drop-off at about 5×10^{-14} m^2. As permeability increases above 10^{-13} m^2, injection rates increase significantly. The corresponding hydraulic conductivity K values (in m/sec) are obtained by multiplying k by the factor 9.81×10^6.

Figure 4.15 shows the injection curves for saturated conditions. **Figure 4.16** demonstrates the radius of the injected CS bulb, as affected by the permeability and the injection pressure. Under saturated conditions, injection rates are slightly smaller than under unsaturated conditions due to the need to displace existing water in the formation under saturated conditions. We observe the same sort of steep edge to the surface defined by the permeability curves as observed in the unsaturated case. However, as permeability increases, we do not see as rapid an increase in injection rates as we see for the unsaturated conditions.

4.5.3. Implications

Assuming (a) a 60-day working period for emplacement operations, (b) 16-hr work-days, i.e. double shifts, and (c) 3 lance injection rigs working simultaneously, a minimum injection rate of 0.35 l/min is needed.

These simulations show that it may be difficult to inject significant quantities of water or gel over any practical time frame into the low-permeability formations expected at the H-Area site. The simulations do not account for permeability heterogeneity or anisotropic permeability, which could permit higher injection rates. To account for the effects of the CS viscosity (expected to be in the 4.5-6 cP range), the pressures or injection rates must be scaled accordingly by dividing (rates) or multiplying (pressures) by the CS viscosity.

4.5.4. Grouting Around Buried Foreign Objects

An integrated approach of vertical and angled lance injection will be used to grout around the different types of foreign bodies (e.g. rip-rap) in the basin. Grouting around rip-rap and asphalt pieces will be performed with the previously described lance injection system, with the use of a drill rig in the event that lancing to depth cannot be accomplished due to the presence of foreign objects. Reinforced concrete structures left in place at the basin outlet are to be grouted using angled lance injection. Ditch and graveled areas will be conservatively grouted to include some area surrounding these features to ensure a continuous barrier.

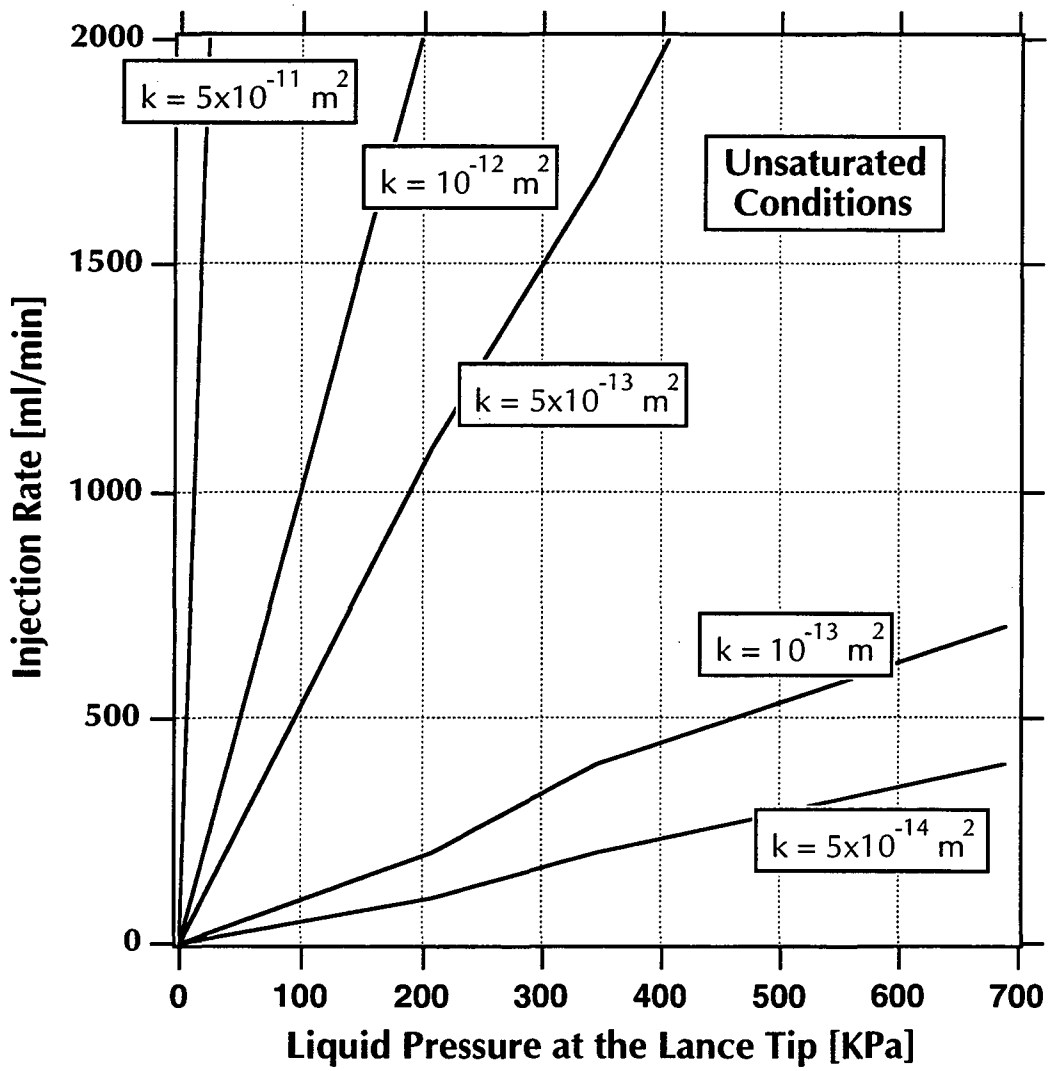

Figure 4.14. Injection curves for unsaturated conditions (water injection).

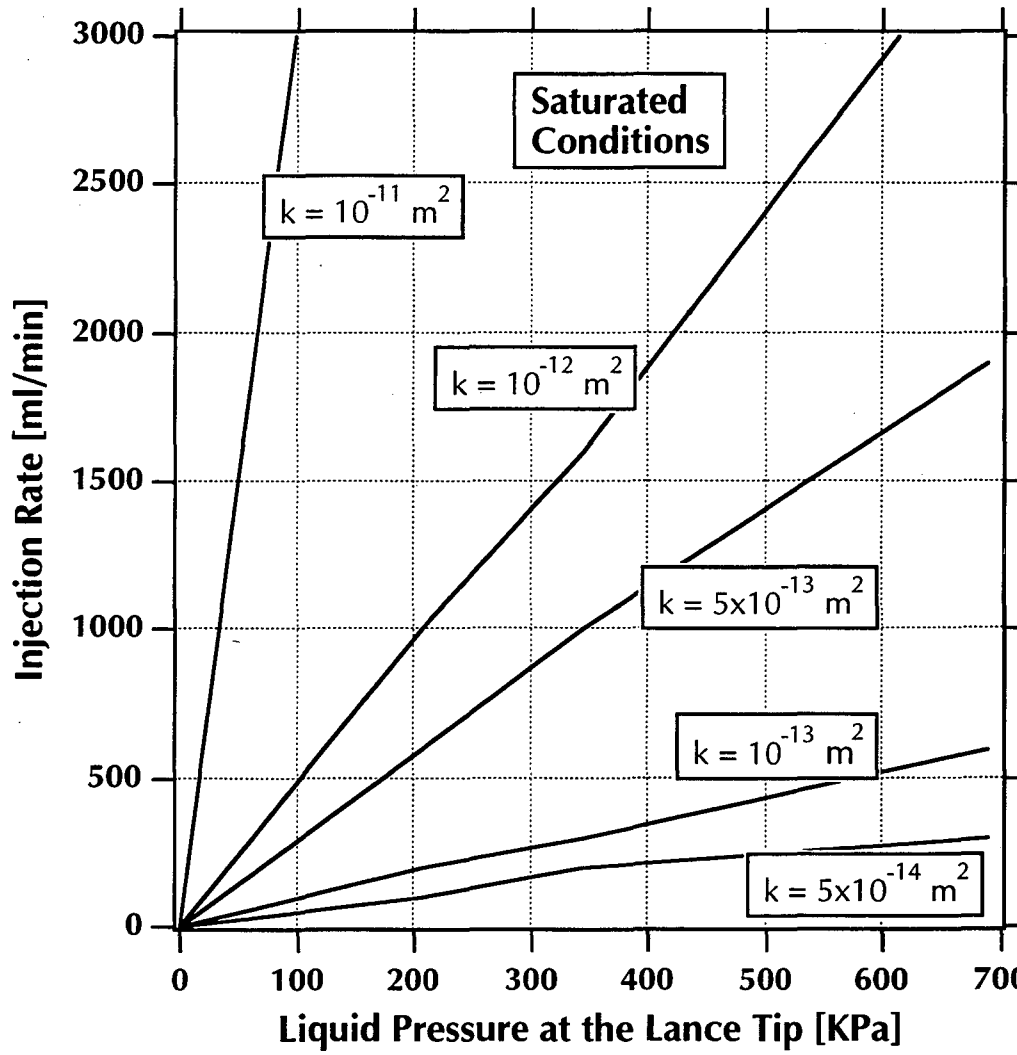

Figure 4.15. Injection curves for saturated conditions (water injection).

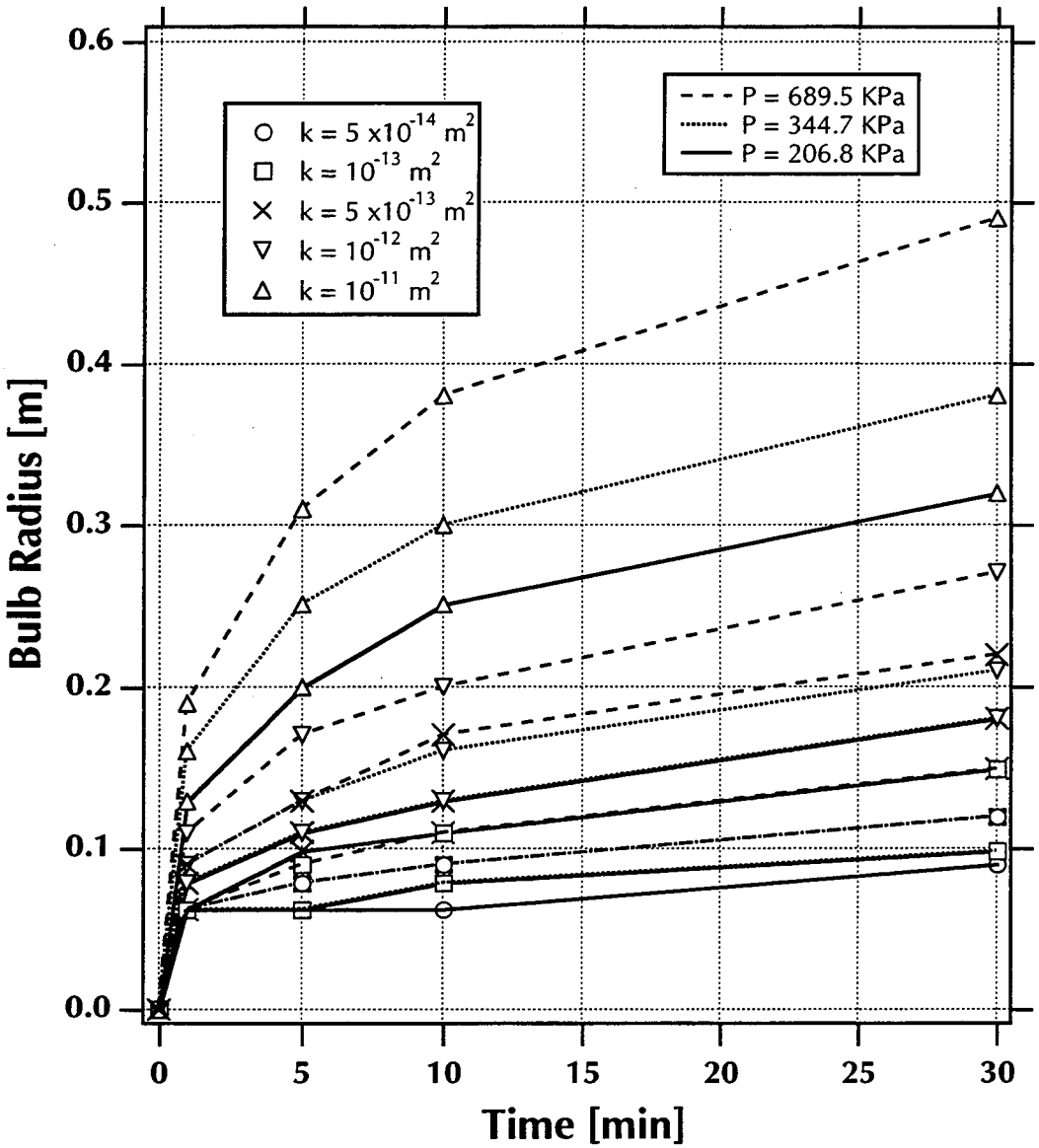

Figure 4.16. Bulb radius of injected CS grout, as affected by injection pressure and permeability (saturated conditions, water injection).

5. THE BARRIER LIQUIDS

The barrier liquid to be used in the pilot-scale field demonstration is CS, a material also used in the first-level field test of the viscous barrier technology [*Moridis et al.*, 1995a, 1996a]. In this section the CS properties and behavior are discussed, as well as the procedure for selecting the CS variant to be used in the field demonstration.

5.1. Design Parameters, Issues, and Implications

(a) The CS to be used in the pilot-scale field demonstration has a viscosity of about 4.5 cP and a density about 1.2 g/cm^3. The viscosity is further decreased upon mixing with the electrolyte.

(b) SRS soils could have an effect on the gelation behavior of CS, but this effect is controllable in the selected material.

(c) The CS gelation may be affected by
- the liquid and surface (air) temperature,
- diurnal and daily variations in air temperature,
- the difference between the liquid and subsurface temperatures.

(d) The design CS gel time is 2-2.5 hrs.

(e) Variability between batches of the barrier liquids could be observed. Testing of each batch prior to injection is therefore necessary.

5.2. Background Information

The barrier fluids used in this work represent a new generation of chemical grouts. Chemical grouts are generally prepared by mixing two or more liquids, and the resulting mixture changes from a liquid to a *solid* state during some period of time. The process of *solidification*, caused by gelling or crosslinking, begins as soon as the ingredients are mixed.

The initial viscosity of the grout is sufficiently low (about 4-6 cSt) to permit injection of the liquid without requiring excessive pressure, but once in place the liquid must solidify and block pores before the barrier liquid plume moves or spreads due to gravity or capillary forces. The time to solidification is called the *gel time*. Control of gel time is essential in the application of the viscous liquid barriers technology.

Gelling of colloidal silica (CS) is induced and controlled by manipulating the inter-particle repulsive forces that stabilize the colloid. Gelling of CS, although thermodynamically favorable, is prevented by a repulsive charge (usually negative) on the particles, which inhibits interaction and prevents Si-O-Si bond formation. For controlled gelling to occur, inter-particle repulsion must decrease sufficiently to allow particles to approach each other more closely. The random motion of the colloidal particles then results in the formation of inter-particle bonds, causing gelling. The means used to destabilize the colloid and make it gel depends upon the mechanism originally used to stabilize the colloid. For CS stabilized at high pH, neutralization reduces the particle charge, inducing gelling. For any CS, increasing the ionic strength by addition of brine compresses the electrical double layer surrounding each particle and permits closer approach of particles, inducing gelling.

In traditional base-stabilized CS systems, particle charge induced by high pH is temporary in the sense that it can be increased, decreased, removed, or even reversed according to the pH value. In surface-modified formulations (which are significantly less susceptible to soil effects [*Moridis et al.*, 1995a]), the CS is stabilized by a permanent particle charge produced by isomorphic replacement of Si by Al on the particle surface (**Figure 5.1**). In the resulting Colloidal Alumina Silica (CAS) the charge is not pH dependent and it is even more environmentally benign because it is stable at a near-neutral pH of 6.5.

Gel time is quantified by observing the gel state over time according to the descriptions given in **Table 5.1**. Typical gel time curves are illustrated in **Figures 5.2** through **5.4** and show that with increasing concentration of added brine, (i.e., with increasing ionic strength) the colloid gels faster. High pH CS also gels faster at lower pH (down to a value near 7), and diluted CS gel more slowly.

When CS grout is injected into soil, changes in pH, ionic strength or electrolytic composition caused by interaction between the grout and the soil or groundwater can affect its rate of gelling. Generally this has the effect of accelerating gelation, but organic compounds in the water can also coat the CS particles and retard gelling. Important interactions include buffering of pH and ion exchange between the grout and clays in the soil. The effects may be great enough to cause rapid gelation even though no brine has been added to the CS; in such conditions, *in situ* gel time could be uncontrollable.

Table 5.1. Jar-Test Gel State Codes
Modified from *Sydansk* [1990].

1.	No detectable gel formed. The gel appears to have the same viscosity (fluidity) as the original polymer solution and no gel is visually detectable.
2.	Highly flowing gel. The gel appears to be only slightly more viscous than the initial polymer solution.
3.	Flowing gel. Most of the obviously detectable gel flows to the bottle cap upon inversion.
4.	Moderately flowing gel. A small portion (about 5 to 15%) of the gel does not readily flow to the bottle cap upon inversion—usually characterized as a *tonguing* gel (i.e., after hanging out of the bottle, gel can be made to flow back into the bottle by slowly turning the bottle upright).
5.	Barely flowing gel. The gel slowly flows to the bottle cap and/or a significant portion (> 15%) of the gel does not flow upon inversion.
6.	Highly deformable non flowing gel. The gel does not flow to the bottle cap upon inversion (gel flows to just short of reaching the bottle cap).
7.	Moderately deformable non flowing gel. The gel flows about halfway down the bottle upon inversion.
8.	Slightly deformable non flowing gel. Only the gel surface deforms slightly upon inversion.
9.	Rigid gel. There is no gel-surface deformation upon inversion.
10.	Ringing rigid gel. A tuning-fork-like mechanical vibration can be felt or a tone can be heard after the bottle is tapped.
11.	Rigid gel no longer ringing. No tone or vibration can be felt or heard, because natural frequency of the gel has increased.

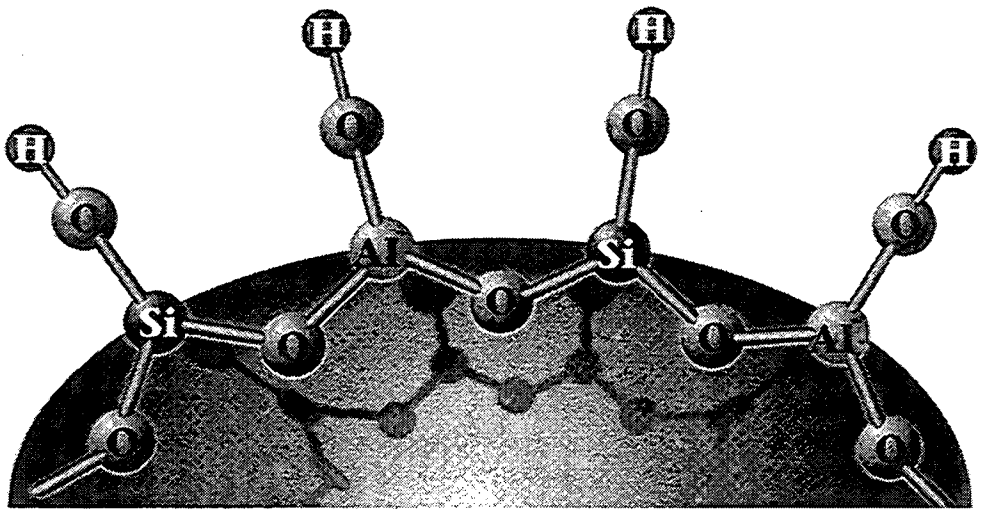

Figure 5.1. Isomorphic substitution of Si by Al on the CS surface in surface-modified CS formulations.

To identify and select types of CS whose gel times could be controlled in the soil, a series of test techniques and criteria were devised. The test methods were developed by testing colloids already on hand, as reported in the following sections. Injected grout also mixes with and is diluted by groundwater. This effect is also recognized in the flow and transport simulations of injected CS grout when using TOUGH2 [*Finsterle et al,* 1994b] to develop this design package.

5.3. Colloidal Silica Samples

Three samples of colloid and brine were received, from two vendors. The colloidal silica samples were received in 5-gallon plastic buckets with pour spouts, identified only by the code numbers CS-1A, CS-2A, and CS-3A. The brines (electrolyte solutions) that were to be used to cause gelation of samples were also identified by the corresponding numbers 1B, 2B, and 3B.

Gel-time curves supplied by the vendors indicated the proportions of brine to be mixed with the colloids to achieve desired gel times (both time to onset of gelation and time to final solidification). These curves necessarily were only valid for gelling the colloid in the absence of soil. The brine originally supplied for sample 2 (identified as *2B original*) was mis-compounded for a 4:1 rather than 5:1 ratio of colloid to brine. As soon as this error was noticed, the vendor revised the brine formula and forwarded a 1-gallon sample of the corrected brine (identified as *2B new*). However, to avoid delay while waiting for arrival of *2B new*, we prepared a replacement

according to the formula specified by the vendor. This replacement was identified as *2B replacement.*

Archive samples of each colloid were taken immediately, so that they could be referred to if necessary to resolve any question of mis-identification. No problems of sample identification were encountered during the work.

5.4. Soils

The soil samples were obtained from a trench near basin 281-3H. Two drums of soil were collected from the 1.52-3.05 m (5-10 ft) depth interval (referred to as soil S1), and two from the 3.05-6.10 m (10-20 ft) depth interval (referred to as soil S2). Only the S2 soil was used in this work. The soil was sieved to eliminate large lumps of kaolinite. The -4 (smaller than 4.76 mm) fraction was homogenized. This is referred to as *native soil.* The water saturation of this soil was approximately 18%.

In addition to the native soil, a clay-sand mixture was prepared to simulate the sandy layers or lenses into which grout is to be injected. To prepare this mixture, the native soil was dried, ground in a mortar and pestle, and sieved. Ten percent by weight of the -30 fraction of this dried and ground native soil was mixed with 90% Monterey sand. This soil is referred to as 10% clay and had negligible moisture content.

Sludge similar to the one at the bottom of the 281-3H basin was used in a series of experiments designed to test the injectability of CS and its ability to gel in the sludge. The sludge posed a significant challenge as it is known to be 0.3-0.6 m (1-2 ft) deep and to contain significant radionuclide contamination. To effectively contain the radionuclide contamination, it is necessary either to place a barrier underneath the sludge or to permeate and gel the sludge at the bottom of the basin.

Finally, soil representative of the contaminated soil (such as the soil pile) to be placed at the bottom of the basin was tested. The SRS native S1 soil which was used as an analog was remolded to a density of 80-85% of Standard Proctor, and was tested for CS injectability and permeation.

5.5. Laboratory Testing

Laboratory testing was conducted to determine (i) whether the samples submitted for evaluation could be made to gel at controlled times, (ii) whether the gel time was significantly accelerated or retarded by the soils (iii) whether the grout could be injected into the soil without excessive injection pressures caused by uncontrolled gelation, and (iv) whether the grout gels in the soil at the desired rate.

The measurements conducted for this evaluation consisted of standard tests, gel-time jar tests with and without soil, and special tests designed to assess the ability of grout to flow and gel in the particular soil to be grouted. While the suppliers could be reasonably certain of the performance of the samples in standard tests, the gel time jar tests with soils and the special tests involved use of soil materials with which the vendors were not familiar; therefore the vendors could not anticipate with certainty the performance of the samples in these tests.

5.5.1. Standard Tests

The pH, viscosity, and solids content of each candidate colloid were measured using both a pH meter and pH paper. The meter was calibrated with pH 7.0 and 10.0 buffers immediately before use. Both methods of measurement agreed. The meter measurements are reported in **Table 5.2**. The pH of sample 2A was 10.28, which is outside the specified range; however this was not considered a sufficiently serious deficiency to disqualify the material. The other two colloids had neutral pH. The pH of the vendor-supplied brines, and of the grouts formed by mixing the brine and colloid, were also measured.

The solids content of each colloid was measured by pouring triplicate-weighed samples into a tared metal dishes, and weighing again after evaporation for 16 hr. Evaporations were done at 65 and 95 °C. The dishes were placed on aluminum foil to detect any spattering of the colloid (if it were to boil) which would cause loss of material; no spattering was noted. Three samples of each colloid were evaporated. No significant difference was detected between the samples at the two evaporating temperatures. Sample 3A had 28% solids, which is below the specified requirement; however this was not considered a sufficiently serious deficiency to disqualify the material.

The viscosity of each material was measured at 20 °C using new, appropriately ranged Ubbelohde viscometers. This instrument measures the kinematic viscosity (centistokes), which is the ratio of the dynamic viscosity (centipoise) to the density. Density was measured by weighing 25 mL of sample in a tared graduated cylinder. The measured viscosities were lower than the values reported in the manufacturer-supplied literature.

5.5.2. Gel Time Jar Tests Without Soil

Gel time tests with and without soil are collectively referred to as Test 1. Colloidal silica is made to gel by adding 1 part by volume of brine to 5 parts colloid. The gel time is controlled by diluting the brine from its concentration as delivered. Four mL of brine, diluted according to the vendor's directions, were slowly added to 20 mL of CS by syringe while swirling the mixture by hand. The mixture was then allowed to sit without agitation between readings. (In a separate study, agitation of the grout was found to delay gelling and weaken the gel.)

The progress of gellation was recorded by assigning gel states according to **Table 5.1**, [*Moridis et al,* 1993a; *Sydansk,* 1990]. For each candidate colloid, gel-time jar tests were run using brine diluted to give four target initial gel times (i.e., time to reach state 2 when the target gel-time is 1, 2, 4, and 8 hr.)

5.5.2. Gel Time Jar Tests With Soil

Because the gel time in the soil (as well as *in vitro*) is an important consideration, the gel time tests were repeated with 0.020 kg of soil added to the jar. All candidate colloids were tested at the four target gel times with both soils.

5.6. Special Tests

5.6.1. Drain-In Test

The drain-in test is used as a screening test to identify (and eliminate) colloids that gel upon contact with the soil even though no brine was added to cause gelling. In previous work, this test was used to identify colloids that were not suitable for use for use in Hanford sand. Because such uncontrolled gelling would prevent CS grout from being injected, the effect of the soil was assessed in drain-in tests.

In this test, 0.1 kg of soil are packed in a vertical column to a height of approximately 0.28 m. Then 85 mL of colloid are poured onto the soil column and the height of the liquid is monitored as the colloid flows into the soil. If the CS does not gel substantially, all of the colloid will flow through the column.

5.6.2. Column Injection Test

Two tests were performed sequentially in a packed column of soil, in which the pressure required to inject the grout into the soil and the rate at which the grout gels in the soil are measured. They are collectively referred to as Test 2. Performance in the gel-time jar tests and the drain in test are considered indicative of performance in these tests, but these two tests are the actual acceptance tests for candidate grouts.

In the first test, soil is packed into a 0.0254 m (1 in) diameter, 0.91 m (36 in) long column. Four pore volumes (PV) of water are pumped through the column, and the injection pressure ($P_{i,w}$) is monitored. The flow rate for all injections is 1 PV in 30 minutes. All injection pressure values are corrected by subtracting the gravity head so that only viscous head loss is measured. The maximum value of $P_{i,w}$ during the four PV of water injection is recorded (in fact, $P_{i,w}$ is always constant during the four PV of water injection). This provides a measure of the hydraulic

conductivity of the soil pack. Then two PV of grout are injected, and the injection pressure ($P_{i,g}$) is monitored.

The maximum value of $P_{i,g}$ during the two PV of grout injection is recorded. One expects $P_{i,g}$ to be greater than $P_{i,w}$ because the viscosity of the grout is initially greater than that of the water, and also increases as the grout gels. An unexpectedly high of $P_{i,g}$ indicates that premature gelling is occurring in the soil, or that the injection of grout has caused some change in the soil that reduces its hydraulic conductivity, such as swelling of clays. The criterion for success is that $(P_{i,g}/P_{i,w})(\mu_g/\mu_w)$ does not exceed 2.5. The viscosity of the grout was taken as the viscosity of the colloid.

All candidate barrier liquids were tested in both native and simulated soils. Results confirm those of the drain-in and gel-time jar tests that premature gellation is not a problem for these grouts in the SRS soils. When the design gel-time is as short as 1 hr, $P_{i,g}$ can become very large. This, however, is due to gelling in the pump and should not be misinterpreted as premature gelling in the soil.

5.6.3. Column Gel-Time In Soil Test

Immediately following the column injection pressure test, the gel time of the grout in the soil is measured by monitoring the mobility of the grout in the grouted soil column. The procedure for measuring the barrier liquid mobility is to impose a hydraulic gradient across the grouted soil column, and record the heights of the two water columns as the gradient decays. The grouted column is removed from the injection manifold and connected to flexible tubes filled with water. By moving one or both of the flexible tubes, the water levels in the two tubes can be made to differ. This imposes a hydraulic gradient across the grouted soil column. As long as the grout remains mobile, this gradient will decay to zero, as in a falling head permeability measurement. By monitoring the heights of the two water columns as the gradient decays, a measure of the mobility of the barrier liquid is obtained.

When equilibrium is reached, the height of the two water columns are not equal, because density of the grout is greater than that of water. The equilibrium height difference is recorded and used to correct the readings. Darcy's law requires that the corrected height difference decay exponentially. The mobility of the grout is proportional to the absolute value of the slopes of the lines, and as the mobility decreases (i.e., as the grout gels), the lines approach horizontal. Finally, when the grout has gelled sufficiently to prevent any water movement, the imposed hydraulic gradient is maintained and no longer decays.

The criterion for success in this test is that the grout remain mobile 2 hours after mixing (and 1 hr after injection ceases) but that it becomes effectively immobile within four hours after mixing.

5.7. CS Evalution Results and Discussion

5.7.1. CS in Native and Simulated Soils

The results of the evaluation are summarized in **Tables 5.2** through **5.8**. **Table 5.2** summarizes the compliance of the CS variance to specifications. CS-1A meets the specifications. CS-2A does not meet the pH requirements. This is undesirable, but not a critical issue compared to its performance in porous media. CS-3A has a marginally lower than specified solids content; however, this is not a fatal shortcoming. This criterion was set because in our experience an increasing solids content effects a lower final permeability. The permeability criterion, a far more rigorous test, is met even with this slightly lower than specified solids content.

Figures 5.2 through **5.4** show typical gel-time curves of the three CS variants (CS-1A, CS-2A, and CS-3A) with and without soil, and for various electrolyte (brine) concentrations. The gel time of dry soils grouted with CS are invariably shorter than the ones for wet soil. This is expected because of the very strong attraction of water by the high-clay content of the oven-dry SRS soils, which removes water from the CS and thus causes the double layers to collapse, resulting in gelation. The CS gelation in wet SRS soils is an appropriate indicator of the CS behavior in field applications.

It is interesting to note that the SRS soil has a delaying effect on gelation; the opposite effect, i.e. acceleration of gelation, had been observed in previous studies [*Moridis et al.*, 1995a]. CS in shallower S1 soil (originating from the 1.5 to 3 m zone) gels slower than the deeper S2 soil (from the 3 to 6.1 m zone). The delaying effect is attributed to the presence of organic acids, and is supported by the fact that increasing amounts of organic content corresponds to longer gel times: the TOC of the S1 soil is significantly larger than the one for the S2 soil (see **Table 3.5**). In the high-TOC sludge (see subsection 5.7.2) the delay in the gelation of CS is even more pronounced .

Tables 5.3 and **5.6** present the results of the jar tests with and without soil at various design gel times. According to the LBNL specifications, jar test results **cannot** be used to disqualify a CS variant. The overall impression is that the gel times of all the CS variants are generally controllable in **jar tests**; flow and field performance, however, may be different.

In **Table 5.7** we present the results of the flow and permeability tests (Tests 2 and 3) **conducted in strict accordance to specifications**. CS-2A could not pass Test 2. Its performance could not be controlled by adjusting the brine concentration. With more concentrated brine the gel time was acceptable but the injection pressure was unacceptably high; with less concentrated brine the injection pressure met the criterion but exhibited unacceptably long gel times.

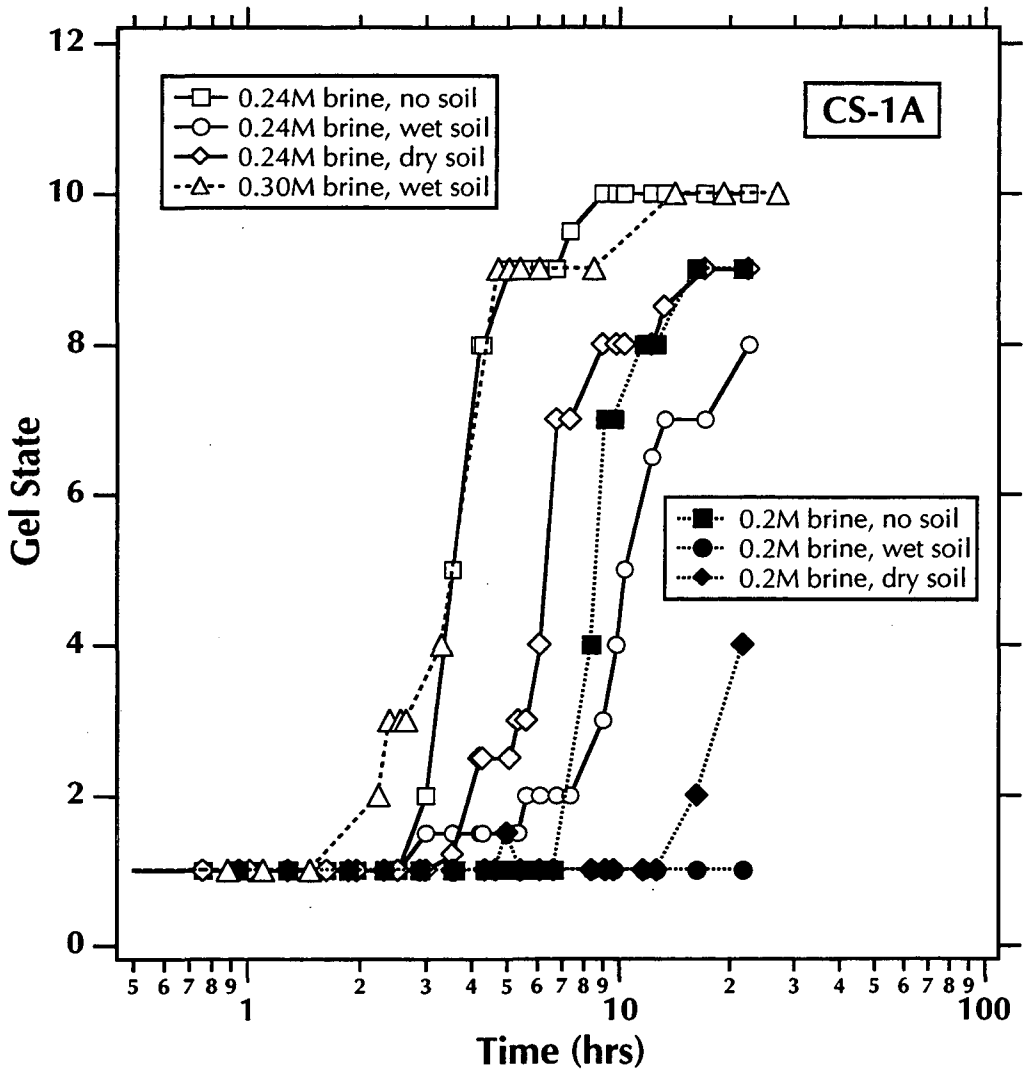

Figure 5.2. S2 soil effect on the gel time of CS-1A.

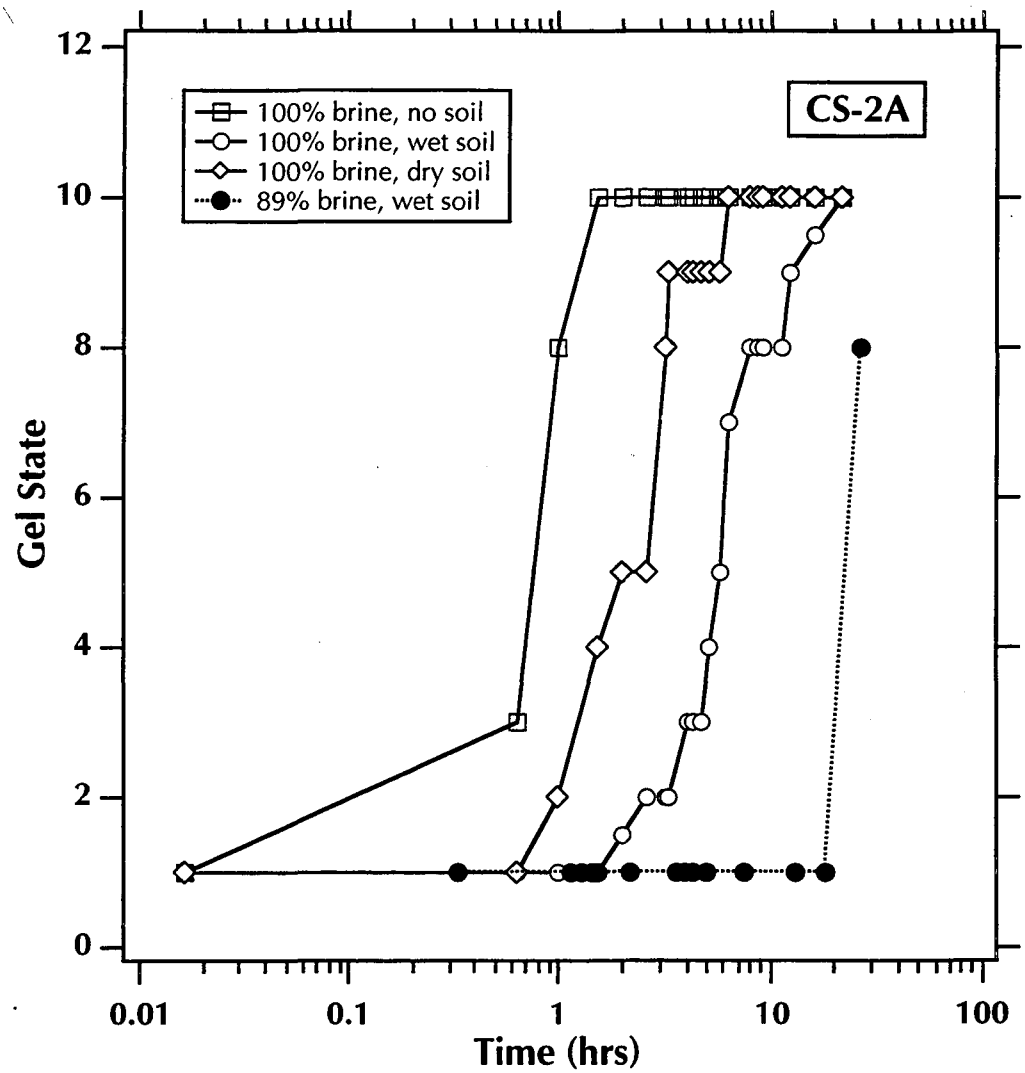

Figure 5.3. S2 soil effect on the gel time of CS-2A.

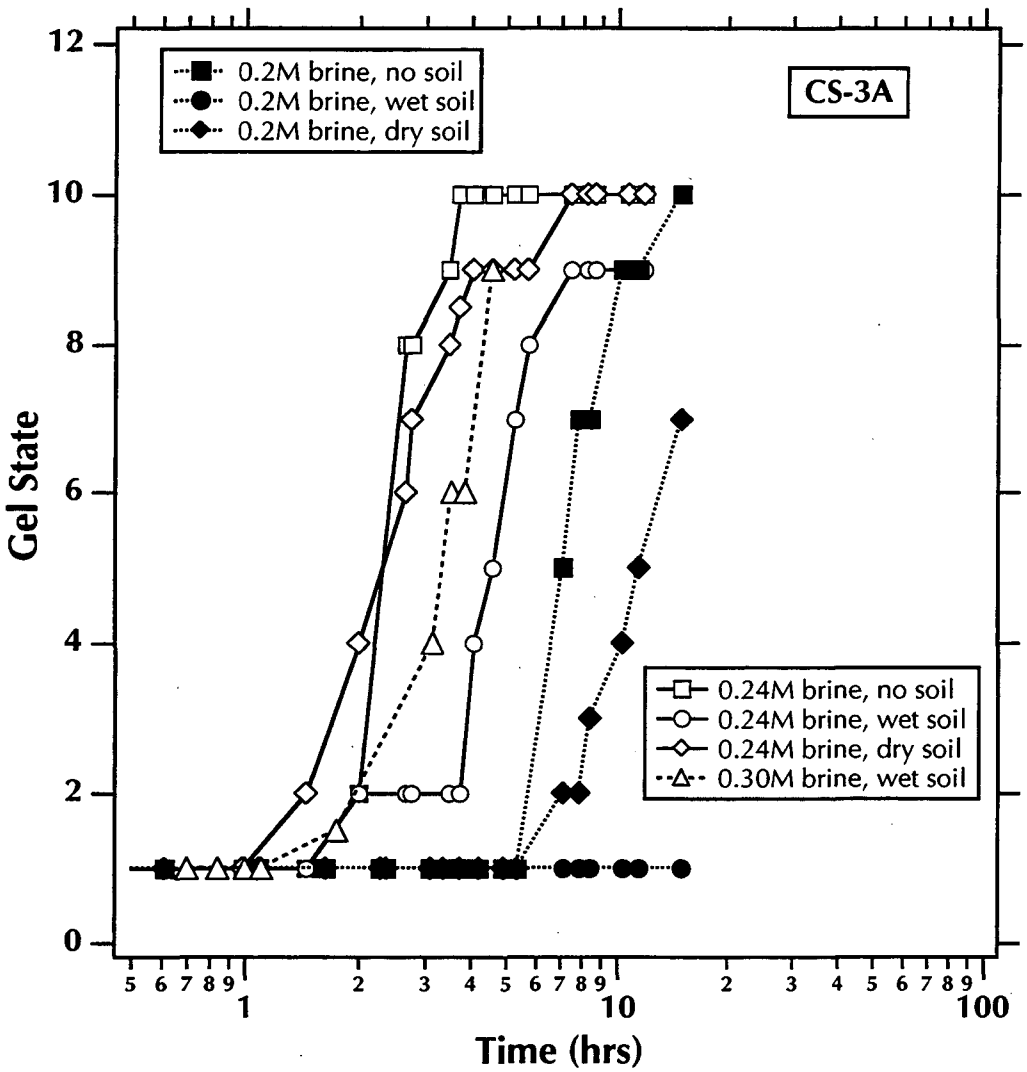

Figure 5.4. S2 soil effect on the gel time of CS-3A.

All three CS variants met the permeability criterion (Test 3) by lowering under optimal conditions the hydraulic conductivity of a Monterey sand core from 10^{-4} m/sec to less than 10^{-10} m/sec.

Finally, **Table 5.7** shows the results of additional tests which we deemed important enough to conduct. The drain-in test showed that the SR soils do not induce premature gelations without brine in any of the three CS variants. The drip test described the CS performance after a long contact with the soil, and confirmed our observation from Test 2 that the gelation of CS-2A may be significantly retarded by the presence of the SR soil.

5.7.2. CS Variant Selection

CS-1A has desirable properties, most important of which is its low initial viscosity (only 4.23 cP). CS-1A does not, however, pass Test 2. CS-2A (which produces a strong gel) fails on a number of significant counts. The initial pH is above the specified 5-10 range; however, this is not a critical issue compared to its performance in porous media. The presence of soil significantly affects the gelation of CS-2A, and these effects cannot be overcome by adjusting the supplied electrolyte concentration to produce **both** an acceptable gel time **and** injection pressure.

CS-2A, moreover, is handicapped by a relatively high viscosity. This parameter has taken on greater importance, because we have determined that the permeabilities of the sediments beneath the H-Area retention basin are significantly lower than we had earlier assumed. Because injection times and pressures are linearly dependent on viscosity, the use of CS-2A (were its retardation in gel time to be overlooked) could result in field operations taking twice as long, or require double the injection pressures with potentially unacceptable hydrofracturing effects during injection. The implication of the high viscosity of CS-2A is that entire zones with relatively low permeability could be left untreated because of the potential for hydrofracturing or impractically long injection times.

CS-3A has the most predictable behavior. It has a marginally lower than specified solids content, but for the reasons previously discussed, this is not deemed a very serious shortcoming. CS-3A has a relatively low initial viscosity (4.41 cP), a significant advantage as it allows faster injection at lower pressures and enables treatment of zones with relatively low permeability.

In summary, because gelling of CS-2A is greatly retarded by native soil, its emplacement cannot be controlled unless the electrolyte concentration is increased, which shortens its pot-life so much that injection becomes impractical. It is this property which causes it to fail test 2. Therefore, CS-2A cannot be recommended as a viable material for injection. CS-1A also does not pass test 2, because it gels too slowly in the clay/sand mixture. We could overcome this problem by adjusting electrolyte properties. Furthermore, the tests required by the specifications do not yield sufficient information to predict with confidence the performance of this material. We consider CS-3A to be the best candidate for field

injection, because it passes test 2, has predictable behavior, and has low viscosity. Therefore, our recommendation is to accept CS-3A for injection under the H-Area retention basin because of its desirable properties.

Additional work will be needed to optimize the CS performance for the SR site-specific conditions. This will, in all likelihood, necessitate refinement of the electrolyte strength and/or composition.

Figure 5.5 shows the temperature dependence of the complex viscosity of the CS-3A variant, an important issue when CS is applied at a site that experiences the temperature extremes common at the SRS. Of importance is the relative rate of onset of gelation (indicated by the steep part of the complex viscosity curve). The maximum viscosities shown in **Figure 5.5** are not accurate because they are affected by the viscometer operation and the temperature. The lack of elasticity of the CS-3A gel and the breaking of the bonds caused by the viscometer motion are indicated by the low maxima in the complex viscosity curves. The jagged appearance and occasional decrease in the complex viscosity are due to the mechanical destruction of the weak bonds in the gel (an inevitable consequence of the viscometer operation). At higher temperatures (30-40 °C) this is further intensified by the evaporation of water and syneresis.

Table 5.2. Compliance of CS Variants to Specifications

Specifications	Required	CS-1A	CS-2A	CS-3A
Colloidal Particle Size (nm)	<15 nm	Not tested-MSE has specs	Not tested-MSE has specs	Not tested-MSE has specs
Solids Content (wt %)	>30	**Pass** 32.2	**Pass** 31.8	**Fail** 27.8
Viscosity (cP)	<10	**Pass** 4.23	**Pass** 7.27	**Pass** 4.41
pH	5-10	**Pass** 7.85	**Fail** 10.28	**Pass** 7.25

Table 5.3. Performance of the CS Variants in Test 1 With a 1 hr Design Gel Time

Specifications	Required	CS-1A(1)	CS-2A(2)	CS-3A(3)
No Soil (Test 1a)	~1 hr to gel time (State 2)	**Fail** 1.4 hrs	**Fail** 0.5 hr	**Pass** 0.82 hr
No Soil (Test 1a)	~2 x gel time to solidification	**Marginal** 3.25 hr	**Pass** 1.08 hrs	**Marginal** 1.4 hrs
Soil S1 (Native SR Soil)	~1 hr to gel time (State 2)	**Marginal** 1.63 hrs	**Fail** 2.3 hrs	**Pass** 1.0 hr
Soil S1 (Native SR Soil)	~2 x gel time to solidification	**Fail** 4.75 hrs	**Fail** 10.08 hrs	**Pass** 1.85 hrs
Soil S2 (Simulated Soil)	~1 hr to gel time (State 2)	**Marginal** 1.63 hrs	**Pass** 1.15 hrs	**Pass** 1.0 hr
Soil S2 (Simulated Soil)	~2 x gel time to solidification	**Marginal** 4.20 hrs	**Pass** 2.17 hrs	**Pass** 1.85 hrs

(1): the brine is a 36 wt% wt $CaCl_2$ solution (diluted from 1M solution provided by the CS supplier)
(2): the brine is at a 100% concentration (undiluted, as provided by the CS supplier)
(3): the brine is a 36 wt% $CaCl_2$ solution (diluted from 1M solution provided by the CS supplier)

Table 5.4. Performance of the CS Variants in Test 1 With a 2 hr Design Gel Time

Specifications	Required	CS-1A(1)	CS-2A(2)	CS-3A(3)
No Soil (Test 1a)	~2 hr to gel time (State 2)	**Pass** 2.1 hrs	**Pass** 2.2 hrs	**Marginal** 1.6 hrs
No Soil (Test 1a)	~2 x gel time to solidification	**Marginal** 5.9 hrs	**Pass** 4 hrs	**Pass** 2.7 hrs
Soil S2 (Native SR Soil)	~2 hr to gel time (State 2)	**Pass** 5.3 hrs	**Pass** 2.5 hrs	**Pass** 2.0 hrs
Soil S2 (Native SR Soil)	~2 x gel time to solidification	**Fail** >12 hrs	**Pass** 9 hrs	**Marginal** 5.5 hrs
Soil SS2 (Simulated Soil)	~2 hr to gel time (State 2)	**Fail** 3.8 hrs	**Fail** 1.01 hrs	**Pass** 2.05 hrs
Soil SS2 (Simulated Soil)	~2 x gel time to solidification	**Pass** 6.6 hrs	**Fail** 1.15 hrs	**Pass** 3.1 hrs

(1): the brine is a 28 wt% $CaCl_2$ solution (diluted from 1M solution provided by the CS supplier)
(2): the brine is at a 89% concentration (diluted from solution provided by the CS supplier)
(3): the brine is a 28 wt% $CaCl_2$ solution (diluted from 1M solution provided by the CS supplier)

Table 5.5. Performance of the CS Variants in Test 1 With a 4 hr Design Gel Time

Specifications	Required	CS-1A(1)	CS-2A(2)	CS-3A(3)
No Soil (Test 1a)	~4 hr to gel time (State 2)	**Pass** 4.75 hrs	**Marginal** 3.2 hrs	**Fail** 2.0 hrs
No Soil (Test 1a)	~2 x gel time to solidification	**Marginal** 8.15 hrs	**Pass** 6.6 hrs	**Pass** 3.35 hrs
Soil S2 (Native SR Soil)	~4 hr to gel time (State 2)	**Marginal** 5.65 hrs	**Fail** 15.6 hrs	**Fail** 2.15 hrs
Soil S2 (Native SR Soil)	~2 x gel time to solidification	**Fail** >21 hrs	**Fail** >27 hrs	**Fail** 7.45 hrs
Soil SS2 (Simulated Soil)	~4 hr to gel time (State 2)	**Fail** 7.05 hrs	**Fail** 2.5 hrs	**Pass** 3.9 hrs
Soil SS2 (Simulated Soil)	~2 x gel time to solidification	**Marginal** 15.0 hrs	**Pass** 5 hrs	**Pass** 8.2 hrs

(1): the brine is a 24 wt% $CaCl_2$ solution (diluted from 1M solution provided by the CS supplier)
(2): the brine is at a 80% concentration (diluted from solution provided by the CS supplier)
(3): the brine is a 24 wt% $CaCl_2$ solution (diluted from 1M solution provided by the CS supplier)

Table 5.6. Performance of the CS Variants in Test 1 With a 8 hr Design Gel Time

Specifications	Required	CS-1A(1)	CS-2A(2)	CS-3A(3)
No Soil (Test 1a)	~8 hr to gel time (State 2)	**Pass** 7.0 hrs	**Pass** 8.2 hrs	**Pass** 8.25 hrs
No Soil (Test 1a)	~2 x gel time to solidification	**Fail** 10.65 hrs	**Fail** 11.5 hrs	**Fail** 12.0 hrs
Soil S2 (Native SR Soil)	~8 hr to gel time (State 2)	**Fail** >21 hrs	**Fail** 16 hrs	**Fail** >10.5 hrs
Soil S2 (Native SR Soil)	~2 x gel time to solidification		**Fail** >38 hrs	
Soil SS2 (Simulated Soil)	~8 hr to gel time (State 2)	**Fail** 15.0 hrs	**Pass** 6.0 hrs	**Pass** 9.25 hrs
Soil SS2 (Simulated Soil)	~2 x gel time to solidification	**Pass** 30.0 hrs	**Fail** 9 hrs	**Pass** 16.75 hrs

(1): the brine is a 20 wt% $CaCl_2$ solution (diluted from 1M solution provided by the CS supplier)
(2): the brine is at a 72.5% concentration (diluted from solution provided by the CS supplier)
(3): the brine is a 20 wt% $CaCl_2$ solution (diluted from 1M solution provided by the CS supplier)

Table 5.7. Performance of the CS Variants in Tests 2 and 3

Specifications	Required(*)	CS-1A	CS-2A(1)	CS-2A(2)	CS-3A
Test 2 - Soil S1 (Native SR Soil)	Pressure ratio criterion(<2.5)	**Pass** 0.67	**Fail** 5.6	**Pass** 0.53	**Pass** 1.1
Test 2 - Soil S1 (Native SR Soil)	Gel time criterion ($1.5 \leq t_0 \leq 2.5$)	**Pass** 1.73 hrs 1h:44 m	**Pass** 2.33 hrs 2h:20m *3:50 to gs 9*	**Fail** 13.83 hrs 13h:50m *18:28 to gs 9*	**Pass** 1.87 hrs 1h:52 m
Test 2 - Soil S2 (Native SR Soil)	Permeability criterion	**Pass**	**Pass**	**Pass**	**Pass**
Test 2 - Soil SS2 (Simulated Soil)	Pressure ratio criterion(<2.5)	**Pass** 1.9	**Fail** 6.1	**Pass** 0.87	**Pass** 1.7
Test 2 - Soil SS2 (Simulated Soil)	Gel time criterion ($1.5 \leq t_0 \leq 2.5$)	**Fail** 4.3 hrs 4h:18m	**Pass** 2.35 hrs 2h:21m *2:21 to gs 9*	**Fail** 2.83 hrs 2h:50m *4:40 to gs 9*	**Pass** 1.6 hrs 1h:36m
Test 2 - Soil SS2 (Simulated Soil)	Permeability criterion	**Pass**	**Pass**	**Pass**	**Pass**
Test 3 (m/sec)	Hydraulic Conductivity $\leq 10^{-10}$ m/sec	**Pass** 1×10^{-10} ±10%		**Pass** 4×10^{-11} ±10%	**Pass** 9×10^{-11} ±10%

(1): the brine is at a 100% concentration (undiluted, as provided by the CS supplier)

(2): the brine is at a 89% concentration (diluted from solution provided by the CS supplier)

Table 5.8. CS Testing Results in Tests Not Included in the RFP (Savannah River Soil S2)

Specifications	Required	CS-1A	CS-2A	CS-3A
Drain-in test	Flow without gelling	**Pass**	**Pass**	**Pass**
Drip test	Controllable gel time	Anomalous **Marginal**	**Fail**	**Pass**

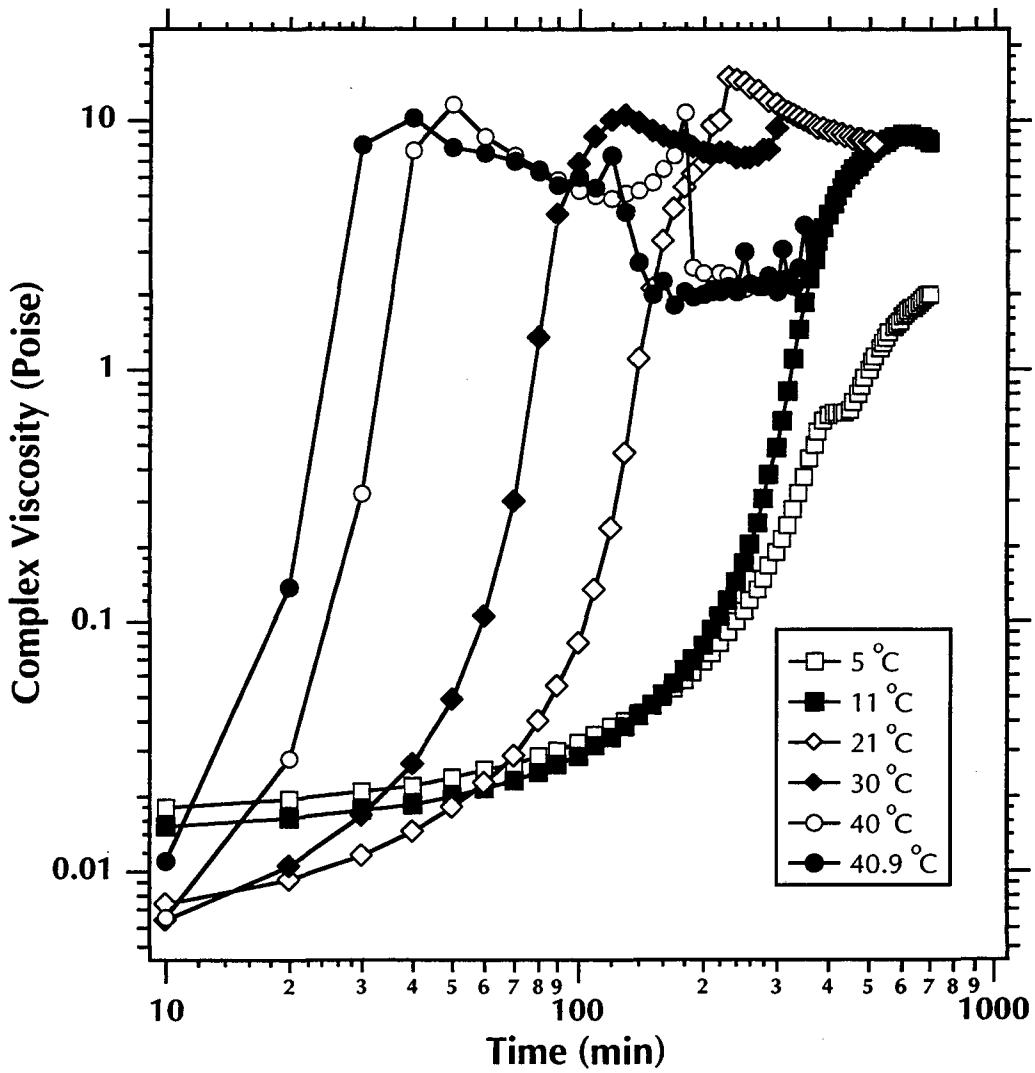

Figure 5.5. Effect of temperature on the complex viscosity of CS-3A.

5.7.3. CS Permeation and Gelling in Sludge

Using a clean sludge, we determined that (a) the gelation of CS was not inhibited by the presence of the sludge, (b) sludge retards the gelation of CS (**Figure 5.6**), and (c) the slower gelation rate does not seem to pose a significant problem as it can be compensated by adjusting the electrolyte concentration and/or by the higher temperatures expected during injection. The slower gelation may be partially attributed to CS dilution due to the high water content of the sludge.

Assuming that the radioactively-contaminated sludge in the 281-3H retention basin is not significantly different, a similar (if not identical) behavior is expected, because the controlling factor in the gel retardation is the amount of organic acids in the sludge. The amount of radioactive cations (mainly Sr, Cs, Pu) is too low to influence the gel behavior, and we do know from previous experiments that radioactivity has no effect on the behavior and stability of the CS gel.

Water and a long-gel-time CS grout (8 hr gel time) were tested under gravity-head conditions in columns filled with sludge. From the rate of percolation, the hydraulic conductivity of the sludge was estimated at 10^{-8} m/sec. Penetration of the CS grout into the sludge over the time of the experiment (i.e. until gelling occurred) was about 1 cm.

Additional water and CS grout injection tests at higher pressures (68.9KPa, i.e. 10 psi) did not yield very useful data, because the sludge permeability varied (decreased) during injection. This was expected due to the very considerable yield and extrusion potential of the sludge, and confirmed our expectation that, although CS could be injected, it would not permeate the sludge.

5.7.4. CS Permeation and Gelling in Remolded S1 Soils

Native SRS S1 soil was remolded to a density of 80-85% of Standard Proctor, and was tested for CS injectability and permeation. Water and CS were injected into the soil in column tests. From the analysis of the injection pressures (less than 28KPa, i.e. 4 psi) and rates (**Figure 5.7**), the hydraulic conductivities of the two soil packs were respectively estimated at 1.2×10^{-5} and 2.5×10^{-5} m/sec. These values are quite large, and indicate easy and fast injection into the remolded native soil.

Effluent samples in fractions of 0.1 Pore Volume (PV) were collected from the soil pack which had been injected with the CS grout. The gelling of the first fraction was retarded the most; each succeeding fraction gelled more rapidly, approaching the design gel-time of the injected CS (**Figure 5.8**). This behavior is entirely consistent with our previous experience in a variety of soils.

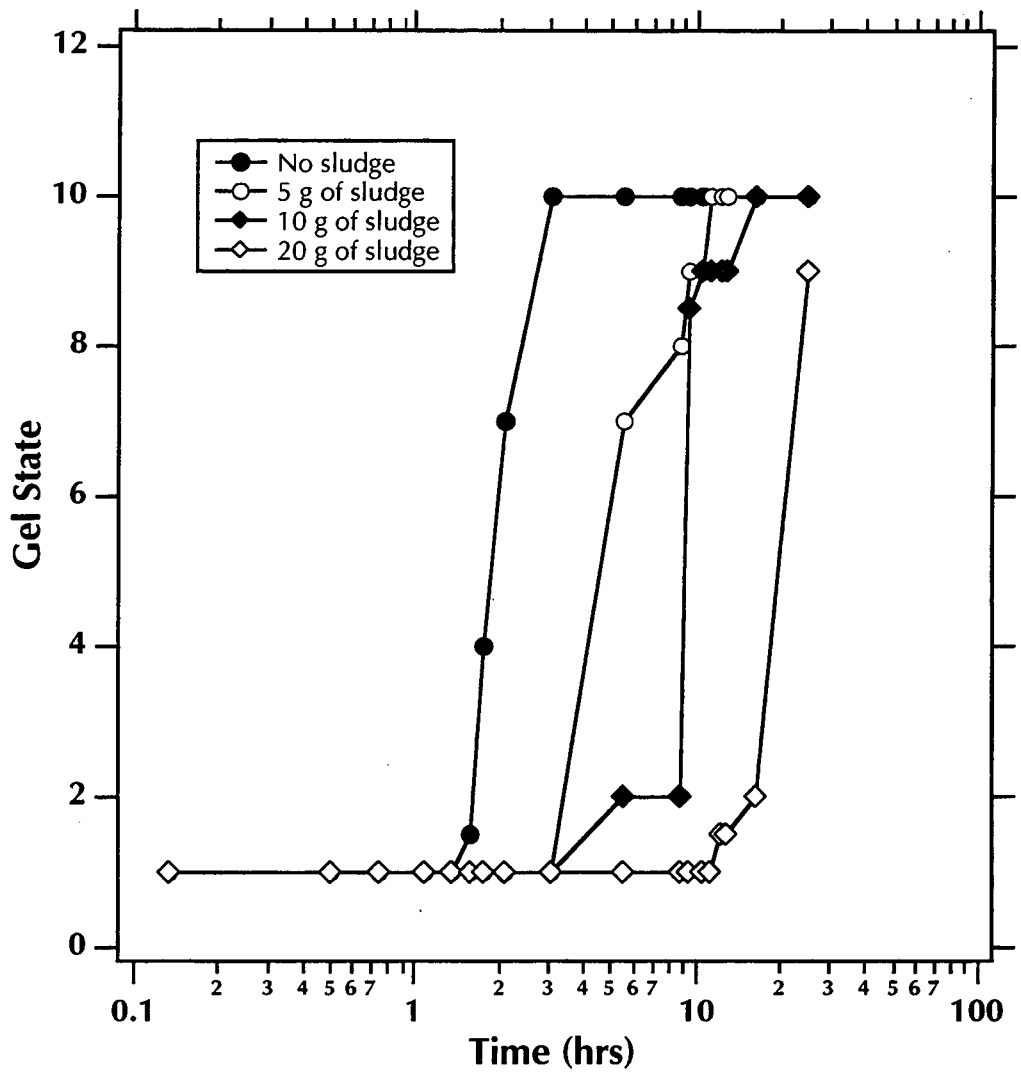

Figure 5.6. Effect of sludge on the gel time of CS-3A.

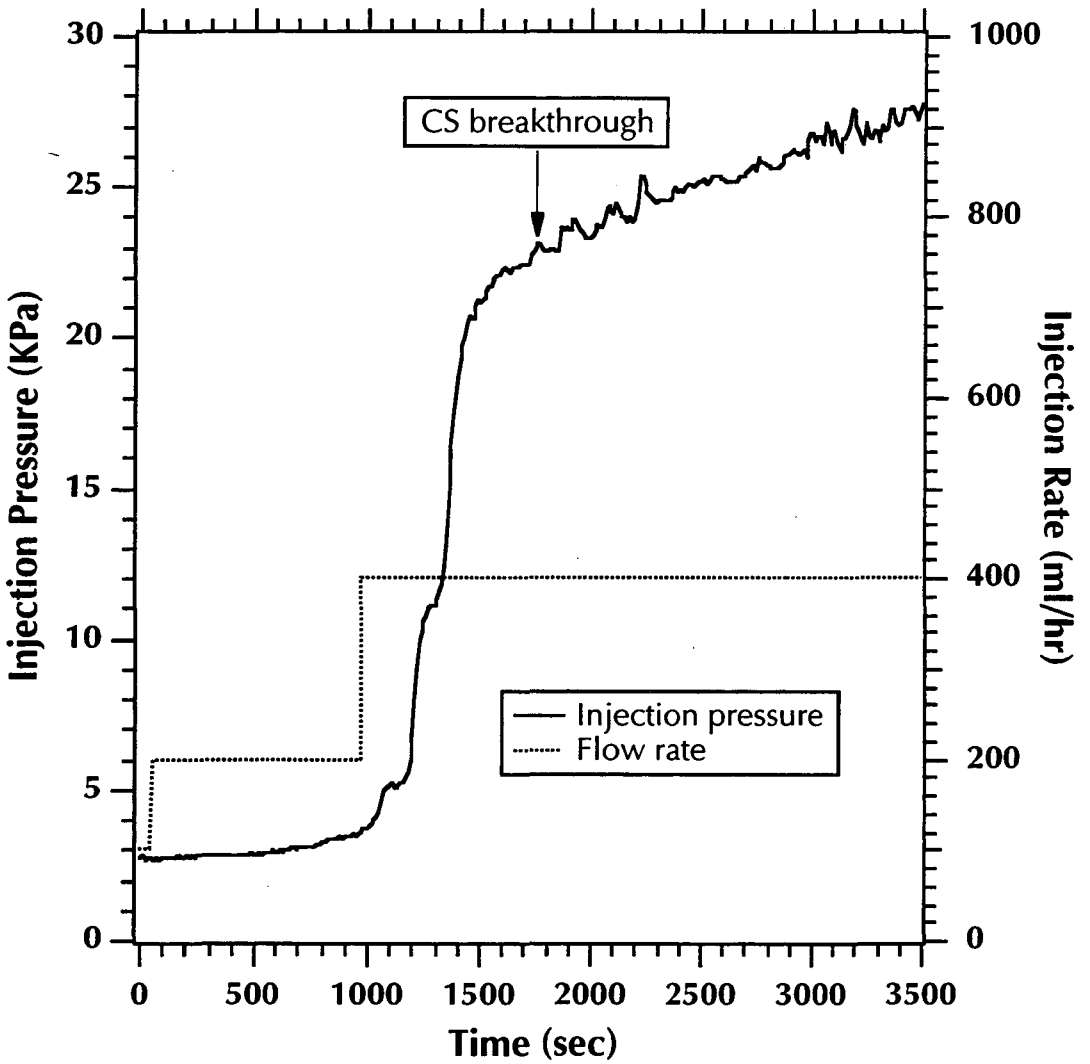

Figure 5.7. Pressure and flow rate during CS-3A injection into remolded S1 soil.

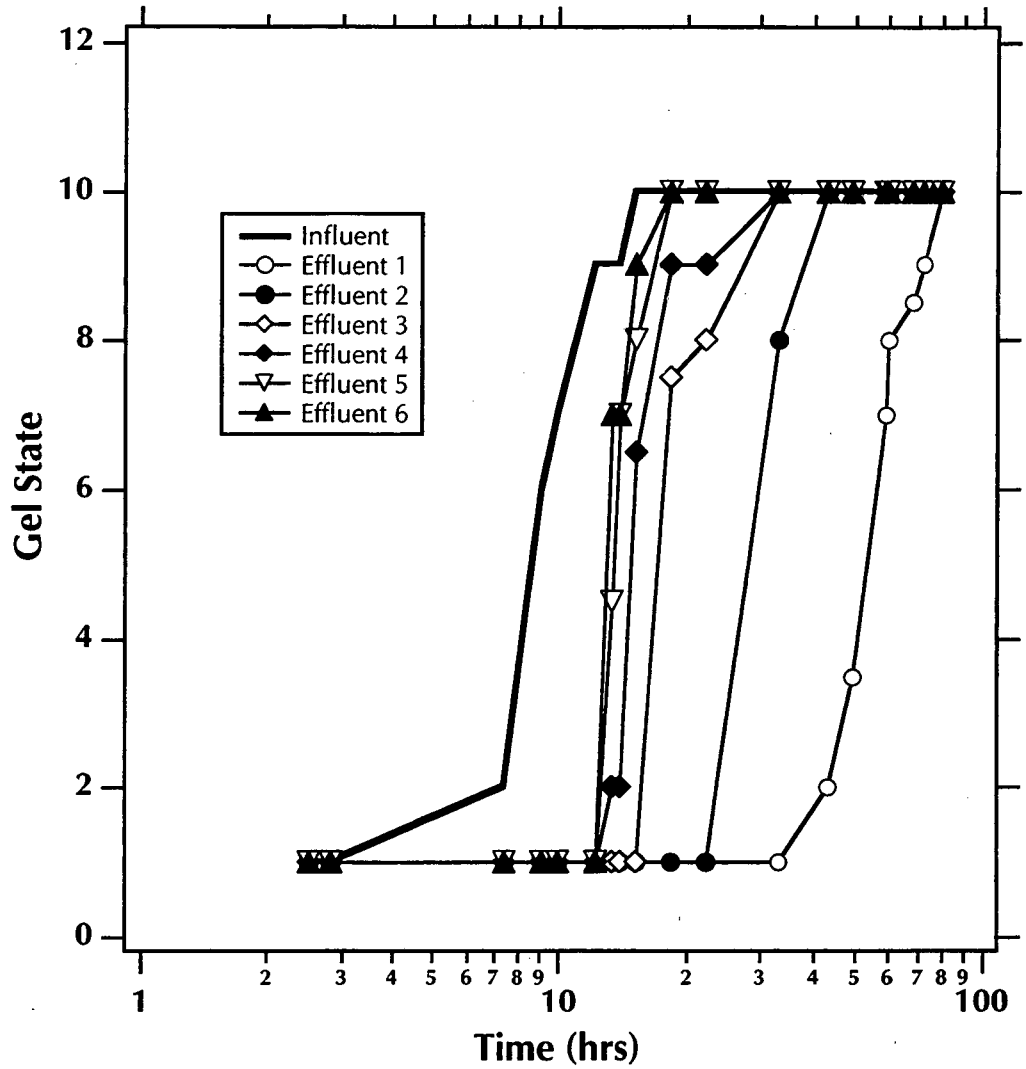

Figure 5.8. Gel time of CS-3A effluent from a column of remolded S1 soil. Each effluent number corresponds to fractions of 0.1 PV.

5.7.5. Effect of γ-Radiation

Two S2 soil cores (one to be used as a control and one to be irradited) were grouted using the CS-3A variant. Exposure to γ-radiation determined that permeability of the CS-grouted core was practically unaffected. The core was exposed to a Co-60 source with a dose rate of 1441 Rem/hr for a period of 3 days, accumulating a dose of 103,696 Rem. This dose is 144,711 times higher than the dose of the total Cs-137 in the basin accumulated after one half-life (≈30 years) decay (based on 33,000 pCi/g measured in SRS soils).

Subsequent laboratory testing determined that the hydraulic conductivities of the irradiated and the control cores were 5.9×10^{-11} m/sec and 1.0×10^{-10} m/sec respectively. Although we did not test the same core before and after irradiation (in order to avoid possible core disturbance due to handling and transportation), the hydraulic conductivity of the irradiated grouted core was close to the minimum possible, indicating an insensitivity of CS to radiation.

6. VERIFICATION AND MONITORING

Monitoring and verification are discussed in this section. A brief overview of sensors and equipment is given, specifications are presented, and the verification implementation plan is discussed.

6.1. Design Parameters, Issues, Implications and Requirements

(a) Surface Ground Penetrating Radar (GPR) surveys are conducted before and after barrier emplacement.

(b) GPR surveys are conducted before and after barrier emplacement using
- 5 vertical 9.15-m (30-ft) wells
- 24 vertical 1.83-m (6-ft) probes (see **Figure 6.4**)
- an unspecified number of horizontal wells underneath the basin

(c) 10 piezometers are installed at a depth of 35 ft using the lance injection equipment (see **Figure 6.2**).

(d) 35 Multifunction Hydrologic Probes (MHPs) are installed on a regular grid using the lance injection equipment or CPT (see **Figure 6.2**)

(e) 63 Dual-Function Probes (DFPs) are installed on a regular grid using the lance injection equipment (see **Figure 6.3**).

6.2. Sensors and Equipment for Barrier Verification

6.2.1. Overview

The objective of hydrologic sensor installation is to provide a means to assess the performance of the emplaced barrier. The sensor network will provide measurements of hydraulic head, tensiometric potential, and parameters to estimate permeability.

Drive point piezometers will be used to measure the hydraulic head around the perimeter of the basin. DFPs measure pressures using pressure transducers and provide access ports for gas tracer testing and gas permeability measurements.

MHPs will be used to

- provide access ports for gas tracer testing and gas permeability measurements
- measure hydraulic head using pressure transducers, and
- assess the tensiometric potential above the water table.

MHPs will allow *in-situ* measurements of permeability above and below the water table. **Figure 6.1** shows the concepts of the DFP and the MHP, as well as important design parameters.

6.2.2. Drive Point Piezometers

The lance injection truck will be used to install drive point piezometers in the ground. The drive point probes will be installed at 10 locations outside the perimeter of the targeted injection area to a depth of 10.7 m (35 ft). The locations of the piezometers are shown in **Figure 6.2**. These piezometers will be instrumented with pressure transducers that are polled by computer controlled logging equipment. The information will be transmitted in real time over a modem to the Berkeley Lab for analysis. The information from these piezometers will provide baseline regional information for the more detailed monitoring that will occur within the grouted region.

The drivepoint piezometer consists of a stainless steel tube, 0.035 m (1.375) in diameter, which is driven into the ground using the same lancing technique that is used for barrier fluid injection. The piezometer is installed with an expendable tip that has a permeable section sheathed within the tube. Once the tube has reached its targeted depth it is disconnected from a drive rod on the lance truck. The expendable tip is pushed down to expose the permeable section. A pressure transducer is lowered down the tube and the cable is run through a fitting threaded into the tube tip.

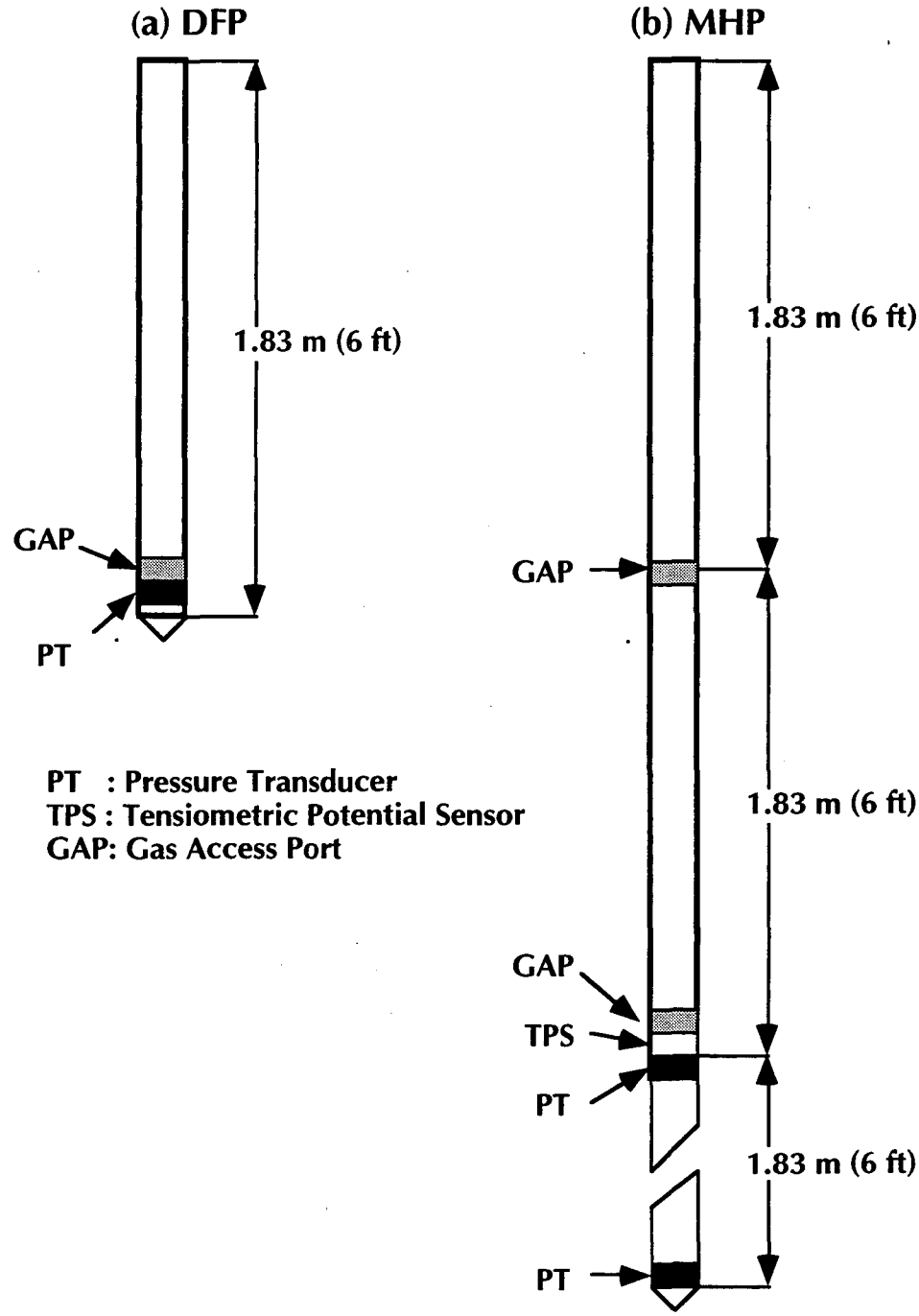

Figure 6.1. Schematic of (a) the Dual-Function Probe (DFP) and (b) the Multifunction Hydrologic Probe (MHP).

6.2.3. Multifunction Hydrologic Probes (MHP)

A sketch of an MHP is shown in **Figure 6.1**. 35 MHPs will be emplaced at the locations indicated in **Figure 6.2**, within and below the targeted injection zone. Because of the difficulties of injecting the barrier with a large number of sensors and their accompanying wires and tubes interfering with vehicle mobility, an iterative approach will be used. The sensors will be installed prior to grout injection, will be grouted in place, but will become connected to the data aquisition systems after completing the CS injections. The MHPs will be logged using the same equipment that is used for the monitoring of the drivepoint piezometers.

Three groups of sensors are included in the MHP. The top group remains immediately above the barrier, the middle group below, and the bottom group is located in the saturated zone. The various types of instruments and their locations are shown in **Figure 6.1.**

MHP emplacement could use the same lance injection truck as will be used for barrier emplacement or a standard CPT system if the stainless steel casing of the MHP is larger than 0.035 m (1.375 in) in diameter. A specially designed injection rod with expendable tips will be used to drive in the sensor to the targeted installation location. The expendable tip will be pushed out and the sensor lowered down the rod. The lance will then be withdrawn to a height six inches above the sensor. Clean sand will be used to fill the annulus around the sensor up to the bottom of the lance. Finally, the lance will be withdrawn and the void will be backfilled to the surface or to the depth of the next sensor package.

6.2.4. Dual-Function Probes (DFP)

A sketch of a DFP is shown in **Figure 6.1**. 63 DFPs will be emplaced at the locations indicated in **Figure 6.3**, within and above the top of the barrier. DFPs have two groups of sensors: an access port for use in gas tracer and/or air permeability tests and pressure transducers to detect air pressure changes. DFPs are inserted into the ground after completing injection, and their tips are located just above the top of the barrier. DFPs consist of a stainless steel tube, 0.035 m (1.375 in) in diameter and 1.83 m (6 ft) in length, and are installed using the same lancing technique.

6.2.5. Gas Tracer Analysis and GPR Instrumentation

Commercially available models will be used for this task. The gas tracer sensors will be connected to the access ports of the DFPs and MHPs.

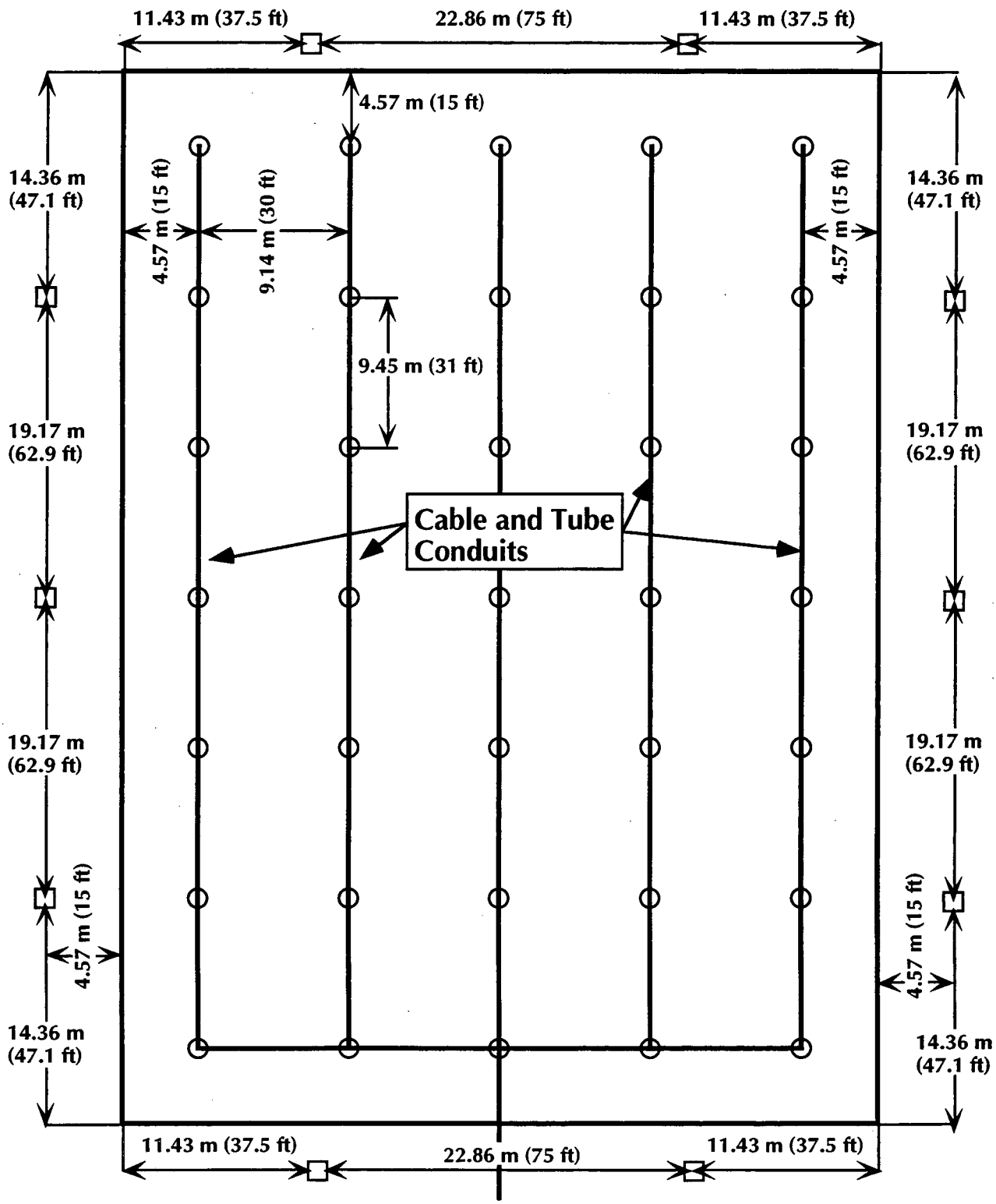

Figure 6.2. Locations of piezometers (squares) and MHPs (circles), as well as layout of the tube and cable conduits for data aquisition.

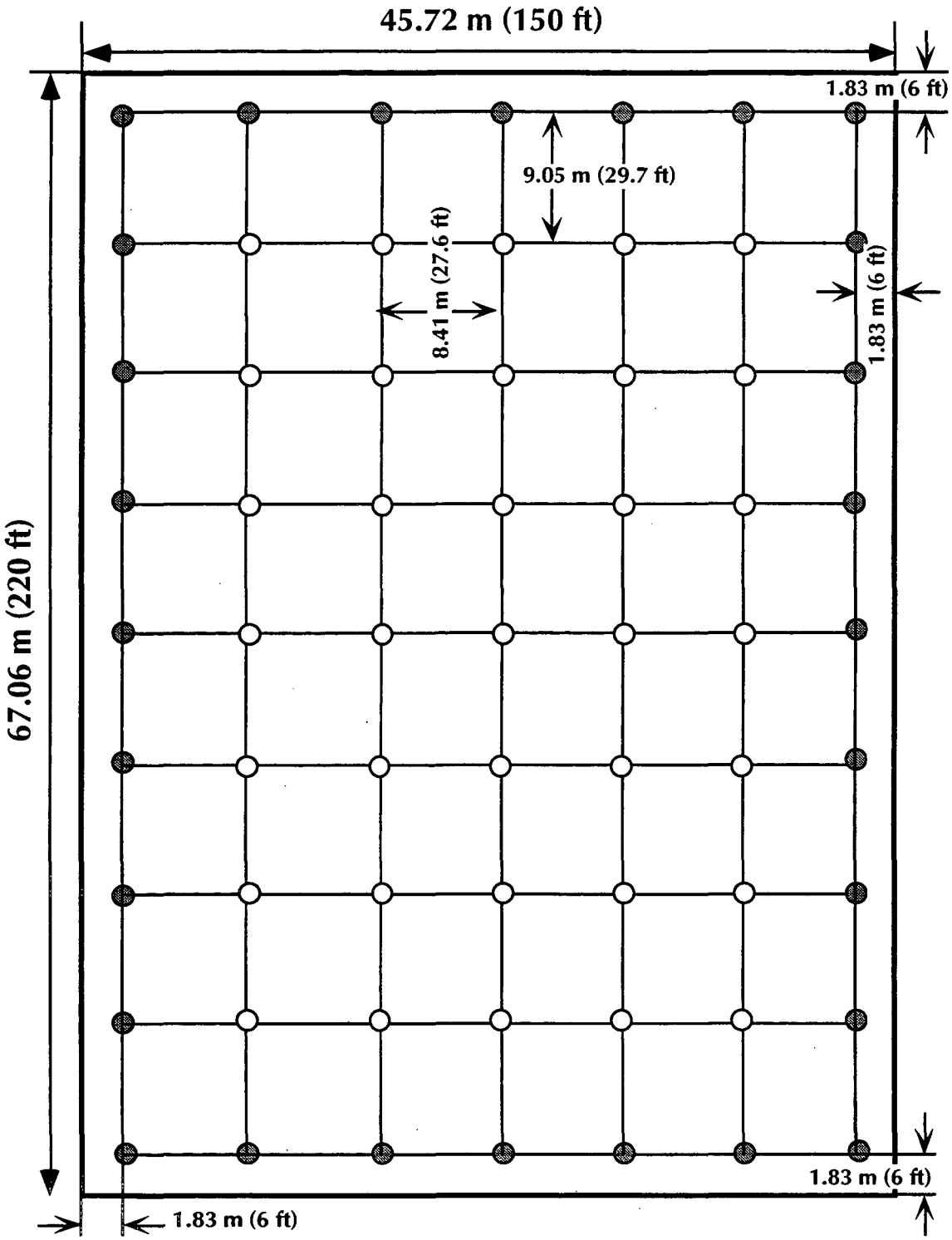

Figure 6.3. Layout of the DFP array.

6.3. Pre-Injection Monitoring- and Verification-Related Activities

(a) The wells resulting from the 9.15-m (30-ft) continuous cores (obtained from 5 locations for contaminant characterization) are completed and equipped for GPR studies.

(b) Horizontal wells are drilled underneath the target area for GPR measurements from below the barrier.

The possibility of a number of potential problems related to the drilling of horizontal wells must be considered. Namely:

- Because the surrounding soils have low permeabilities, the presence of an open well communicating with the formation could disrupt the hydraulic measurements (i.e. the direct measurements of the most important parameter of interest) by short-circuiting flow patterns. Therefore, the well must be grouted and not communicate at all with the formation. In addition, health and safety issues preclude bringing contaminated water to the surface, an inevitable event if the well is not isolated from the formation.
- If closed (isolated) wells are to be installed, these are notoriously difficult to grout and isolate and can leave (due to incomplete grouting or grout shrinkage) very conductive pathways. This raises the problem previously discussed. In essence, use of GPR might jeopardize **H**ydraulic, **P**neumatic and **T**racer (HPT) measurements, the most reliable and relevant method monitoring and verification.
- With the current design, a total of 45 metal tubes will extend to a depth of 10.7 (35 ft) from the surface. The question which needs to be answered is whether the presence of so many metal tubes could disturb the GPR measurements. Due to the extremely high resistance to penetration of the soil at the site, there is no alternative, but to using metal tubes.
- For GPR from underneath to be useful, measurements must be made before and after the CS barrier emplacement. Potential scheduling problems requirements must be resolved and institutional/regulatory requirements met before the beginning of injection.

(c) GPR surveys (surface, using the 5 vertical wells, and subsurface) of the site are conducted.

(d) 10 drive-point piezometers are installed outside the perimeter of the basin using the lance system.

(e) 35 MHPs are installed on a regular grid within the perimeter of the basin using the lance system. The metal-tube housing of the probes can be up to 0.051 m (2 in) in diameter, and either the lance system or CPT could be used to install them.

(f) Hydrologic data collection from the piezometers begins. Because the basin will be isolated, the piezometric head is expected to begin falling immediately after tbarrier installation. However, due to the naturally low permeability of the SR soils,

- the decline is expected to be slow, and
- care must be taken to isolate the basin effects from the regional groundwater fluctuations.

6.4. Monitoring and Verification During Emplacement

(a) The injection presssures and flow rates of CS will be monitored during the barrier emplacement. This will provide continuously updated information on the distribution of the subsurface permeability (giving the measure of anticipated behavior in the vicinity of the last injection) in preparation of the next injection, as well as the measure of the total injected CS volume.

The field operations contractor and LBNL will be jointly responsible for the task.

(b) The CS barrier location and thickness are determined by employing inverse modeling of the pressure and flow rate data [*Finsterle et al.*, 1995].

(c) The MHPs in the covered (grouted) areas are connected to the data collection system and data recording begins (LBNL). While grouting operations continue, data from the two lower groups of sensors are collected: pressure and potentiometric values from the middle group, and piezometric data from the bottom group.

6.5. Post-Emplacement Verification

For barrier verification, HPT methods will be used for direct measurements of the barrier permeability to confirm compliance with the regulatory requirement of a maximum hydraulic conductivity of 10^{-7} cm/sec. GPR will be used to determine (to the extent possible) the CS barrier location and thickness, providing the information for satisfying the second requirement of the TS.

The sensors discussed in subsection 6.2 will be used for the hydraulic barrier verification. Two types of hydraulic tests will be employed: short-term active tests, and long-term passive tests (monitoring). Before and during the lancing process a number of wells and pressure probes will be installed. It must be pointed out that there will be NO open wells within the isolated basin, and all the probes will be safely placed under the basin cover.

In the short-term tests (a) air and (b) gaseous tracers will be injected into the subsurface underneath the barrier using the access port of the middle group. Pressure and gas tracer concentration will be monitored at all the other pressure sensors and gas access ports above (and below) the barrier . A limited number of such active tests is being planned.

The long term tests do not involve water injection, but will instead involve the monitoring of pressures at the sensors outside, inside, and within the barrier zone in response to seasonal fluctuations of the regional water-table. An effectively isolated basin would demonstrate a change in pressure outside the barrier, and no response inside and within the barrier zone. Pressure monitoring is expected to continue for several months or years, until the necessary data to demonstrate isolation has been collected. The pressure probes can safely continue to gather data for a very long time.

Barrier verification will be accomplished by determining *in situ* permeability from measurements of hydraulic head. Hydraulic head and moisture potential fluctuations occur naturally due to seasonal changes in the water table, rain events, atmospheric loading, and earth tidal effects. At all the piezometers in the saturated zone the piezometric head will be continuously monitored using pressure transducers. Above the water table the pressure transducers will be operated as tensiometers to reflect moisture potential.

GPR will be used to determine the location and thickness of the barrier. To accomplish this, GPR measurements will be made from:

- the five vertical wells
- surface surveys
- subsurface horizontal wells
- 24 vertical access ports installed immediately after the end of injection (**Figure 6.4**).

All the GPR measurements will be conducted before the installation of the DFPs so as to minimze the effect of metal on the measurements. The verification implementation at this stage of the project includes the following activities:

(a) All MHPs are connected to the data collection system.

(b) 24 vertical access tubes (12 inside and 12 outside the basin) for GPR measurements are installed using the lance system.

(c) GPR surveys (surface, using the 5 vertical wells and the 24 access tubes, and subsurface) of the site are conducted.

(d) 63 DFPs are installed on a regular grid within the perimeter of the basin above the barrier using the lance system.

(e) Air and gaseous tracers are injected underneath the barrier, the responses of the various sensors are recorded, and the areal distribution of the barrier permeability is determined.

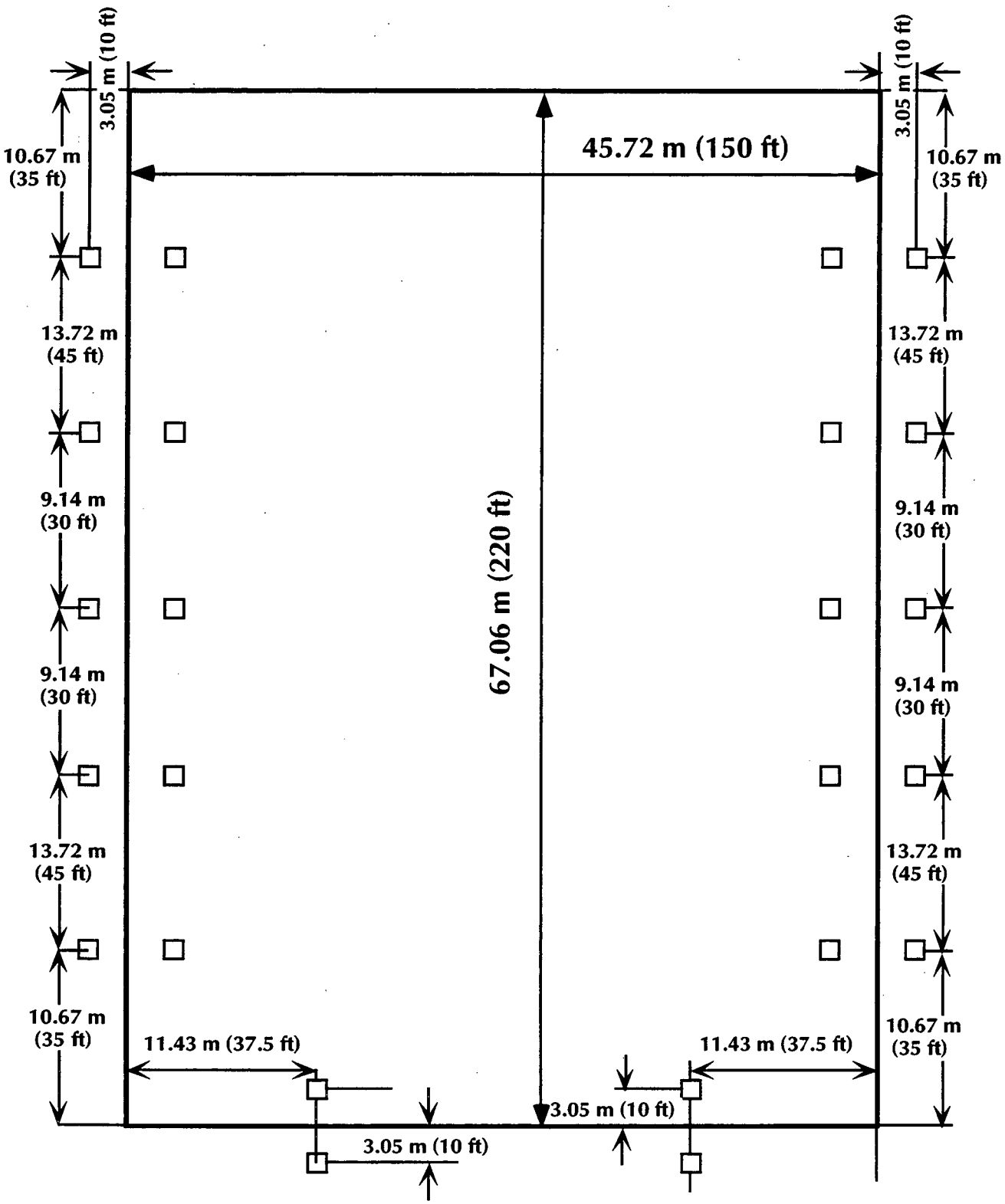

Figure 6.4. Layout of the GPR vertical access tubes.

(f) Based on the results of the air injection and gas tracers (as supported and enhanced by the GPR analysis in c), weak areas of the barrier with incomplete CS coverage are identified.

(g) Following the data analysis in 2.6.f, if areas of the barrier are found to not be in compliance with the design criteria for permeability and thickness, finishing and *touch-up* CS injection operations begin and target incompletely grouted horizons.

7. THE LANCE WATER INJECTION TEST (LWIT)

In this test we discuss the results and consequences of a Lance Water Injection Test (LWIT) conducted in the immediate vicinity of the 281-3H basin. The LWIT was a vital characterization step (see Section 3), as well as a precursor to the field application of the VLB techhnology because it involved the same type of equipment intended for use during the CS barrier emplacement. A detailed discussion of the LWIT can be found in the companion report of *Freifeld et al.* [1996].

7.1. Objectives of the LWIT

The objectives of the LWIT were as follows:

(a) To evaluate the general performance of the lance injection technique for grout emplacement at the site, including the range and upper limits of injection pressures and flow rates applicable for site conditions, and the mechanical forces needed for lance penetration.

(b) To obtain detailed information on the injectability of the soils immediately adjacent to the H-area retention basin.

(c) To identify any high permeability zones and evaluate their spatial distribution.

7.2. Synopsis of the LWIT Results

Here we summarize the most important results and observations of the test [*Freifeld et al.*, 1996]:

(a) A very hard layer (characterized by kaolinitic clay and quartz pebbles) was identified at a depth between 1.5 m (5 ft) and 3 m (10

ft) below the land surface. This stratum seemed to be continuous over the tests plot area.

(b) At the hard layer, holes were augured and split spoon samples were taken to a depth at which the lance system could resume operation. The bottom of the hard layer was generally 4.3 to 4.9 m (14 to 16 ft) below land surface.

(c) The force available to the particular lance injection system used in the LWIT was insufficient to penetrate this hard layer; a heavier system was needed for the task. It appears that only a fraction of the 89,000 N (20,000 lbs) of the weight of the lance injection truck was available for lance penetration.

(d) Above the hard layer the injection rates were invariably below the detection limit of our instruments (i.e. 0.01 L/min, corresponding to a soil hydraulic conductivity of less than 1.6×10^{-8} m/sec at pressures as high as 827 kPa (120 psi).

(e) At the hard layer the injection rates were invariably below the detection limit of our instruments (i.e. 0.01 L/min, corresponding to a soil hydraulic conductivity of less than 1.6×10^{-8} m/sec at pressures as high as 1,380 KPa (200 psi). This layer seems to have considerable mechanical strength, as it did not show any signs of fracturing at these high pressures. It must be pointed out that these data were obtained from the top boundary of the hard layer; no field hydrologic data could be acquired within the hard layer.

(f) Below the hard layer we identified injectable strata. Most injectable intervals were between 6 m and 9 m (20 and 30 ft). Although some correlation could be found between adjacent holes, no continuous injectable layer could be identified. There was very little vertical correlation at each hole, and intervals 0.3 m (1 ft) apart could exhibit drastically different behavior.

(g) Soil fracturing was frequently observed below the hard layer at injection pressures ranging between 380 and 760 KPa (55 to 110 psi). Such soil fracturing was characterized by a sudden drop in injection pressure coupled with a jump in the injection rate. For permeation grouting, however, under the conditions of the radionuclide-contamination at the basin, such fracturing is undesirable.

(h) Below the hard layer, the injection rates before obvious fracturing were as high as 2 L/min at relatively high pressures 620 KPa (90 psi). There is no direct evidence, however, that the uptake before fracturing was not due to yielding (a distinct possibility in the kaolinitic soils at those depths).

(i) Even at reasonable injection rates, the pressure and injection rate data indicate a relationship which cannot confirm permeation grouting. Although numerical simulation managed to predict similar (to the measurements) behavior, there is strong indication that the water uptake is not due to permeation but to incipient yielding or soil

fracturing. This would not be uncommon in the clay-rich soils of the subsurface at the site. If this is the case, numerical simulation could not presently predict such behavior because none of the available models of flow and transport account for effects in soils with significant yield.

7.3. Conclusions and Implications

Considering the goals of the project and the hydraulic behavior and properties of the site, we felt that an attempt to install a barrier underneath the basin according to any of the discussed conceptual models **could not be defended scientifically** for a number of reasons:

(a) near-zero or low permeabilities (and consequently impractically long injection times),

(b) strong evidence indicating lack of continuity of the injectable zones,

(c) no compelling evidence that the water uptake was due to permeation and not to fracturing/yielding,

(d) tendency of the soils to fracture at the injection pressures needed to effect reasonable injection rates, and

(e) inability to permeate the contaminated sludge lying on the bottom of the basin (emplacement of the barrier in the contaminated fill above the sludge would leave significant contamination in the sludge outside the containment system).

Following these conclusions, a decision was reached to discontinue the attempt to emplace a VLB at the 281-3H retention basin. Consequently, no further design analyses (e.g. simulations to optimize lance spacing, injection sequence, CS gel time, etc.) were conducted.

In concluding, it is important to emphasize that the inability to emplace a VLB barrier at the 281-3H basin **must under no circumstances be misinterpreted** as a failure of the VLB technology. For a successful VLB application, a minimum hydraulic conductivity of 10^{-6} m/sec is required, with a grain size distribution of less than 20% passing through a #200 sieve (although the latter is not critical if the permeability criterion is met). The very low permeabilities at that site preclude any kind of permeation, and an attempt to apply the VLB technology by injecting into the undisturbed native soils would be tantamount to trying to inject a barrier liquid into a site which may already be a natural barrier. It is important to clarify that our effort was not intended to determine the natural containment ability of the site, as this would have been beyond the scope of this project.

8. SUMMARY AND CONCLUSIONS

This report is a description of the design study for a pilot-scale field demonstration of a new subsurface containment technology for waste isolation developed at the Lawrence Berkeley National Laboratory, in which Colloidal Silica (CS, a new barrier liquid) is used for permeation grouting. The demonstration site was Retention Basin 281-3H, a shallow catchment basin at the Savannah River Site (SRS) originally built to control contaminated runoff from the H Reactor, and which has been contaminated mainly by radionuclides. Of particular concern were ^{137}Cs, ^{90}Sr, and ^{238}Pu. The basin dimensions were originally designed to be 200 ft by 120 ft by 6 ft. Most of the contamination (estimated at about 200 Ci) was believed to be contained in the first 1-2 ft from the surface and from the basin bottom.

The specific objectives of this study were:

(a) To demonstrate the ability to create a continuous subsurface barrier isolating the contaminants.

(b) To demonstrate the continuity, performance, and integrity of the barrier, and its compliance with the functional requirements [*WSRC*, 1996].

The functional requirements included:

(1) Spatially averaged hydraulic conductivity between the isolated soil volume and the surroundings of 10^{-9} m/sec or less.

(2) Demonstrated lack of hydraulic communication between the isolated volume and the surrounding soils.

(3) Minimum cumulative thickness of the grouted soil horizons in the direction of potential flow of 0.9 m (3 ft).

The site geology, pedology, geochemistry, and hydrology were studied. Preliminary hydraulic conductivity data were obtained from the laboratory analysis of Shelby tube and split-spoon cores from locations adjacent to the basin, and indicated the possibility of permeable zones as targets for injection. This information, however, was insuffiecient for the development of the design for the barrier emplacement, and a field study to measure the *in situ* hydraulic conductivity was deemed necessary. The state

of knowledge on the contaminant characterization was reviewed, and the necessary activities to fill important knowledge gaps were discussed.

Based on the site characteristics and the functional requirements, a conceptual model was developed that involved the sealing of all permeable zones to a depth of 6 m. The barrier geometry and specifications were defined, and lance injection was selected as the emplacement method. The injection strategy and patterns, as influenced by the saturation conditions of the subsurface, were analyzed using numerical simulations. Baseline calculations and numerical simulations were conducted to determine the effect of soil conditions and properties on the injection pressure and flow rates. Curves relating injection pressures to injection rates, as influenced by the soil hydraulic conductivity and saturation, were developed.

The site soils appeared to delay gelling, a behavior attributed to the high organic content of the soils. An appropriate CS variant was selected as the barrier liquid based on its relative insensitivity to interactions with the site soils. Although the SRS soils had an effect on the gelation behavior of the CS, this effect was controllable. The selected CS had a viscosity of about 4.5 cP and a density of about 1.2 g/cm^3. Laboratory experiments demonstrated that the selected CS could easily penetrate and grout disturbed site soils remolded to a density of 80-85% of standard Proctor. Tests with sludge similar to that present at the bottom of the basin indicated that the sludge retarded the CS gelling, but could still be controlled. However, injection into the sludge was not possible due to its impermeability and tendency to deform or be extruded.

A barrier verification strategy including hydraulic, pneumatic, tracer, and geophysical methods, was developed. The location, layout and configuration of the appropriate sensors was designed, and a sampling strategy to minimize potentially adverse interactions between the various verification methods was devised.

The hydraulic conductivity data obtained from the soil cores were insufficient to fdesign the barrier. Therefore, a Lance Water Injection Test (LWIT) was conducted in order to obtain representative estimates of the hydraulic conductivity and its distribution, and thus identify injection zones. Additionally, the LWIT was expected to provide technical information on the general performance of the lance injection technique for grout emplacement at the site, including the range and upper limits of injection pressures and flow rates applicable for site conditions, and the mechanical forces needed for lance penetration. The LWIT demonstrated the absence of any permeable zones suitable for injection.

Considering the goals of the project and the hydraulic behavior and properties of the site, the installation of a barrier underneath the basin could not be defended scientifically for a number of reasons:

(a) near-zero or low permeabilities (and consequently impractically long injection times),
(b) strong evidence indicating lack of continuity of the injectable zones,
(c) no compelling evidence that the water uptake was due to permeation rather than fracturing/yielding,
(d) tendency of the soils to fracture at the injection pressures needed to effect reasonable injection rates, and

(e) an inability to permeate the contaminated sludge lying on the bottom of the basin. Emplacement of the barrier in the contaminated fill above the sludge would leave significant contamination in the sludge outside the containment system.

Following these conclusions, a decision was reached to discontinue the attempt to emplace a VLB at the 281-3H retention basin. Consequently, no further design analyses (e.g. simulations to optimize lance spacing, injection sequence, CS gel time, etc.) were conducted.

9. ACKNOWLEDGEMENTS

This work was supported by the U.S. Department of Energy, Office of Environmental Management, Office of Technology Development, Subsurface Contamination Focus Area, under Contract No. DE-AC03-76SF00098. Drs. S. Finsterle and K. Karasaki are thanked for their helpful review comments.

9. Acknowledgements

10. REFERENCES

Altaner, S.P., *Savannah River Site Native Soil Mineralogical Analyses*, Letter report to J. Apps, July 24, 1996.

Morrey, J. R., *FASTCHEM™ Package, Volume 4: User's Guide to the ECHEM Equilibrium Geochemistry Code*, Electric Power Research Institute, EPRI EA-5870-CCM, 1988..

Finsterle, S., G.J. Moridis, K. Pruess, and P. Persoff, *Physical Barriers Formed From Gelling Liquids: 1. Numerical Design of Laboratory and Field Experiments.* LBL Report No. 35113, January 1994a.

Finsterle, S., G.J. Moridis, and K. Pruess, *A TOUGH2 Equation-of-State Module for the Simulation of Two-Phase Flow of Air, Water, and a Miscible Gelling Liquid*, LBL Report No. 36086, May 1994b.

Freifeld, B., L. Myer, G. Moridis, P. Cook, A. James, L. Pellerin, and K. Pruess, *Lance Water Injection Tests Adjacent to the 281-3H Retention Basin at the Savannah River Site, Aiken, South Carolina*, LBNL Report No. 39028, September 1996.

Hasbrouck, J.C., O.A. Dickenson, T.M. Boyd, and W.P. Hasbrouck, *3D/3C Seismic Baseline Technology Report* , Technical Task Plan No. AL94C242, 3D/3C Seismic for site characterization, Report DOE/ID/12584-251, GJPO-GP-25, U.S. Dept. of Energy, Grand Junction Projects Office, April 1996.

Huddlestun, P.F., *A Revision of the Lithostratigraphic Units of the Coastal Plain of Georgia*; The Miocene Through Holocene, Georgia Geological Survey Bulletin 104, 162 p., 1988.

Kegley, W. P., Distribution of Permeability at the MWD Well Field, Savannah River Site, Aiken, South Carolina, M.Sc. thesis, Clemson University, South Carolina, 186 p., 1993.

Kuelske, K.J., Removal Site Evaluation report for the H-Area retention Basin (281-3H)(U), WSRC Report No. 95-1533, Savannah River Site, Aiken, South Carolina, August 1995.

Moridis, G.J., P. Persoff, H.-Y. Holman, S.J. Muller, K. Pruess, P. Witherspoon, and C.J. Radke, *FY93 ANNUAL REPORT, Containment of Contaminants Through Physical Barriers From Viscous Liquids Emplaced Under Controlled Viscosity Conditions.* LBL Report No. 35114, October 1993a.

Moridis, G.J., P. Persoff, H.-Y. Holman, S.J. Muller, K. Pruess, and C.J. Radke, *New Barrier Fluids for Subsurface Containment of Contaminants.* In Proceedings of the ER '93 Environmental Remediation Conference, pp. 941-948, October 24-28, Augusta, Georgia, and LBL Report No. LBL-34673, October 1993b.

Moridis, G.J., L. Myer, P. Persoff, S. Finsterle, J.A. Apps, D. Vasco, S. Muller, P. Yen, P. Williams, B. Freifeld, and K. Pruess, *First-Level Field Demonstration of Subsurface Barrier Technology Using Viscous Liquids*, LBL Report No. 37520, July 1995a.

Moridis, G.J., P. Persoff, J.A. Apps, L. Myer, K. Pruess, and P. Yen, *A Field Test of Permeation Grouting in Heterogeneous Soils Using a New Generation of Barrier Liquids*, LBL Report No. 37554, August 1995b.

Moridis, G.J., P. Yen, P. Persoff, S. Finsterle, P. Williams, L. Myer, and K. Pruess, *A Design Study for a Medium-Scale Demonstration of the Viscous Barrier Technology*, LBNL Report No. 38916, September 1996a.

Moridis, G.J., K. Nihei, K.H. Lee, W. Frangos, D. Hopkins, C. Garbesi, S. Finsterle, D. Vasco, and K. Pruess, *Technologies for Subsurface Barrier Monitoring and Verification*, LBNL Report No. 38917, September 1996b.

Nystrom, P. G, and R.H. Willoughby, Cretaceous, *Tertiary, and Pleistocene Stratigraphy of Hollow Creek and Graniteville Quadrangles, Aiken County, South Carolina*, in Geological Investigations Related to the Stratigraphy in the Kaolin Mining District, Aiken County, South Carolina, (Nystrom, P. G, and Willoughby, R. H., Eds.), Carolina Geological Society Field Trip Guidebook, p.80-113, 1982.

Persoff, P., G.J. Moridis, J. Apps, K. Pruess, and S. Muller, *Designing Injectable Colloidal Silica Barriers for Waste Isolation at the Hanford Site* (LBL Report No. 35447), Proceedings of the 33rd Hanford Symposium on Health and Environment, "In-Situ Remediation: Scientific Basis for Current and Future Technologies", pg. 87-101, November 1994.

Serrato, M., *Viscous Liquid Barrier Demonstration Information*, Letter report to G. Moridis, April 4, 1996a.

Serrato, M., *Viscous Liquid Barrier Demonstration at the SRS H Area Retention Basin, - Shelby Tube Data (U)*, Letter report SRS-ESS-96-201 to G. Moridis, March 22, 1996b.

Sydansk, R.D., *A Newly Developed Chromium (III) Technology*, SPE Reservoir Engineering, 5(3), 346-352, 1990.

Westinghouse Savannah River Company (WSRC), *Phase II, Revision 1, Remedial Investigation Work Plan for the H-Area Retention Basin (281-3H)(U)*, WSRC Report No. 94-499, Rev. 1, Savannah River Site, Aiken, South Carolina, October 1994.

Westinghouse Savannah River Company (WSRC), *H-Area Retention Basin (281-3H) Treatability Study Work Plan (U)*, WSRC Report No. 96-00134, Savannah River Site, Aiken, South Carolina, April 1996.

Williams, K., Savannah River Site Visist, Memorandum to G. Moridis, March 4, 1996.

Wolery, T.J., EQ3/6, A software package for geochemical modeling of aqueous systems: Package overview and installation guide (Version 7.0), *Lawrence Livermore National Laboratory UCRL-MA-110662-PT-I*, Livermore, CA, 1992.

11. APPENDIX

Soil Cores from Shelby-Tube Samples

Sampling Markers

— Intact or Consecutive Shelby Tubes

— Split Spoon Samples

— No Core Recovered

Texture Markers

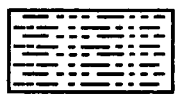

— Silt or Clay layer with sand < 5%

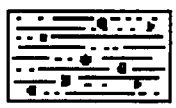

— Silt or Clay layer with weathered pebbles and Rock fragments > 2 cm in size

Mineralogy Markers

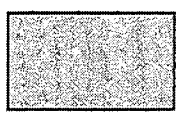

— Kaolinite dominated layer

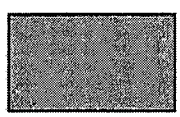

— Goethite(or yellow Fe oxide) dominated layer

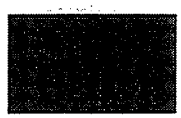

— Hematite dominated layer

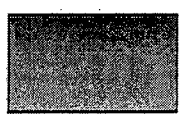

— Transition in layer from Hematite dominant mineralogy to Goethite dominant or increasing concentrations of mottling that has been homogenized during sampling

— Mottling - Typically mottles are in the form of banding or precipitated nodules of hematite, goethite, or kaolinite within a matrix of hematite or goethite. Banding is representative of contiguous portions of minerals that dominate a horizon, rather than disparate nodules.

Cores HAA-3AA-1, 2, 3, & 4

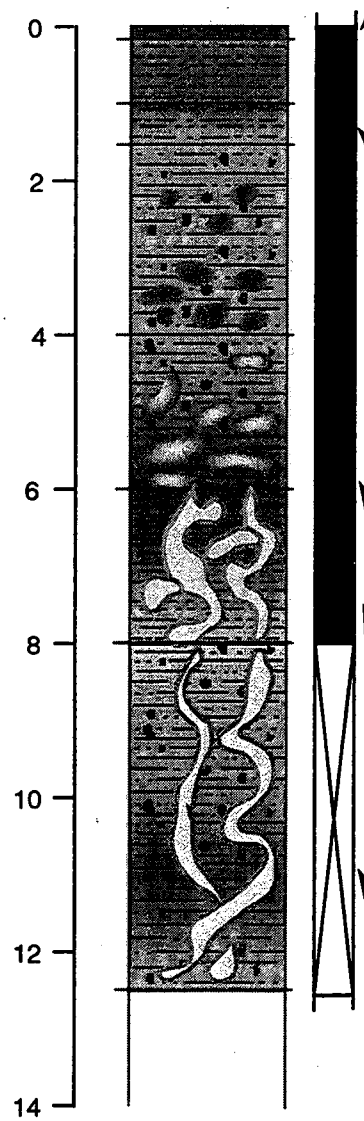

0-1.5" Moderately to weakly developed surficial soil (A horizon), with low concentrations of OM. Surface may have been eroded and soil began developing again.

1-12" Red-brown clay-rich B or AB horizon. Red color indicative of greater oxidation than lower horizons, and structure appears to be that of a more loosely aggregated layer with 15-25% clay. Brown color is indicative of residual OM that has leached through the surface layers of soil. Brownish hue in this layer is indicative of a more mature soil than the thin A, surficial horizon, indicates.

1-1.6' Yellow, goethite-rich sediment below 1', a BC1 horizon with obvious weathering, but lower degree of oxidation and transformation. Presence of goethite without red, hematite mottling (as seen in lower horizon) is indicative of some residual OM present which stabilizes the goethite and prevents transformation into hematite (this is based on conjecture without chemical data to support this assumption)

1.6-4' Yellow, goethite rich layer with mottles of hematite,.a BC2 horizon with weathering and pebbles (<2.5 cm in diameter). Clay content is approximately 10-15% with significant sand and clay films of iron oxides within the matrix. The lithic fragments, pebbles, are quartz rich, implying that the sediment has undergone weathering.

#10 $K_H = 4.3 \times 10^{-5}$
$K_V = 1.2 \times 10^{-3}$

4-6' Mottled layer, with predominantly goethite coloring, rich in kaolinite (potentially a BC3 horizon formed prior to the surface erosion and formation of the current surface soil). Mottling is comprised of yellow (goethite), browns (mixtures of goethite, hematite, and kaolinite), and reds (hematite) mottles and with quartz pebbles (predominantly ≤2.5 cm with larger fragments of 3-5 cm)and sand present. Permeability sample #10 was taken from the 5 to 5.5' section of this core, and it has a preliminary texture determination of sandy clay (clay content of ~25%). This layer is quite massive and compact (although this may partly be a result of the coring procedure). Kaolinite concentration in this horizon appears to increase with depth, giving the lower portion a grey to white color between mottles of red and yellow. The kaolinite appears to be responsible for the dense, lithified nature of portions of this layer.

6-8'+ This is a dense clay layer with highly weathered minerals such as hematite and kaolinite. Little-to-no goethite is present, and there appears to be a sharp transition (discontinuity) into this oxidized, weathered layer at approximately 6'.

8-12.5' There is a gap in the shelby tube samples between 7 or 8' and ~12.5', where recovery of the sediment using shelby tubes was impossible. Split spoon samples through this section revealed that the sediment is of similar composition as the overlying sections with more pebbles surrounded by a hematitic clay matrix. It is difficult to determine the actual composition of this layer after split spoon acquisition.

K_V and K_H are expressed in units of cm s^{-1} with K_V and K_H representing the hydraulic conductivity in the vertical and horizontal direction respectively.

Cores HAA-3AA-1, 2, 3, & 4

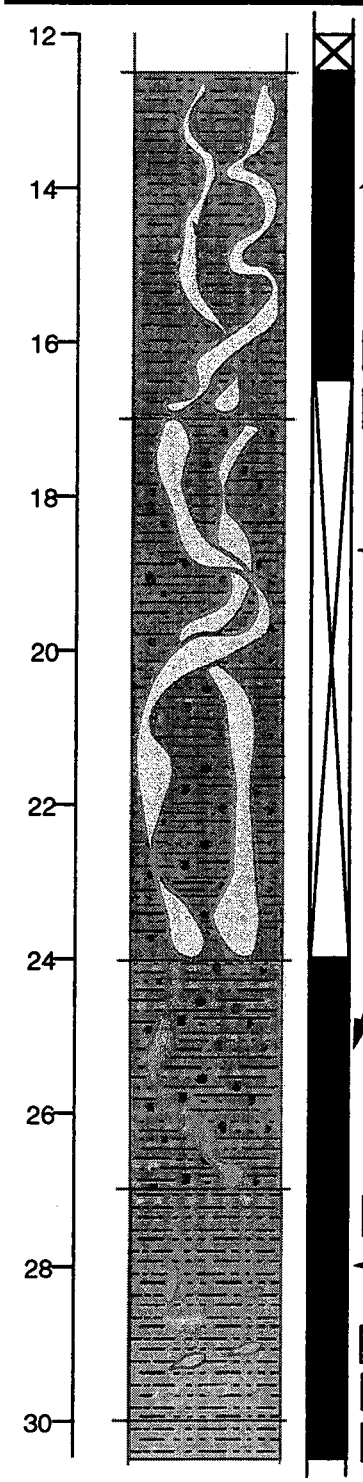

12.5-17' Composition and degree of weathering indicate that this layer was not weathered as part of the current soil development processes. It has many of the same minerals found in the layers between 6-8', but the concentration of highly crystallized hematite and kaolinite are greater. Undulating layers of kaolinite form streaks through the red to purple, well crystallized hematite. Some mica and sand are present, but clay concentration is extremely high (25+% clay). Origin is either that of highly altered material (Eocene coastal sedimentary rock that has been highly weathered and buried) or buried, highly weathered Pleistocene soil. Without further information regarding the history of the site, it is impossible to determine. Permeability sample 9 was taken from the 15-15.5' increment of this series of cores. It is predominantly kaolinite with stains of goethite on the edges of the hematite-kaolinite margins. Permeable in this layer is expected to be extremely low. Sample #8 was taken from the 16.5-17' depth in a kaolinite/hematite mixed sample where the ratio was approximately 50/50.

#9 $K_H = 2.4 \times 10^{-4}$, $K_V = 2.8 \times 10^{-4}$

#8 $K_H = 4.9 \times 10^{-5}$, $K_V = 4.8 \times 10^{-5}$

17-24' Quartz rich layer missing in cores (split spoon has shown that it is quartz conglomerate layer with kaolinite and hematite matrix). Despite the high concentration of pebbles in this layer, it has a high concentration of clays in the matrix, making the permeability extremely low.

24-27'+ Red oxide conglomerate layer with purple stains on pebbles due to well crystallized hematite. Banding of goethite and hematite in the matrix surrounding sands and pebbles form layers of alternating yellow and red. Although the texture of this layer is skeletal (matrix surrounding a conglomerate layer) the matrix is composed of well lithified clays with low concentrations of sands. Both permeability samples #6 and 7 were taken from this layer at a depth of 25-25.5'. Proximity to the water table changes the appearance of this layer dramatically from well hole to well hole. As a result, adjacent holes have cores with very different appearance. Sample #5 was taken at a depth of 25.75 to 26.25' in a layer with an approximate texture of clayey loam (~15% clay).

The water table appears to be somewhere between at 26 to 28' feet in depth. This can be determined both by the degree of saturation in the sediments removed by the cores, but also the increasing concentration of goethite and lighter yellow colors.

#6&7 K not testable

#5 $K_H = 1.2 \times 10^{-6}$, $K_V = 1.5 \times 10^{-6}$

#4 $K_H = 9.5 \times 10^{-7}$, $K_V = 1.2 \times 10^{-3}$

27-30'+ This is a layer that is high in clay and quartz sand (25-30% clay). It is difficult to determine its original morphology because of the proximity of the water table and the degree of saturation of the sediments (cores appear to be slurries of the original samples). These layers appear very mixed and yellow in color due to the lower redox potential and available oxygen (making goethite more stable). Sample #4 and 3 were removed from this series of layers, with 4 taken out of a layer of unconsolidated sandy clay at 27 to 27.5'. Sample #3 came from a depth of 28.25 to 28.75' in a sandy clay layer with mottling of goethite within a matrix mixture of hematite and goethite.

#3 $K_H = 2.6 \times 10^{-6}$, $K_V = 1.1 \times 10^{-6}$

#2 $K_H = 1.7 \times 10^{-4}$, $K_V = 7.2 \times 10^{-5}$

#1 $K_H = 6.0 \times 10^{-6}$, $K_V = 4.7 \times 10^{-6}$

There is a sandy clay loam layer below the water table at 29.5 to 30', where sample #2 was obtained (~15% clay). A clayey sand texture was found at approximately 30-30.5' where sample #1 was taken. Mineralogy of both samples is similar; a matrix of goethite and small amounts of hematite dominate the profile. The presence of goethite is indicative of the lower oxygen content as discussed above.

Cores HR3-13-1 & 2

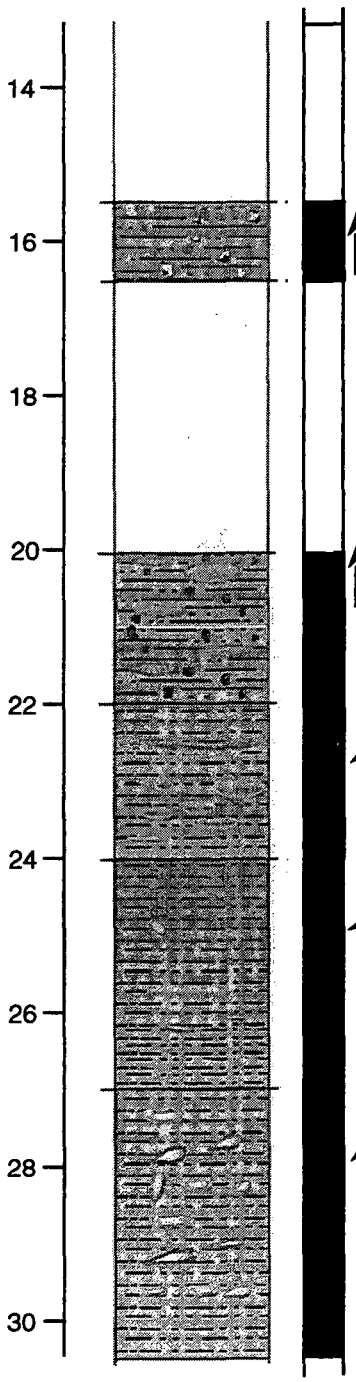

0-20' A single core from 16 to 17' was recovered from this section, and it appears to have similar mineralogy to the 18' section of well HAA-3AA-1 to 4. There are fewer quartzite pebbles in this core, and no kaolinite present. Sample #15 was removed from this layer between 16.25 and 16.75'. The sample layer was described as a pebble rich sandy clay.

#15 $K_H = 2.5 \times 10^{-5}$
$K_V = 1.2 \times 10^{-5}$

20-22 At 20' recovery of cores using shelby tubes was possible showing that the mineralogy and composition of the sediment was very similar to the overlying layers at 16-17', more goethite present altering the color to a lighter brown-yellow hue. Where sample #14 was taken at a depth of 20.25 to 20.75' in a mixed hematite-goethite mineralogy with loamy sand texture tending to goethite conglomerate at the bottom of the sample.

#14 $K_H = 2.2 \times 10^{-5}$
$K_V = 1.7 \times 10^{-6}$

22-24' This layer appears to be in the capillary fringe above the water table where the transition from red, oxidized sediments to yellow, reduced sediments occurs (~23'). Sample #13 was taken from a layer at a depth of 23.25 to 23.75', where the texture was sandy clay, and although the layer was more lithified than the overlying slough, it was wet and high in both hematite and goethite.

#13 $K_H = 8.9 \times 10^{-5}$
$K_V = 1.5 \times 10^{-5}$

24-27' This is a continuation of the transition layer in the capillary fringe, in which the goethite increases dramatically over 3'. Sample #12 was taken at a depth of 25 to 25.5', in the center of this clay rich mixed mineralogy zone.

#12 $K_H = 1.6 \times 10^{-5}$
$K_V = 7.2 \times 10^{-8}$

27-29' At the bottom of the transition layer, 26.75 to 27', there is a sharp transition to goethite-rich, yellow sediments with hematite and kaolinite mottling. It is a loamy clay with dense layers of kaolinite throughout the horizon, and smaller pockets of hematite. Sample #11 comes from a depth of 28 to 28.5'.

#11 $K_H = 1.3 \times 10^{-5}$
$K_V = 5.0 \times 10^{-6}$

ERNEST ORLANDO LAWRENCE BERKELEY NATIONAL LABORATORY
ONE CYCLOTRON ROAD | BERKELEY, CALIFORNIA 94720

Prepared for the U.S. Department of Energy under Contract No. DE-AC03-76SF00098